

DTIC FILE COPY

1

AGARD-R-734 / ADDENDUM

AGARD-R-734 ADDENDUM



AD-A198 702

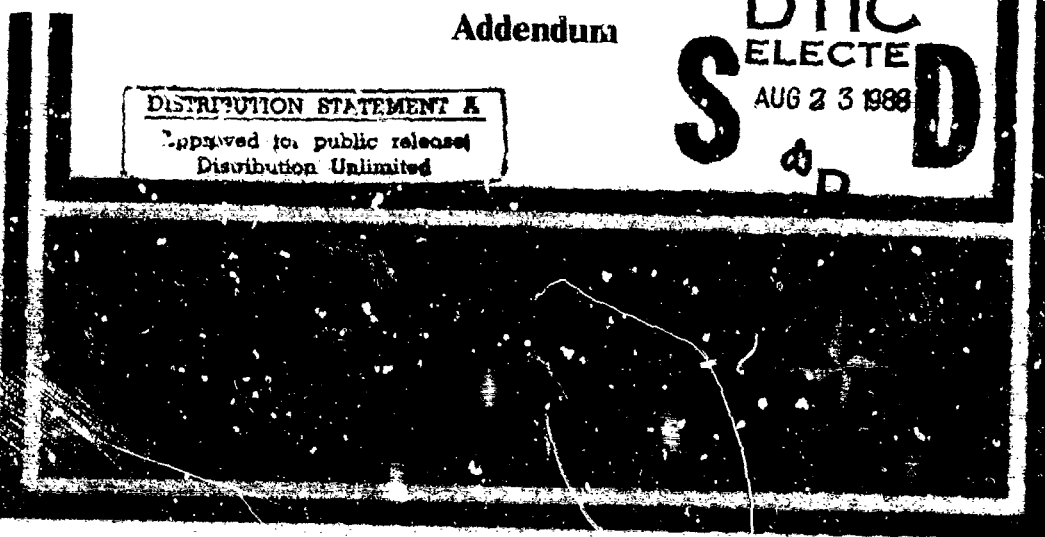
AGARD REPORT No.734

**The Flight of Flexible Aircraft in
Turbulence — State-of-the-Art in the
Description and Modelling of
Atmospheric Turbulence**

Addendum

DTIC
ELECTE
AUG 23 1988
S **D**

DISTRIBUTION STATEMENT A
Approved for public release
Distribution Unlimited



**DISTRIBUTION AND AVAILABILITY
ON BACK COVER**

88 8 23 037

AGARD-R-734
(Addendum)

NORTH ATLANTIC TREATY ORGANIZATION
ADVISORY GROUP FOR AEROSPACE RESEARCH AND DEVELOPMENT
(ORGANISATION DU TRAITE DE L'ATLANTIQUE NORD)

AGARD Report No.734

ADDENDUM

THE FLIGHT OF FLEXIBLE AIRCRAFT IN TURBULENCE --
STATE-OF-THE-ART IN THE DESCRIPTION AND MODELLING OF
ATMOSPHERIC TURBULENCE



Accession For	
NTIS GRA&I	<input checked="" type="checkbox"/>
DIC TAB	<input type="checkbox"/>
Unannounced	<input type="checkbox"/>
Justification	
By	
Date Recd.	
Priority Series	
Dist	Aviation or Special
A-1	

Papers presented at the 65th Meeting of the Structures and Materials Panel in Cesme, Turkey on
4-9 October 1987.

THE MISSION OF AGARD

According to its Charter, the mission of AGARD is to bring together the leading personalities of the NATO nations in the fields of science and technology relating to aerospace for the following purposes:

- Recommending effective ways for the member nations to use their research and development capabilities for the common benefit of the NATO community;
- Providing scientific and technical advice and assistance to the Military Committee in the field of aerospace research and development (with particular regard to its military application);
- Continuously stimulating advances in the aerospace sciences relevant to strengthening the common defence posture;
- Improving the co-operation among member nations in aerospace research and development;
- Exchange of scientific and technical information;
- Providing assistance to member nations for the purpose of increasing their scientific and technical potential;
- Rendering scientific and technical assistance, as requested, to other NATO bodies and to member nations in connection with research and development problems in the aerospace field.

The highest authority within AGARD is the National Delegates Board consisting of officially appointed senior representatives from each member nation. The mission of AGARD is carried out through the Panels which are composed of experts appointed by the National Delegates, the Consultant and Exchange Programme and the Aerospace Applications Studies Programme. The results of AGARD work are reported to the member nations and the NATO Authorities through the AGARD series of publications of which this is one.

Participation in AGARD activities is by invitation only and is normally limited to citizens of the NATO nations.

The content of this publication has been reproduced directly from material supplied by AGARD or the authors.

Published June 1988

Copyright © AGARD 1988
All Rights Reserved

ISBN 92-835-0458-5



Printed by Specialised Printing Services Limited
40 Chigwell Lane, Loughton, Essex IG10 3TZ

PREFACE

This is the second of two Workshops on turbulence held by the Panel in the 1986—87 time period. The first Workshop concentrated on the measurement of turbulence and methods of data collection. The theme of the second Workshop concerned the criteria, analysis methods and regulations involved in the design and certification of aircraft for turbulence. Taken together, these two Workshops will provide invaluable guidance in the formulation of an AGARD Manual on turbulence, scheduled for publication in late 1988 or early 1989.

The authors are to be congratulated for the interesting and valuable presentations at the Workshop, and the appreciation of the Panel is hereby extended to them. A special note of thanks is offered to the FAA and the AGARD Flight Mechanics Panel for the contributions sponsored by those organizations.

Le présent rapport rend compte des travaux de la deuxième réunion de travail organisée par le Panel, sur le thème de la turbulence pendant la période 1986—1987. La première réunion fut consacrée aux mesures des turbulences et les procédures de recueil des données. La deuxième réunion de travail concerne les critères, les méthodes d'analyse et les règlements intervenant dans l'étude et l'homologation des aéronefs du point de vue de leur aptitude au vol dans les turbulences atmosphériques.

Les travaux de ces deux réunions de travail devraient déboucher sur des directives qui seront d'une grande utilité lors de l'élaboration du Manuel AGARD de la turbulence, dont la parution est prévue fin 1988 début 1989.

Nous tenons à féliciter les auteurs de l'intérêt et de la valeur des exposés qui ont été présentés lors de la réunion, et de la part du Panel, nous leur présentons nos vifs remerciements. Nous ne saurions conclure ce résumé sans exprimer notre reconnaissance pour les contributions effectuées sous l'égide de la FAA et du Panel AGARD de la Mécanique du vol.

CONTENTS

	Page
PREFACE	iii
<i>cont fr p 7-15</i>	
Reference	
CURRENT AND PROPOSED GUST CRITERIA AND ANALYSIS METHODS - AN FAA OVERVIEW by T.J. Barnes	1
FLIGHT TEST EQUIPMENT FOR THE ON-BOARD MEASUREMENT OF WIND AND TURBULENCE by G. Schänzer, M. Swolinsky and P. Vörsmann	2
MATCHING P.S.D. - DESIGN LOADS by R. Nohack	3
A SUMMARY OF METHODS FOR ESTABLISHING AIRFRAME DESIGN LOADS FROM CONTINUOUS GUST DESIGN CRITERIA by R.N. Moon	4
COMPARISON OF THE INFLUENCE OF DIFFERENT GUST MODELS ON STRUCTURAL DESIGN by M. Molsow	5
MEASURED AND PREDICTED RESPONSES OF THE <u>NORD 260</u> AIRCRAFT TO THE <u>LOW ALTITUDE</u> ATMOSPHERIC TURBULENCE by J.L. Meurtec and F. Poirion	6
Erratum to AGARD Report No. 734	
A REVIEW OF MEASURED GUST RESPONSES IN THE LIGHT OF MODERN ANALYSIS METHODS . Keywords: Flight characteristics; Data reduction by V. Card <i>Airborne accelerometers. (eds)</i>	7

**CURRENT AND PROPOSED GUST CRITERIA AND ANALYSIS METHODS
AN FAA OVERVIEW**

by

Terence J. Barnes
Federal Aviation Administration
ANM-105N
P.O. Box C-68966
Seattle, WA 98168, USA

INTRODUCTION

This paper presents an FAA overview of the gust criteria and analysis methods used in the various types of flight vehicle certified under the FAR's (Reference 1). The current criteria for small airplanes, transports, and rotorcraft are presented, and the status of proposed criteria for the tilt rotor and aerospace plane are discussed. The amount of discussion on each class of vehicle depends on the significance of gust loads as design loads, and the importance of vehicle flexibility. Transport airplane gust criteria development, usage and problems are discussed in some detail. Analysis methods used by U.S. Industry are covered in a separate paper.

Units used throughout this paper (Standard English) are those accepted world wide for certification to FAR-25 and JAR-25 standards.

PHILOSOPHY OF REGULATIONS

Structural design limit load criteria are chosen such that there is sufficient structural margin around normal operating loads that, in combination with the factor of safety, the probability of catastrophic failure is acceptably low.

The structural criteria used to establish the required strength levels have changed over the years to reflect changes in airplane configurations, knowledge of the atmosphere and ability to analyze.

To ease the analysis burden, criteria are presented in the simplest form consistent with obtaining acceptable safety levels. However, it is necessary to recognize the impact of the simplifications on a particular vehicle. A typical example is the definition of gust velocities without spanwise variation. The combinations of airplane size and current criteria have proven adequate, however, a transport with a significantly larger wing span than the Boeing 747 would likely receive special attention in this area.

Similarly, transport airplanes have gradually introduced active controls and non-linear systems. Although recognized by the AC (Reference 2) and special conditions, the basic criteria have not yet been changed.

DISCUSSION

For each class of flight vehicle, the following are discussed (if applicable):

- ° Summary of current regulations, and their historical development.
- ° Adequacy of current regulations for conventional configurations.
- ° Adequacy of current regulations and methods of analysis for anticipated configurations.
- ° Identified Problems.
- ° Actions to address identified problems.

SMALL AIRPLANES

Small airplane gust criteria (Part 23 of Reference 1), with the exception of the evaluation of dynamic response, are the same as the transport criteria. Most configurations of small airplanes certified to date have been relatively stiff, slow and conventional. Special conditions have been written and rule changes proposed to cover the certification of canard configured airplanes. The evaluation of dynamic response to turbulence has not been considered necessary. The current rules are presented in FAR Part 23 §23.333(c) and §23.341 as follows:

§23.333(c) Gust envelope. (1) The airplane is assumed to be subjected to symmetrical vertical gusts in level flight. The resulting limit load factors must correspond to the conditions determined as follows:

(i) Positive (up) and negative (down) gusts of 50 f.p.s. at V_C must be considered at altitudes between sea level and 20,000 feet. The gust velocity may be reduced linearly from 50 f.p.s. at 20,000 feet to 25 f.p.s. at 50,000 feet.

(ii) Positive and negative gusts of 25 f.p.s. at V_C must be considered at altitudes between sea level and 20,000 feet. The gust velocity may be reduced linearly from 25 f.p.s. at 20,000 feet to 12.5 f.p.s. at 50,000 feet.

(2) The following assumptions must be made:

(i) The shape of the gust is -
$$U = \frac{U_{de}}{2} \left(1 - \cos \frac{2\pi s}{25C} \right)$$

Where -

s = Distance penetrated into gust (ft.);

C = Mean geometric chord of wing (ft.); and

U_{de} = Derived gust velocity referred to in subparagraph (1) of this section. §23.341 Gust Load Factors.

In the absence of a more rational analysis, the gust load factors must be computed as follows:

$$n = 1 + \frac{K_g U_{de} V_a}{198(W/S)}$$

Where -

$K_g = 0.88 \mu_g / 5.3 + \mu_g$ = gust alleviation factor;

$\mu_g = 2(W/S) / \rho C a g$ = airplane mass ratio;

U_{de} = Derived gust velocities referred to in §23.333(c)(f.p.s.);

ρ = Density of air (slugs/cu.ft.); at altitude;

W/S = Wing loading (p.s.f.);

C = Mean geometric chord (ft.);

g = Acceleration due to gravity (ft/sec.²)

V = Airplane equivalent speed (knots); and

α = Slope of the airplane normal force coefficient curve C_{NA} per radian if the gust loads are applied to the wings and horizontal tail surfaces simultaneously by a rational method. The wing lift curve slope C_L per radian may be used when the gust load is applied to the wings only and the horizontal tail gust loads are treated as a separate condition.

FIXED WING TRANSPORTS

° Summary of current regulations, and their historical development.

The starting point for this discussion is the gust load formula (FAR Part 25 §25.341(b)(3), Reference 1). A good overall technical discussion of gust criteria development is given by Noback in his report NLR TR 82134U, Reference

4. The current gust load formula (frequently referred to as the "Pratt Formula") was developed based on an evaluation of V-G records from 9 civil transports from 1933 to 1950 and presented in Reference 3.

As can be deduced from the table (Figure 1) below, these were essentially straight wing, stiff airplanes flying slowly at low altitudes.

Air plane	Design gross wt., W, lb	Wing area, S, sq ft	Wing span, b, ft	Mean geometric chord, c, ft	Aspect ratio, A	Design cruising speed, V_c , mph	Estimated operating altitude, ft
A	13,400	836	74	11.3	6.6	180	5,000
B	18,560	939	85	11.0	7.7	215	5,000
C	41,000	1,340	118.2	11.3	10.4	181	5,000
D	50,000	2,145	130	16.5	7.9	168	5,000
E	25,200	987	95	10.4	9.1	211	5,000
F	45,000	1,486	107.3	13.9	7.8	230	5,000
G	94,000	1,650	123	14.7	9.2	271	10,000
H	70,700	1,461	117.5	13.6	9.5	224	10,000
J	39,900	864	93.3	10.1	10.1	256	5,000

Figure 1

As airplane configurations, speeds and cruise altitudes changed, it was recognized that airplane dynamic response should be considered. The current rules are presented in §25.305(c) and (d), and §25.341 as follows:

§25.305(c) where structural flexibility is such that any rate of load application likely to occur in the operating conditions might produce transient stresses appreciably higher than those corresponding to static loads, the effects of this rate of application must be considered.

§25.305(d) the dynamic response of the airplane to vertical and lateral continuous turbulence must be taken into account. The continuous gust design criteria of Appendix G of this part must be used to establish the dynamic response unless more rational criteria are shown.

The airplane is assumed to be subjected to symmetrical vertical gusts in level flight. The resulting limit load factors must correspond to the conditions determined as follows:

(1) Positive (up) and negative (down) rough air gusts of 66 fps at V_B must be considered at altitudes between sea level and 20,000 feet. The gust velocity may be reduced linearly from 66 fps at 20,000 feet to 38 fps at 50,000 feet.

(2) Positive and negative gusts of 50 fps at V_C must be considered at altitudes between sea level and 20,000 feet. The gust velocity may be reduced linearly from 50 fps at 20,000 feet to 25 fps at 50,000 feet.

(3) Positive and negative gusts of 25 fps at V_D must be considered at altitudes between sea level and 20,000 feet. The gust velocity may be reduced linearly from 25 fps at 20,000 feet to 12.5 fps at 50,000 feet.

The following assumptions must be made:

(1) The shape of the gust is

$$U = \frac{U_{de}}{2} (1 - \cos) \frac{2s}{25C}$$

Where -

s = distance penetrated into gust (ft);

C = mean geometric chord of wing (ft); and

U_{de} = derived gust velocity referred to in paragraph (a) (fps).

(2) Gust load factors vary linearly between the specified conditions B' through G', as shown on the gust envelope in §25.333(c).

(3) In the absence of a more rational analysis, the gust load factors must be computed as follows:

$$n = 1 + \frac{K_g U_{de} V_a}{498 (W/S)}$$

Where -

$$K_g = \frac{0.88g}{5.3+g} = \text{gust alleviation factor};$$

$$g = \frac{2(W/S)}{\rho C a g} = \text{airplane mass ratio};$$

U_{de} = derived gust velocities referred to in paragraph (a) (fps);

ρ = density of air (slugs cu. ft.); at altitude

W/S = wing loading (psf);

C = mean geometric chord (ft);

g = acceleration due to gravity (ft/sec²);

V = airplane equivalent speed (knots); and

a = slope of the airplane normal force coefficient curve C_{NA} per radian. If the gust loads are applied to the wings and horizontal tail surfaces simultaneously by a rational method. The wing lift curve slope C_{AL} per radian may be used when the gust load is applied to the wings only and the horizontal tail gust loads are treated as a separate condition.

The first step in the development of the necessary techniques to include airplane dynamic response was taken toward the end of the era of piston engine transports. At that time it became apparent that the earlier airplanes had satisfactory service and safety records, even though no provision had been made in their design loads for dynamic effects that were known to be present. Thus it became evident that the design gust velocities had been set high enough so that for these airplanes no increase in design loads for dynamic effects was needed. On the other hand, it was apparent that, with the noted trends, the relative dynamic effects might well increase. Sooner or later, design to static loads alone could lead to a structure of inadequate strength.

Consequently, to prevent any deficiency in strength that might otherwise have resulted from this trend, the CAA at that time adopted a policy which was summarized as follows:

"During the AIA-CAA Gust Loads Meeting in Washington, it was agreed that if a manufacturer showed that for his new model the percentage increase in load, due to transient effects, was no greater than that of his previous models, it would not be necessary to design for the increased load; however, if the increase was greater than for the previous models, this increase should be designed for."

This policy, reflecting what may be called the concept of "limited dynamic accountability", was applied, for example, in the design of the Lockheed Model 1649 Constellation and the Electra. As was the practice at that time, primary emphasis was placed on a comparison of dynamic magnification factors of wing bending moment.

The major objection to a continuation of this type of approach was that detail engineering data on the various satisfactory existing airplanes were available only to the manufacturers of those airplanes. Consequently, a manufacturer whose past airplanes may not have been gust-critical, or for other reasons may have had more than the required strength, had to design a new aircraft to more severe criteria than the manufacturer whose past aircraft happened to have less margin. Further, with few exceptions, no criteria short of "full dynamic accountability" were available to a manufacturer who had no previous aircraft in operation with a long, satisfactory service life.

FAA decided to develop new gust criteria using the power spectral technique. The results of study contracts let to Lockheed and Boeing for the purpose of helping FAA define procedures and criteria are summarized in References 5 and 6 (ADS-53 and 54).

The criteria that FAA incorporated into the regulations as Appendix G to FAR 25 (Reference 1) in September 1980 were the result of extensive negotiations between FAA and U.S. Industry. The primary difference between the criteria prescribed in FAA-ADS-53 and current FAA criteria are in the specified design gust velocities and their variation with altitude. These FAA criteria provided the basis for all current continuous turbulence criteria, regardless of the certifying agency. For example, the European civil regulations as of January 1987 are specified in JAR-25, Reference 9. The continuous gust design criteria given here are identical to those given in Appendix G of FAR 25 with one major exception. JAR-25 makes no reference to reducing design gust velocities for airplanes that have an extensive satisfactory service experience with design gust velocities that are less than 85 fps. This will be discussed later.

As specified in Appendix G of FAR 25, power-spectral gust loads criteria are presented in two basic forms; the design envelope analysis and the mission (flight profile) analysis. Provision is also made for a modification of the design envelope analysis that considers the service life of existing airplanes.

The design envelope criterion is similar to past discrete criteria as well as to current limit design maneuver loads criteria. Operational usage of the aircraft is ignored. Instead, the aircraft response is evaluated for a specified design envelope of speed, altitude, gross weight, fuel weight and center of gravity, c.g., position.

Appendix G of FAR 25, Item (b)(3)(i), provides for reduced design values of U sigma. Specifically, "Where the Administrator finds that a design is comparable to a similar design with extensive satisfactory service experience, it will be acceptable to select U sigma at V_C less than 85 fps, but not less than 75 fps, with linear decrease from that value at 20,000 feet to 30 fps at 80,000 feet." To apply the reduced U sigma values requires that:

- (1) Transfer functions of the new design are similar to the prior designs.
- (2) Typical missions of the new airplane are substantially equivalent to that of the similar design.

This modification to the design envelope criterion came about from an AIA proposal to the FAA after extensive studies of mid-range to long-range transports, such as the L-1011, DC-9 and DC-10, and the Boeing 727, 737, and 747, that showed U sigma of 75 fps at V_C was permissible under FAR Appendix G for this type of transport. The higher U sigma values, specified by the unmodified design envelope criterion, are more appropriate for the lower cruise altitude more-severe types of operation. The more severe types of operation are represented by short range or commuter operations where cruise altitudes of 20,000 to 30,000 feet are typical. The mid-range to long-range airplanes normally have cruise altitude in the vicinity of 35,000 feet.

As originally developed in FAA-ADS-53, the mission analysis approach was a "stand alone" method. It was, however, suggested that the most appropriate criterion would be a combination of the design envelope approach and the mission analysis approach. Combining these two approaches now constitutes the Mission Analysis Criterion specified in FAR 25, JAR-25 and the various U.S. MIL SPECS.

In addition to a mission profile analysis the Mission Analysis Criterion requires that a design envelope analysis be performed similar to the design envelope criterion, but with reduced U sigma values to provide a design envelope floor. The U sigma value at V_C is specified as 60 fps from 0 to 30,000 feet with a linear reduction to 25 fps between 30,000 feet and 80,000 feet. The V_B value is still 1.32 times the V_C value and V_D is still 0.5 times the V_C value.

There was a transition period, during which dynamic response to both single gust encounters and continuous turbulence was considered. Depending on the manufacturer, there was a different balance of reliance on the two methods. Dynamic analysis of the single gust encounter was accomplished by requiring an evaluation of the 1 minus cosine gust shape and 25 chord length of §25.341(b)(1), including the rigid body and flexible airplane responses.

The Boeing 747 was the last airplane certified during the transition period. All subsequent new airplane certifications commencing with the Lockheed L1011 and Douglas DC-10 used gust criteria similar to those currently published.

Atmosphere	Single Gust Encounter	Continuous Turbulence	
	Airplanes	Essentially Rigid Slow	Flexible High Subsonic Swept Wings
Criteria	Pratt Formula/1-Cos	PSD Pratt Formula/1-Cos	
Analysis Methods	Rigid	Frequency domain plus static elastic solution	Frequency domain plus supplemental time history plus static elastic

*L1011-500, A-320

Transition
Period

Current Situation

Figure 2

*Adequacy of current regulations for conventional configurations.

Sufficient service has been built up on airplanes certified to the Appendix G PSD gust criteria to be confident that the criteria are adequate for these configurations. However, these airplanes have gradually included more non-linear systems and active controls. In general, the group of airplanes identified as "flexible high subsonic swept wings" in Figure 2 included only a yaw damper in addition to a limited authority autopilot. However, the last group, which currently includes only the Lockheed L-1011-500 and the Airbus A320, have systems which interact with vertical gust response, and have non-linear characteristics. Even though FAA prepared special conditions for the certification of these airplanes, they discussed the technical concerns without defining an acceptable means of compliance.

*Adequacy of current regulations and methods of analysis for anticipated configurations.

As more airplanes are certified with increasing levels of system interaction with structure, the need for changes in the regulations increases. For example, if the control surfaces deflect at high rates to large deflections to maintain a desired airplane attitude in turbulence, the way in which these effects are accounted for in the analyses should be defined by the FAA, and not left to the imagination of the manufacturer. In addition, concerns increase about the need for consideration of, for example, spanwise variation of gust velocity.

*Identified Problems

The following are considered to be problems with the current regulations:

- Difficulties using current PSD criteria to produce design loads.
- Definition of realistic turbulence to evaluate active controls and gust load alleviation.
- Criteria for reduction of PSD Gust Intensity below 85 ft/sec.

The difficulty using the current PSD criteria to produce design loads is how to fit them into the routine by which design loads are obtained and stress analysis is conducted. Normal stress analysis practice utilizes design conditions each of which is defined over the whole of some major structural component at a given instant. Power-spectral methods, however, do not result in this sort of design condition. They lead, instead, to individual design-level values of load of equal probability at various points in the structure, or of various components of load such as wing shear, bending moment, and torsion, with the phasing undetermined. For example, it is not determined whether maximum up shear combines with maximum nose-up or maximum nose-down torsion or with some intermediate value. This difficulty can be circumvented to some extent by determining design-level values of internal loads or stresses, such as front and rear beam shear flows. As discussed earlier, the methods used by U.S. Industry are reviewed in detail in a separate paper.

The definition of realistic turbulence to evaluate active controls and gust load alleviation becomes more important as the use of active controls becomes more prominent in modern airplane design.

The criteria for allowing a reduction of PSD gust intensity below 85 ft/sec are qualitative. It is not possible to evaluate transfer functions and typical missions to arrive at a value between 85 and 75 ft/sec. Typically the jet transports which cruise at 30,000 to 40,000 feet can substantiate the use of 75 ft/sec, while the turboprop shorter range transports which cruise at 20,000 to 30,000 feet have found to require the use of 85 ft/sec.

°Actions to address identified problems.

Two of the problem areas identified above are being actively addressed.

Most Airworthiness Authorities and Transport Manufacturers outside the U.S., and some smaller U.S. Transport Manufacturers indicated an interest in developing a time domain continuous turbulence gust analysis that would produce complete sets of correlated loads on an airplane. FAA agreed to sponsor an evaluation of methods including the Statistical Discrete Gust (SDG) analysis method (Reference 7) proposed by Mr. J. Glynn Jones of RAF Farnborough, England. Originally Mr. Jones' Statistical Discrete Gust (SDG) method was seen only as a possible alternate means of compliance which produced complete sets of time correlated loads. It is now recognized in addition as a possible tool for directly analyzing the response of nonlinear systems such as gust load alleviation to continuous turbulence. An International Ad Hoc Committee has been formed under the chairmanship of Mr. Terence J. Barnes, FAA's National Resource Specialist for Flight Loads/Aeroelasticity.

The committee met for the first time on May 22, 1986 and agreed that the first step should be to validate the "overlap" between PSD and SDG. As discussed by Jones in Reference 8, since both methods reflect a variation of gust velocity with gust length (in the PSD method by the von Karman spectrum, and in the SDG method by assuming that gust velocity is proportional to gust length to the power 1/3) there is a fixed mathematical relationship between the methods. This is, however, valid only for linear systems. NASA has agreed to assist FAA in the validation of this overlap between the two methods. In the interim, several manufacturers including British Aerospace, Canadair and de Havilland Canada are conducting their own evaluations. A workshop is planned for October 12/13, 1987 in London at which users will discuss the status of their evaluations, and have an opportunity to discuss any problems with Mr. Jones. No recommendations for use will be made until the method is well understood and it has been evaluated on several representative airplanes.

The JAR Authorities are considering allowing a gust intensity reduction similar to that allowed by FAR 25 Appendix G. However they have suggested that the qualitative evaluation required by Appendix G to allow a reduction in gust intensity should be replaced by a quantitative evaluation for ease of compliance, and to possibly allow the use of values between 75 and 85 ft/sec. A simplified mission analysis, where the scope is reduced to a small number of missions, and where the loads are evaluated at a few key locations, has been discussed. FAA will review any acceptable proposal by the European Authorities with U.S. Industry, and consider it as a possible replacement for the current rule.

Helicopters

The gust criteria of FAR Part 29 are very basic, since helicopters are relatively insensitive to gust encounters. Loads analysis techniques are therefore unsophisticated, and based on data developed in the 1940 time period.

The concerns regarding helicopters in turbulence relate more to controllability and fatigue.

The current rules for gust loads criteria are presented in §29.341 as follows:

Each rotorcraft must be designed to withstand, at each critical airspeed including hovering, the loads resulting from vertical and horizontal gusts of 30 feet per second.

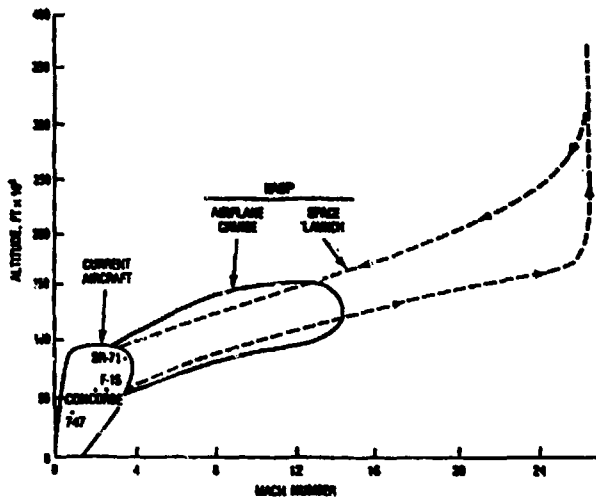
Tilt Rotor

At first sight, it would appear that a tilt rotor configuration could use the existing helicopter criteria in the hover mode and the transport criteria in the cruise mode, with the only area of concern being transition. However, due to the size and flexibility of the blades, and the configuration, there are significant blade/wing aerodynamic/aeroelastic interactions in all modes. This subject was discussed extensively by the Airframe Technical Issues Panel at the Powered Lift Conference in Fort Worth, Texas on 23/26 June 1987. The consensus of the experts was that these concerns justified a complete re-evaluation of the gust criteria. Some form of time history gust criteria will likely be proposed.

National Aerospace Plane (NASP)/Orient Express

The Orient Express concept focuses on sustained supersonic cruise at Mach 5 or 6, and hypersonic cruise vehicles derived from the aerospace plane may achieve speeds to Mach 10 and beyond in the altitude region of 100,000 ft. Initiated under DARPA, the U.S. Air Force will head the aerospace plane development program, with NASA having major technical responsibility. This is intended as a multiple purpose airplane, - hypersonic cruise and single stage to orbit -, propelled by an airbreathing (Scramjet) propulsion system. The ascent dynamic pressure will be high. New design concerns arise for this airplane due to major thermal effects on static and dynamic aeroelasticity, and dynamic loadings on the huge liquid hydrogen tank. 1986 saw the release of funds to begin NASP technology development. Aircraft conceptual design studies are being conducted by Boeing, General Dynamics, Lockheed, McDonnell Douglas and Rockwell International. These contractors will recommend gust criteria as appropriate for their individual design concepts. At the present time proprietary aspects prevent revealing the various proposed criteria.

Although FAA is not directly involved in the initial development phase, it already has begun thinking about the job of certificating a Mach 5 or Mach 6 transport for commercial use.



FLIGHT ENVELOPE FOR EXPERIMENTAL HYPERSONIC VEHICLE

Figure 3

REFERENCES

1. Federal Aviation Administration, Department of Transportation Airworthiness Standards: Part 23, Normal, Utility, and Acrobatic Category Airplanes, Part 25, Transport Category Airplanes and Part 29, Transport Category Rotorcraft.
2. AC 25.672-1, Federal Aviation Administration, Department of Transportation Advisory Circular; Active Flight Controls.
3. NACA Report 1206, A Revised Gust - Load Formula and a Re-evaluation of V-G Data Taken on Civil Transport Airplanes from 1933 to 1950 by Kermit G. Pratt and Walter G. Walker.
4. NLR TR 82134 U Review and Comparison of Discrete and Continuous Gust Methods for the Determination of Airplane Design Loads by R. Noback, NLR.
5. FAA-ADS-53 Development of a Power-Spectral Gust Design Procedure for Civil Aircraft by F. M. Hoblit, N. Paul, J. D. Shelton, and F. E. Ashford.
6. FAA-ADS-54 Contributions to the Development of a Power-Spectral Gust Design Procedure for Civil Aircraft by J. R. Fuller, L. D. Richmond, C. D. Larkins, and S. W. Russell.
7. R.A.E. Tech Memo FS 208 on the Formulation of Gust Load Requirements in Terms of the Statistical Discrete-Gust Method by J. G. Jones.
8. AIAA-86-1011-CP, A Unified Procedure for Meeting Power-Spectral-Density and Statistical-Discrete-Gust Requirements for Flight in Turbulence by J. G. Jones.
9. JAR-25, Joint Airworthiness Requirements - Large Airplanes.

Continuous Gust Design Criteria

The continuous gust design criteria in this appendix must be used in establishing the dynamic response of the airplane to vertical and lateral continuous turbulence unless a more rational criteria is used. The following gust load requirements apply to mission analysis and design envelope analysis:

(a) The limit gust loads utilizing the continuous turbulence concept must be determined in accordance with the provisions of either paragraph (b) or paragraphs (c) and (d) of this appendix.

(b) Design envelope analysis. The limit loads must be determined in accordance with the following:

(1) All critical altitudes, weights, and weight distributions, as specified in § 25.321(b), and all critical speeds within the ranges indicated in paragraph (b)(3) of this appendix must be considered.

(2) Values of $\bar{\Lambda}$ (ratio of root-mean-square incremental load root-mean-square gust velocity) must be determined by dynamic analysis. The power spectral density of w at atmospheric turbulence must be as given by the equation—

$$\phi(\omega) = \frac{w^2 L}{v} \frac{1 + \frac{\omega}{2} (1.333 L \omega)^2}{[1 + (1.333 L \omega)^2]^2}$$

where:

ϕ = power spectral density (ft./sec.)²/rad./ft.

v = root-mean-square gust velocity, ft./sec.

ω = reduced frequency, radians per foot.

L = 2,500 ft.

(3) The limit loads must be obtained by multiplying the $\bar{\Lambda}$ values determined by the

dynamic analysis by the following values of the gust velocity U_g :

(i) At speed V_1 : $U_g = 85$ fps true gust velocity in the interval 0 to 30,000 ft. altitude and is linearly decreased to 30 fps true gust velocity at 30,000 ft. altitude. Where the Administrator finds that a design is comparable to a similar design with extensive satisfactory service experience, it will be acceptable to select U_g at V_1 less than 85 fps, but not less than 75 fps, with linear decrease from that value at 30,000 feet to 30 fps at 30,000 feet. The following factors will be taken into account when assessing comparability to a similar design:

(1) The transfer function of the new design should exhibit no unusual characteristics as compared to the similar design which will significantly affect response to turbulence; e.g., coalescence of modal response in the frequency regime which can result in a significant increase of loads.

(2) The typical mission of the new airplane is substantially equivalent to that of the similar design.

(3) The similar design should demonstrate the adequacy of the U_g selected.

(ii) At speed V_2 : U_g is equal to 1.32 times the values obtained under paragraph (b)(3)(i) of this appendix.

(iii) At speed V_D : U_g is equal to $\frac{1}{2}$ the values obtained under paragraph (b)(3)(i) of this appendix.

(iv) At speeds between V_2 and V_C and between V_C and V_D : U_g is equal to a value obtained by linear interpolation.

(4) When a stability augmentation system is included in the analysis, the effect of system nonlinearities on loads at the limit

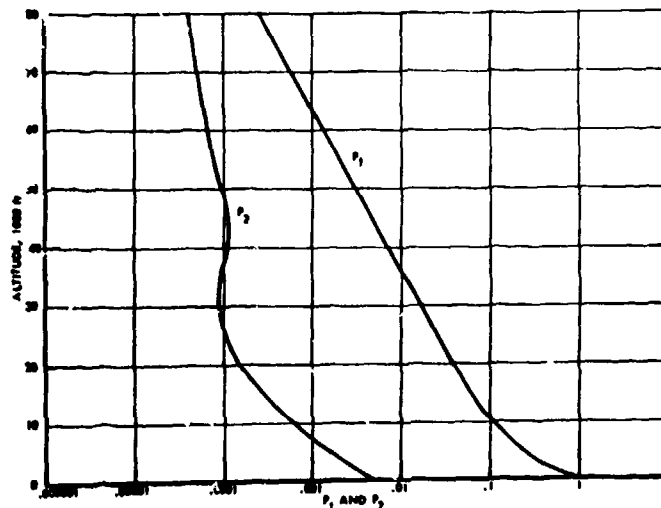


FIGURE 1 P_1 AND P_2 VALUES
(APPENDIX G)

load level must be realistically or conservatively accounted for.

(c) *Mission analysis.* Limit loads must be determined in accordance with the following:

(1) The expected utilization of the airplane must be represented by one or more flight profiles in which the load distribution and the variation with time of speed, altitude, gross weight, and center of gravity position are defined. These profiles must be divided into mission segments or blocks, for analysis, and average or effective values of the pertinent parameters defined for each segment.

(2) For each of the mission segments defined under paragraph (c)(1) of this appendix, values of \bar{A} and N_y must be determined by analysis. \bar{A} is defined as the ratio of root-mean-square incremental load to root-mean-square gust velocity and N_y is the radius of gyration of the load power spectral density function about zero frequency. The power spectral density of the atmospheric turbulence must be given by the equation set forth in paragraph (b)(2) of this appendix.

(3) For each of the load and stress quantities selected, the frequency of exceedance must be determined as a function of load level by means of the equation—

$$N_{ex} = \sum (N_y) \left[P_1 \exp \left(-\frac{y^2}{\bar{A}^2} \right) + P_2 \exp \left(-\frac{y^2}{\bar{A}^2} \right) \right]$$

where—

t = selected time interval.

y = net value of the load or stress.

N_{avg} = value of the load or stress in one-g level flight.

$N(y)$ = average number of exceedances of the indicated value of the load or stress in unit time.

Σ = symbol denoting summation over all mission segments.

N_y, \bar{A} = parameters determined by dynamic analysis as defined in paragraph (c)(2) of this appendix.

P_1, P_2, b_1, b_2 = parameters defining the probability distributions of root-mean-square gust velocity, to be read from Figures 1 and 2 of this appendix.

The limit gust loads must be read from the frequency of exceedance curves at a frequency of exceedance of 2×10^{-8} exceedances per hour. Both positive and negative load directions must be considered in determining the limit loads.

(4) If a stability augmentation system is utilized to reduce the gust loads, consideration must be given to the fraction of flight time that the system may be inoperative. The flight profiles of paragraph (c)(1) of this appendix must include flight with the system inoperative for this fraction of the flight time. When a stability augmentation system is included in the analysis, the effect of system nonlinearities on loads at the limit load level must be conservatively accounted for.

(d) *Supplementary design envelope analysis.* In addition to the limit loads defined by paragraph (c) of this appendix, limit loads must also be determined in accordance with paragraph (b) of this appendix, except that—

(1) In paragraph (b)(3)(i) of this appendix, the value of $U_0 = 85$ fps true gust velocity is replaced by $U_0 = 60$ fps true gust velocity on the interval 0 to 20,000 ft. altitude, and is, linearly decreased to 25 fps true gust velocity at 20,000 ft. altitude; and

(2) In paragraph (b) of this appendix, the reference to paragraphs (b)(3)(i) through (b)(3)(ii) of this appendix is to be understood as referring to the paragraph as modified by paragraph (d)(1).

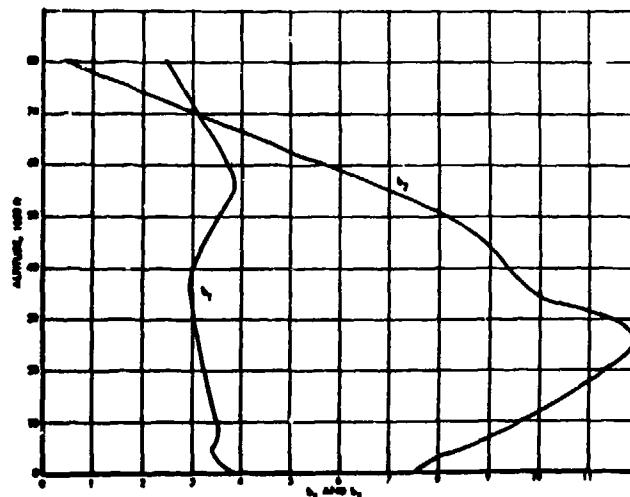


FIGURE 2 b_1 AND b_2 VALUES
(APPENDIX G)

FLIGHT TEST EQUIPMENT FOR THE ON-BOARD MEASUREMENT OF WIND TURBULENCE

by

G.Schünzer and M.Swolinsky
Institute for Guidance and Control
Technical University of Braunschweig
D-3300 Braunschweig, Federal Republic of Germany

and

P.Vörsmann
Aerodata Flugmesstechnik GmbH
D-3300 Braunschweig, Federal Republic of Germany

Abstract

The knowledge of the actual wind and turbulence situation along the flight path of an aircraft is an important factor in the area of meteorological and aeronautical research. In this paper different flight test programs for the on-board implementation of off-line and on-line wind and turbulence measuring systems are presented. The theoretical principle of the determination of all three components of the wind vector is stated. A summary of the installed sensors, the data acquisition systems and computer equipment is represented and the essential effects of sensor errors on the accuracy of wind determination are discussed.

Notation

f_i	sensor parameter
INS	Inertial Navigation System
H	altitude, height
\dot{H}	vertical speed of the aircraft
\ddot{H}	vertical acceleration of the aircraft
L	distance between flight log and inertial navigation system
PCM	Pulse Code Modulation
p_s	static pressure
q	dynamic pressure
\dot{q}	angular velocity about the aircraft y-axis
\dot{r}	angular velocity about the aircraft z-axis
t	time
T_t	total temperature
u_p	North component of true airspeed
u_{kg}	North component of inertial velocity
u_w	North component of the wind vector
\underline{u}	true airspeed vector
v_p	East component of true airspeed
v_{kg}	East component of inertial velocity
\underline{v}_k	inertial velocity
\underline{v}_w	East component of the wind vector
\underline{v}	Wind vector
w_p	vertical component of true airspeed
w_{kg}	vertical component of inertial velocity
w_w	vertical wind component
α	aircraft angle of attack
α_f	flight log angle of attack
β	aircraft angle of sideslip
β_f	flight log angle of sideslip
γ	flight path angle
δ	differential operator
Δ	sensor error or wind component error
Θ	pitch angle
λ	longitude
σ	standard deviation
Σ	sum
φ	latitude
Θ	bank angle
Ψ	true heading
\underline{X}_w	wind direction

1. Introduction

Wind and atmospheric turbulence are essential parts of the weather process. Consequently the measurement of the wind vector and its turbulent fluctuations is the domain of meteorologist for several decades. From aeronautical point of view wind and turbulence are disturbance variables affecting the aircraft dynamic, the load of aircraft and pilot, the passenger comfort and wind shear and downdraft may restrict flight safety especially during take-off and landing. Hence, this meteorological phenomena have to be subject of intensive research in the field of aeronautics, too.

At the Institute for Guidance and Control of the Technical University of Braunschweig different flight test

programs for the wind determination on board of aircraft have been initiated during the last ten years. One of them used an AIRBUS A300 of the DEUTSCHE LUFTHANSA collecting raw data during take-off and landing for the off-line wind calculation (Fig. 1). The experiments demonstrated, that the standard-equipment of an airliner gives sufficient results, if there is performed an extensive and accurate data preparation and fitting [1],[2]. A higher level of accuracy as well as an increase in frequency range can be obtained using a special equipped research aircraft. On board the DO 28 research aircraft (Fig. 2) of the Technical University of Braunschweig an on-line wind and turbulence measuring system has been implemented, which calculates all three components of the wind vector in real time at a sampling rate of 23 Hz [3]. A modified system has been developed in collaboration with the AERODATA Flugmeßtechnik GmbH just now for the second research aircraft of the TU Braunschweig, a DO 128 (Fig. 3), using more powerful computer and sensor systems. The DO 128 is bare also for the flight test of the newest development of AERODATA Flugmeßtechnik GmbH in the field of airborne wind and turbulence measuring systems, the so-called METEOPOD (Fig. 4). This system is installed in a slender body attached under the wing of the research aircraft instead of the auxiliary fuel tank. Its advantage is the high flexibility of the hole wind determination and processing system.

The results of the measuring projects are used to get more information about wind shear and turbulence phenomena, and to perform investigations of the aircraft response. Furthermore it succeeds the development of flight control systems as well as wind and turbulence engineering models for flight simulation and hazard investigation.

2. The principle of on-board wind and turbulence determination

On board of an aircraft wind can not be measured directly. Only by taking the vector difference between the inertial velocity \underline{v}_{kg} and the true airspeed \underline{v} the wind vector \underline{v}_w may be computed (Fig. 5). Following the German Aviation Standard the wind components are defined in the earth-fixed coordinate system as shown in Fig. 6: A wind blowing from the south represents a positive north component u_{wg} , a wind from the west yields a positive east component v_{wg} , and a downdraft indicates a positive vertical wind component. The components expressed in earth-fixed coordinates can be written in the following form:

$$\begin{bmatrix} u_w \\ v_w \\ w_w \end{bmatrix}_g = \begin{bmatrix} u_k \\ v_k \\ w_k \end{bmatrix}_g - \begin{bmatrix} u \\ v \\ w \end{bmatrix}_g \quad (1)$$

with

$$w_{kg} = -\dot{h} \quad (2)$$

and the true airspeed components

$$u_g = V \cdot (\cos\alpha \cdot \cos\beta \cdot \cos\Theta \cdot \cos\Upsilon + \sin\beta \cdot (\sin\Theta \cdot \sin\Theta \cdot \cos\Upsilon - \cos\Theta \cdot \sin\Upsilon) + \sin\alpha \cdot \cos\beta \cdot (\cos\Theta \cdot \sin\Theta \cdot \cos\Upsilon + \sin\Theta \cdot \sin\Upsilon)) \quad (3)$$

$$v_g = V \cdot (\cos\alpha \cdot \cos\beta \cdot \cos\Theta \cdot \sin\Upsilon + \sin\beta \cdot (\sin\Theta \cdot \sin\Theta \cdot \sin\Upsilon + \cos\Theta \cdot \cos\Upsilon) + \sin\alpha \cdot \cos\beta \cdot (\cos\Theta \cdot \sin\Theta \cdot \sin\Upsilon - \sin\Theta \cdot \cos\Upsilon)) \quad (4)$$

$$w_g = V \cdot (-\cos\alpha \cdot \cos\beta \cdot \sin\Theta + \sin\beta \cdot \sin\Theta \cdot \cos\Theta + \sin\alpha \cdot \cos\beta \cdot \cos\Theta \cdot \cos\Theta) \quad (5)$$

The equ. 3-5 are representing the complete computation algorithm for the transformation of the true airspeed components in the earth-fixed coordinate system considering any kind of aircraft manoeuvre [3].

Besides of the inertial velocity components (u_{kg} , v_{kg} , w_{kg}) and the magnitude of the airspeed $|V|$ five angles have to be measured on-board the aircraft: The flow angles of the air relative to the aircraft (α , β) and the attitude data true heading Υ , pitch angle Θ and bank angle Θ . Since the air velocity sensors may not be located near to the sensors for the inertial data, a corrective term $\underline{Q}_p \times \underline{l}$ has to be added, where \underline{Q}_p is the vector of the angular velocity of the aircraft and \underline{l} the distance from the inertial sensors to the air data sensors. For approximate calculations this effect can be expressed by additional terms for the angle of attack and angle of side slip:

$$\alpha = \alpha_f - \Delta\alpha \quad (6)$$

$$\beta = \beta_f - \Delta\beta \quad (7)$$

with

$$\Delta \alpha = -\frac{q \cdot l_x}{V} \quad (8)$$

and

$$\Delta \beta = \frac{r \cdot l_x}{V} \quad (9)$$

where l_x is the longitudinal distance between the inertial data sensors and the air data sensors. The expressions q and r are representing the pitch rate respectively yaw rate of the aircraft, which also have to be measured on-board.

3. The instrumentation and data processing system of the research aircraft

3.1 The measuring system of the AIRBUS A300

The AIRBUS wind shear project started in 1980 [2]. Subject of this research program was the investigation of character, magnitude and frequency of wind variations in the terminal area of airports. One requirement for describing statistical properties of wind shear is to gather data from a large number of take-offs and landings. Due to the medium and short range service of LUFTHANSA AIRBUS A300 in the European and the North African region the high number of operations were guaranteed. The A300 is equipped with a modern Aircraft Integrated Data System for recording numerous signals and sensor outputs about the flight conditions of the aircraft. Most of the required parameters shown in equ. 3-5 were available on-board in one way or another. During normal service air data from the Air Data Computer (ADC) along with other signals is sent to the Flight Data Acquisition Unit (FDAU) which performs the signal processing for the Performance Maintenance Recorder (PMR), see Fig. 7. In order to overcome legal problems in the field of collecting personal data and to consider flight safety aspects, a second FDAU and PMR were installed in parallel to the primary set used by the LUFTHANSA for their maintenance purposes. Hence, an output sequence of 24 parameters with a sampling rate up to 4 Hz could be recorded independently of airline requirements.

One problem was to make the INS-data available for acquisition. On-board no INS-data was processed by FDAU for recording. Thus a special airworthy INS-interface had to be built and installed which converted and reduced the 32 bit serial INS-data bus (ARINC 561) into parallel 12 bit format for the digital input channels of the FDAU. This interface box also was used to house a timer switching the PMR on and off and specific take-off, landing and go-around conditions.

The recorded raw-data have been converted by LUFTHANSA from PCM structure into readable data at the University computer. Here an off-line data processing was performed according to equ. 3-5. But it turned out that an extensive post processing of the raw-data had to be performed, like filtering, wildpoint check and error modelling, to get acceptable accuracy of the results. The problem of influence of sensor errors on the accuracy of wind determination will be pointed out later on.

3.2 The measuring equipment of the DO 28/Do 128 research aircraft

It is easy to realize that a high accuracy of on-board wind determination requires a specifically equipped aircraft. In this case the sensor equipment and its location can be chosen with regard to the specific requirements, and calibration may be performed when ever it is required.

In 1980 the TU Braunschweig acquired the DO 28 aircraft from the BODENSEEWERK Gerätetechnik (BGT) where it was formerly used as a company research aircraft. Since then a CAROUSEL IV Inertial Navigation System, powerful computer hardware and several sensors have been installed. This was a prerequisite for the realization of the on-line wind measuring systems.

The DO 28 computer system consists of two digital computers (Fig. 8). In the main computer, a NORDEN 11/34 (military version of the PDP 11/34), the wind vector is calculated in real time at a sampling rate of 23 Hz. For handling input and output of analog, digital and synchro signals a MUDAS processor designed by DORNIER System is used. This processor also transfers these signals to the main computer. Meteorological data can be viewed during flight on a CRT terminal of the main computer on an alphanumeric cockpit display. For example the average of the wind vector and corresponding aircraft data like position, altitude, heading and flight time can be displayed and may also be selected as output on the printer. Data storage is performed by a PCM recording system, which can sample 32 channels at 92 Hz on one tape recorder. As another quick look feature the flight path and its horizontal wind vector are plotted in real time on an XY-recorder. Fig. 9 shows an example with a ten second average of the wind vector.

The location of the computer and the PCM hardware as well as the location of the essential sensors is illustrated in Fig. 10.

Most parameters, which are required for the wind vector determination can be measured directly except true airspeed and the vertical speed of the aircraft. On-board the DO 28 the vertical speed is synthetically derived by means of complementary filter using the high frequency information of the vertical acceleration signal and low frequency information of the barometric altimeter. This filter obtains a 1-σ accuracy for the vertical speed of the aircraft of about 0.05 m/s [3]. The true airspeed is derived in the ordinary way from dynamic pressure, static pressure and total temperature.

It is planned a medium-term replacement of the DO 28 by the DO 128 research aircraft which has been acquired by the TU Braunschweig in 1985. The DO 128 has an air frame similar to the DO 28. But instead of two piston engines it is equipped with turboprop engines, which give improvements in flight performance and noise abatement.

The airdata sensors are located at the tip of a new designed carbon fibre composite nose boom about 3 m in front of the aircraft nose. Available are the DORNIER flight log or a five-hole probe which can be completed by fixed wind vanes for measurement of the higher frequency turbulent fluctuations (Fig. 11). The eigenfrequency of

the nose boom including the sensor-mass is about 15 Hz. The cutting-off frequency of the fixed wind vanes is roughly 100 Hz. Hence, the lowest turbulence wave length which can be measured by this system has a value of 2 metres.

The inertial data are measured by a strap down inertial navigation system, a Honeywell LASER-NAV. The concept for the data acquisition and processing system, which is implemented at present, is illustrated in Fig. 12. The idea is to realize an integrated navigation system. For the calculation of high accuracy position data a combination of INS-data and data from a Global Position System (working in a differential mode) is projected. Investigation shows that this complementary system also produces a flight path velocity calculation of very high accuracy, which reduces the error in wind determination. The wind determination including the complete coordinate transformation is performed in the main computer, probably a ruggedized Micro-Vax. For data recording a streamer tape recorder is used.

3.3 The AERODATA METEOPOD

The AERODATA Flugmeßtechnik GmbH has developed an aircraft and helicopter pod for application in air pollution and meteorological research. It incorporates an on-board measuring system for wind turbulence and other meteorological parameters. This system integrates the whole sensor equipment (Fig. 13) like 5-hole probe, temperature-, pressure- and humidity-probes, INERTIAL NAVIGATION SYSTEM, radar altimeter, as well as the real time data processing system in a slender body, which may be attached to a pylon under an aircraft wing or at a wire beneath a helicopter. Like the aircraft integrated system of the DO 28/128 the METEOPOD performs real time processing of the wind vector inclusively compensation of the aircraft motion and complete processing of navigation and aircraft data. The specific advantages of METEOPOD are turbulence measurement with a sampling rate of 100 Hz, extremely small distances between the different sensors and exchangeability between aircraft and helicopter. There are no measuring results available up to now, because the in-flight test program with the DO 128 research aircraft starts in October 1987.

4. The effect of errors in measurement on the accuracy of the wind determination

An important factor in estimating errors in measurement and in correcting aircraft wind determination are in-flight calibrations. Completed by specific error models for the 3-dimensional wind determination a far-reaching elimination of sensor errors can be obtained. The error effects are demonstrated by a linear error model, using the north component of the wind vector. The calculated value u_{Wg} consists of the true component u and its error Δu :

$$u_{Wg,c} = u_{Wg} + \Delta u_{Wg} \quad (10)$$

For the total error Δu_{Wg} the following linear model is used:

$$\Delta u_{Wg} = \sum_i \frac{\partial u_{Wg}}{\partial f_i} \Delta f_i \quad (11)$$

The total error of the wind component is the sum of all partial derivatives multiplied with the corresponding sensor error Δf_i . The example in Fig. 14 illustrates the errors of the horizontal wind components caused by errors in true airspeed and angular parameters. These are a function of the SINE and the COSINE of the true heading while of course the error of the vertical wind component does not depend on true heading [3]. As a second general statement can be made that the wind component errors, which are caused by angular parameters, are directly proportional to the true airspeed of the aircraft. This also means an increase in error magnitude of wind speed and direction with increasing true airspeed. Fig. 12 demonstrates this relation for the vertical wind component. It can be seen from this figure, that in the case of level flight ($\gamma, \phi = 0$) only errors in the angles of attack and pitch and an error in the vertical speed of the aircraft contribute to the total error in the vertical wind component.

Because of the error behaviour of the horizontal wind components shown in Fig. 14, a reconstruction of sensor errors or at a combination of sensor errors can be carried out by flying specific flight pattern. Fig. 16 illustrates the calculation of the horizontal wind components respectively the magnitude and wind direction in a standard turn [4]. Curve 1 shows the typical error behaviour. In curve 2 the error effects are eliminated using the above mentioned linear error model. Furthermore this figure demonstrates, that the static sensor errors essentially affect the mean wind accuracy. Whereas the accuracy of the measured turbulent fluctuations are influenced by the sensor dynamic.

5. Samples of flight test results and derived wind models

A lot of wind and turbulence measurement have been carried out by means of the AIRBUS A300 and the DO 28 research aircraft in the field of wind shear investigations, aircraft response on wind and turbulence as well as in the area of meteorological experiments. Flight tests for the in-flight measurement of pollution transport in the atmosphere also have been carried out in the middle of this year. In this case the simultaneous measurement of the wind vector is an important factor for the interpretation of the data. Samples of results of the different research activities will be demonstrated in this chapter.

In Fig. 17 results of the AIRBUS experiment are presented showing wind and temperature profiles in connection

with temperature inversions. On the one hand these examples indicate a significant influence of inversion on wind speed and direction. On the other hand the temperature profile is affecting the intensity of turbulence. There is a much lower turbulence intensity above the inversion layer compared with the region beneath the inversion. Obviously a sample rate of 4 Hz is sufficient to identify these effects.

The next two examples feature research activities in the area of low-level-jet phenomena which have been performed in cooperation with the Institute for Meteorology and Climatology of the University of Hannover. Fig. 18 shows typical profiles of wind speed, direction and temperature of a low-level-jet measured by means of the LUFTHANSA AIRBUS. This wind phenomenon has been found in the northern part of Germany approximately in 10% of all nights [6]. Typical features are:

- a jet like wind profile in connection with intensive ground based temperature inversion
- low turbulence intensity
- horizontal homogeneity of the wind field

Additional measuring points in the diagram originate from mast measurement which have been performed 70 to 100 km distant from the airport Bremen. This underlines the horizontal homogeneity of this phenomenon.

Fig. 19 compares measurements of the DO 28 research aircraft, a meteorological mast and data of a low-level-jet engineering model developed at the Institute for Guidance and Control [6]. The example shows a good agreement of the different measurements and the model. This engineering model has been used for the approximation of numerous measured low-level-jets for hazard investigations. In a similar way modeling of other hazardous wind phenomena like downburst and warm- and cold-fronts has been performed [6].

In general a turbulent wind profile can be separated in a large scale mean wind or trend and a short scale turbulent portion (Fig. 20). The simulation of the complete wind flow field may be synthesized of these two portions. Fig. 21 illustrates the analysis of the turbulent fluctuations and the fitting by the Dryden respectively the v. Karman turbulence model. Subject of this research is the evaluation of relations between the model parameters and meteorological conditions.

The last example relates to DO 28 measurements of the wind situation influenced by a mountain ridge near to Stuttgart airport. Investigations by means of very simple wind model concepts have demonstrated that flight safety may be affected during take-off and go-around by lee-effects of the hill in one-engine-out operation [7]. The measured wind data indicate a much higher hazard level and force to correct the model concepts. Fig. 22 illustrates the results of a take-off simulation with an engine failure at v_{LO} , using measured wind data. The aircraft cannot clear the obstacle on the hill as required under this conditions.

6. Summary

This paper presents the principles of in-flight wind and turbulence determination and the hardware realization of on-board measuring and data processing systems. The results of several measuring projects including tower fly-by and comparison with other reference data show a relative high accuracy in on-board wind computation. The horizontal wind speed is calculated with a precision between 0.5 m/s and 0.7 m/s (1 σ -value). For the vertical wind component a precision of 0.3 m/s can be stated. But high measuring accuracy presumes extensive in-flight calibration as well as the use of specific error models for the compensation of sensor errors. Further increase in precision may be obtained by modification of the measuring equipment, especially by future installation of GPS as an additional sensor system to compensate the bad long term accuracy of the INS-system. First flight tests with different GPS receivers have been performed just now and a research project in this field will be started in 1986.

7. References

- | | | |
|-----|-----------------------------------|---|
| [1] | Krauspe
Swellinsky
Vörsmann | Wind Determination and Wind Shear Detection from Flight Test and Airline Data.
First International Conference on Aviation Weather System, May 4-6, 1981,
Montreal, P.Q., Canada |
| [2] | Swellinsky
Krauspe | Windbestimmung aus Flugmeßdaten eines Linienflugzeuges.
Meteorol. Rdsch. 37, 72-81 (Juni 1984) |
| [3] | Vörsmann | An On-Line Realization for Precise Wind Vector Measurements on Board the
DO 28 Research Aircraft.
14 th ICAS-Congress, Sept. 9-14, 1984, Toulouse, France |
| [4] | Swellinsky
Vörsmann | Windmessungen an Bord des Forschungsflugzeuges DO 28 Skyservant für das
MERKUR-Experiment.
Bericht des Instituts für Flugführung, 1982 |
| [5] | Kettmeier | Die Vertikalstruktur nächtlicher Grenzschichtströmungen.
Thesis at Institut für Meteorologie und Klimatologie, University of Hannover, 1982 |
| [6] | Swellinsky | Wind Shear Models for Aircraft Hazard Investigation.
2nd International Symposium on Aviation Safety, Toulouse, Nov. 1986 |
| [7] | Hahn | Take-off flight path along a lee side of a flat mountain ridge under flight safety
aspects.
2nd International Symposium on Aviation Safety, Toulouse, Nov. 1986 |



Fig.1: Measuring aircraft AIRBUS A 300



Fig.2: The D0 28 research aircraft

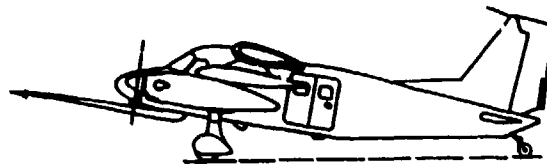


Fig.3: The D0 128 research aircraft



Fig.4: The AERODATA METEOPOD

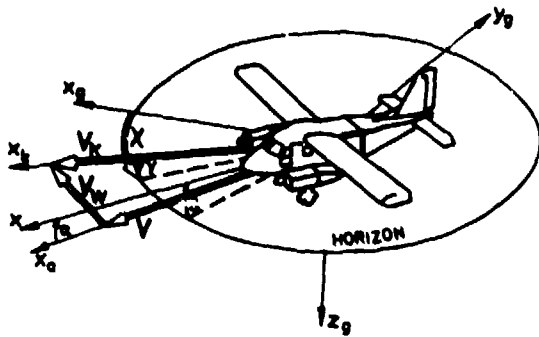


Fig. 5: Determination of the Wind Vector



Fig. 6: Definition of Wind Components

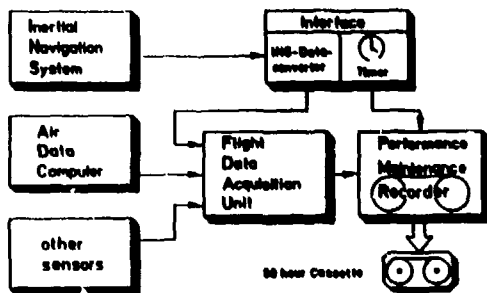


Fig. 7: Wind Shear Acquisition System for Airline Flight Data

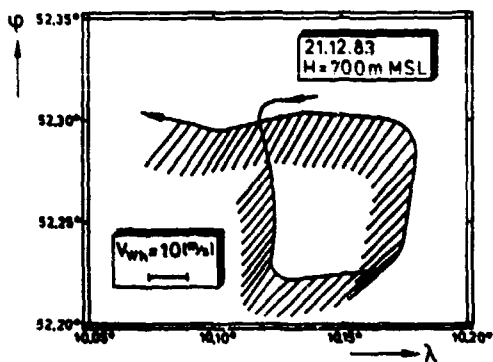


Fig. 9: On-line Flight Path and Wind Vector Plot

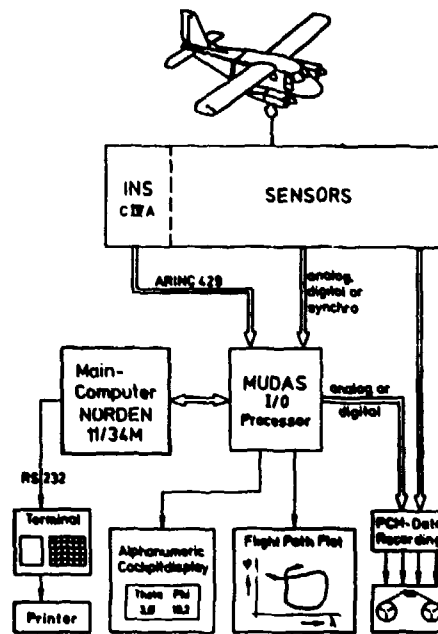


Fig. 8: DO 28 Data Processing System

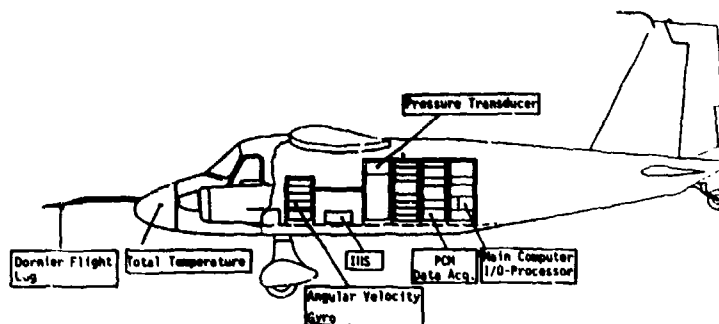


Fig. 10: Hardware Location in the DO 28 Aircraft



DORNIER flight log



Fixed wind vane

Fig. 11: Sensors for air data measurement used in the D0 28/128 aircraft

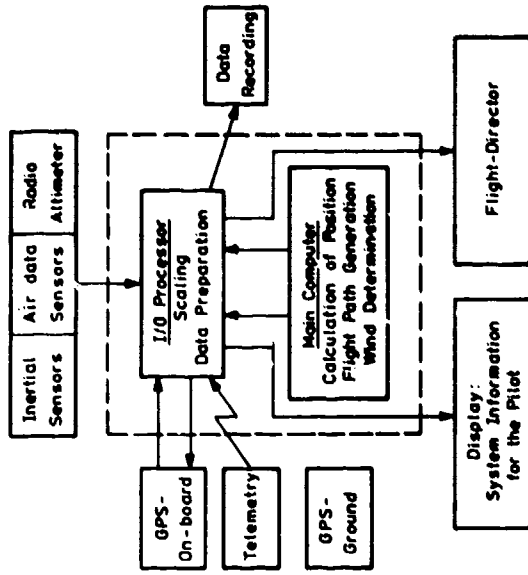


Fig. 12: Concept for the D0 128 Integrated Navigation System

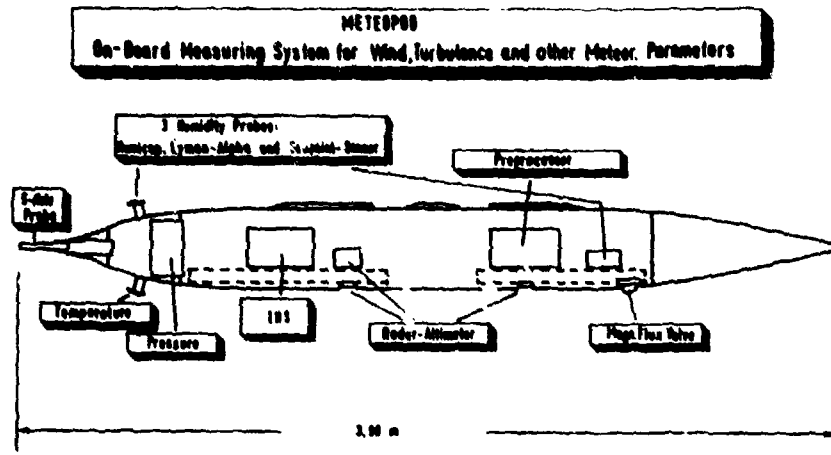


Fig.13: Hardware location in the METEPOD (AERODATA)

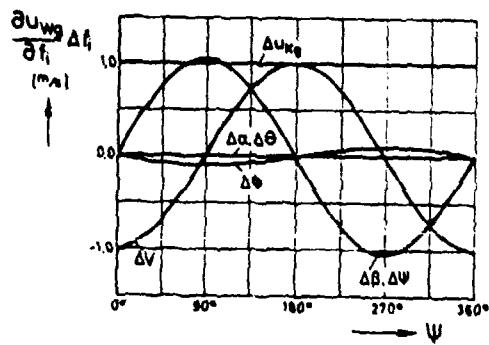


Fig.14: Error of the Northwind Component due to Sensor Errors

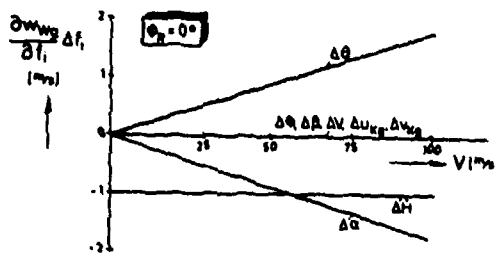


Fig.15: Error of the Vertical Wind Component due to Sensor Errors

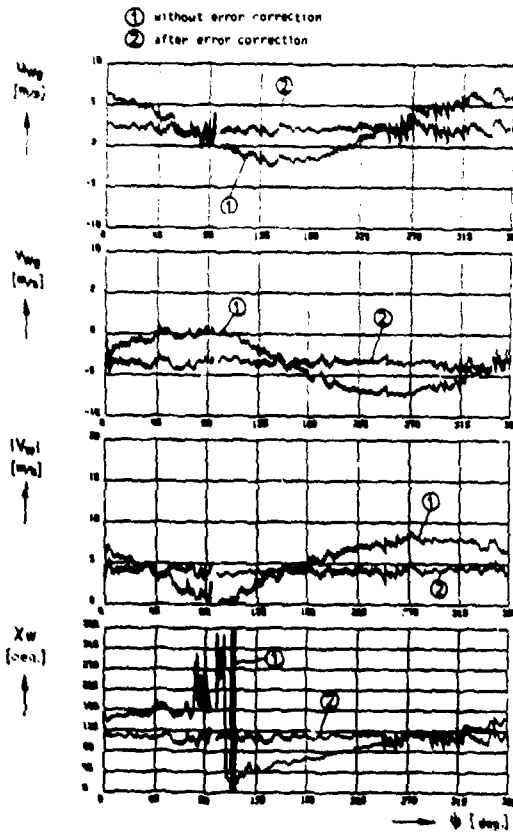


Fig.16: Measurement correction by means of an error model

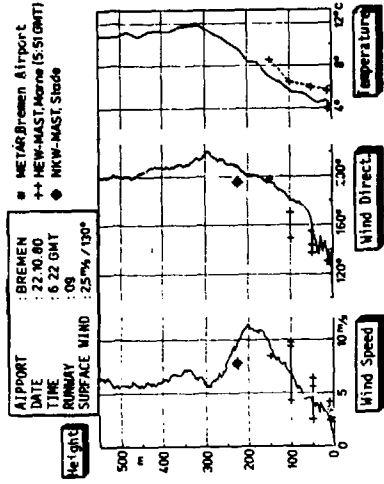


Fig.18: Sample of flight measured low level jet

MAST SPRUMENSEIL 10.08.83 05.43-05.51 MESZ
 00 28 05.42-05.45 MESZ

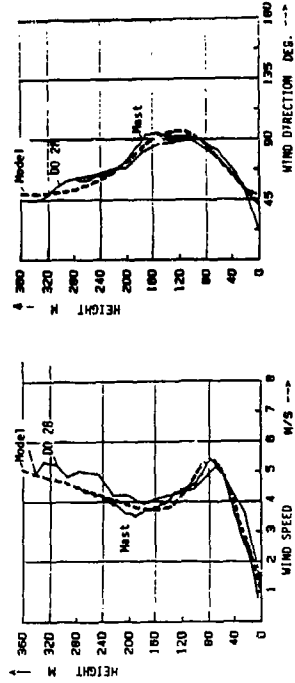


Fig.19: Comparison of aircraft and mast measurement with a low level jet model

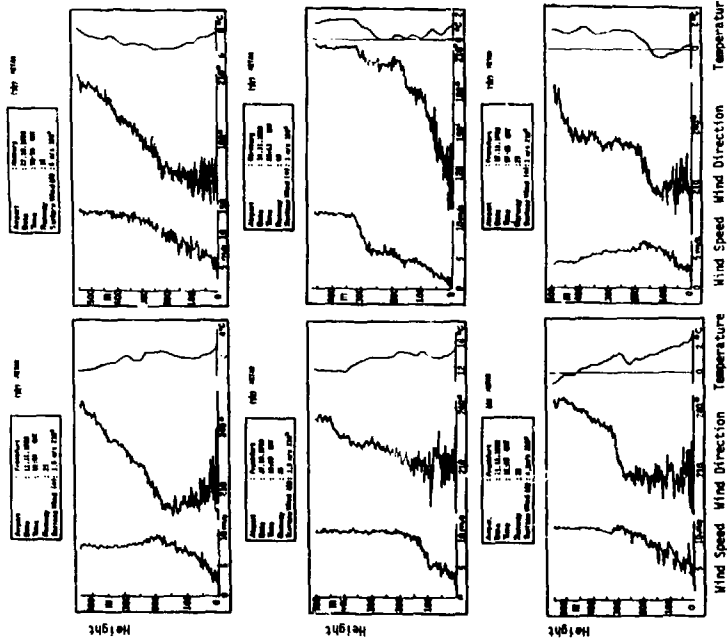


Fig.17: Influence of temperature inversion on wind profile

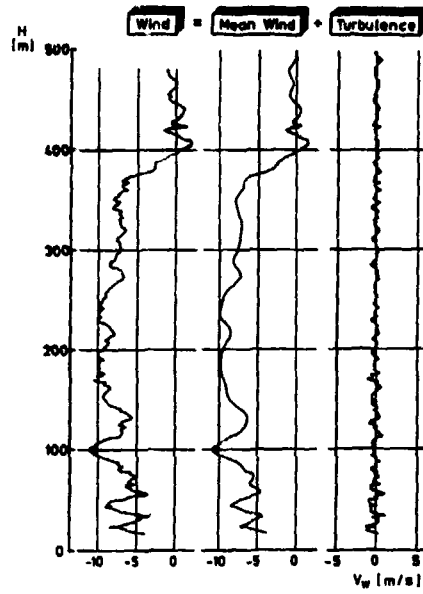


Fig.20: Separation of turbulence and wind shear measured on board

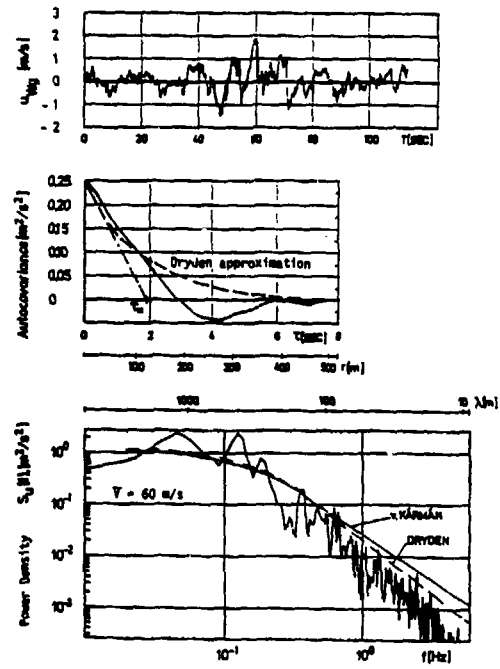


Fig. 21: Autocovariance-function and power spectrum from measurement compared with approximations

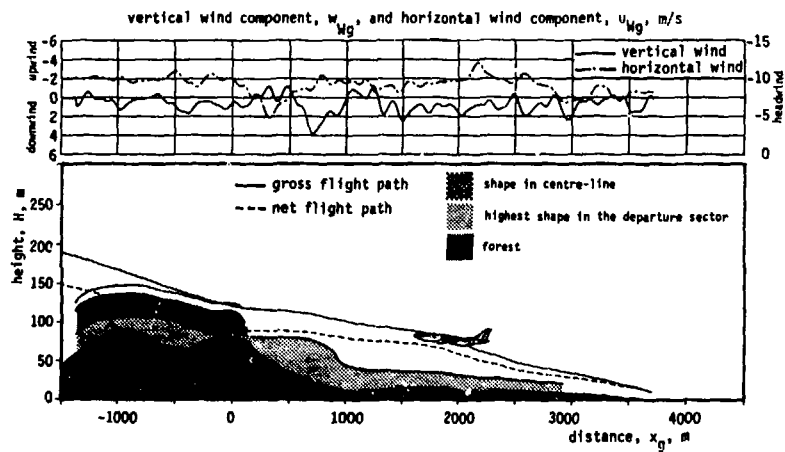


Fig. 22: Take-off path over a hill under the influence of measured wind data

MATCHING P.S.D. - DESIGN LOADS

by
R. Noback
National Aerospace Laboratory NLR
P.O. Box 153, 8300 AD Emmeloord,
The Netherlands

SUMMARY

A method to match loads obtained with the Design Envelope criterion of the P.S.D.-method is presented. Consistent sets of design load conditions can be generated using the correlation coefficients between the loads.

Two of these sets are proposed for practical use.

1. INTRODUCTION

The Power-Spectral-Density (P.S.D.)-method for the calculation of airplane loads is based on the assumption that atmospheric turbulence is a random quasi-stationary Gaussian process, acting as input to a linear system, the airplane. The output, i.e. loads, accelerations, stresses, etc. also are quasi-stationary Gaussian processes.

The calculation of design loads y_{id} with the P.S.D.-method can be based on two criteria as described in references 1 and 2.

The first one is the Design Envelope criterion. The ratio of the standard deviations of the load and turbulence is multiplied with a design value U_{σ} to obtain the design load y_{id} .

$$y_{id} = \bar{A}_1 U_{\sigma} = \frac{\sigma_1}{\sigma_w} U_{\sigma} \quad (1)$$

It should be noted that here and in the following the design load or stress is the load or stress due to turbulence. For the real design value the lg-load has to be added.

The second criterion is the Mission Analysis criterion. The number of exceedances of load level y_1 in a certain flight-segment (k) is calculated with

$$N(y_1)_k = t_k N_{01k} \left\{ P_{1k} \exp\left(-\frac{y_1 - y_{g1k}}{\bar{A}_{1k} b_{1k}}\right) + P_{2k} \exp\left(-\frac{y_1 - y_{g1k}}{\bar{A}_{1k} b_{2k}}\right) \right\} \quad (2)$$

\bar{A}_{1k} is the ratio σ_1/σ_w and N_{01k} is the number of zero crossings of load y_1 pertaining to segment k.

P_{1k} , P_{2k} , b_{1k} and b_{2k} are constants describing the atmospheric turbulence in segment k.

y_{g1k} is the lg-load of load y_1 in segment k.

The total number of exceedances of load level y_1 is obtained by summing Eq. (2) over all flight segments. The design load is defined as the load for which the number of exceedances is equal to the design value N_{des} .

The P.S.D.-method produces the design loads, however not the mutual relation or phasing. If the positive and negative values of these design loads are used to calculate a stress, depending on more than one load, the design stress usually will be overestimated. Besides that the design loads will not be in equilibrium.

Hence a method is needed to combine or match loads such that stresses as calculated with such a combination of loads or design load condition will give a good estimate of the correct values of the stresses.

In the discrete gust case design load conditions usually will be defined as the loads, occurring at the same time, usually at the time that one of the loads is at its maximum or minimum value. Estimates for the stress in a part of the structure can then be calculated for each one of the design load conditions.

The maximum positive or negative value of the stresses thus obtained will be the design stress. It will be clear that this calculated value of the stress will be lower than or just equal to the maximum value of the stress. The stress generally will have its maximum positive or negative value not exactly at the time that one of the loads reaches its design value (see Fig. 1).

A method to generate design load conditions or to match design loads, obtained with the Design Envelope criterion of the P.S.D.-method will be described in this paper. Only the case with two loads will be treated. The derivation for the general case with N loads is given in reference 3, only the results will be given here.

2. CORRELATION AND EQUAL PROBABILITY

In the P.S.D.-method it is assumed that atmospheric turbulence is a quasi-stationary random process, with Gaussian probability-density function (p.d.f.) and with normalized power spectrum ϕ_w^u and standard deviation σ_w . This random process acts as input to a linear system, the aircraft. The outputs, loads and stresses, have the same properties as the input.

The power spectrum of the output y_1 is

$$\phi_{y_1}(w) = \sigma_w^2 |H_{1w}(w)|^2 \phi_w^u(w) \quad (3)$$

The ratio of the standard deviations of output y_1 and input w is

$$\bar{\lambda}_1 = \frac{\sigma_{y_1}}{\sigma_w} = \left[\int_0^\infty |H_{1w}(\omega)|^2 \Phi_w^n(\omega) d\omega \right]^{\frac{1}{2}} \quad (4)$$

$H_{1w}(\omega)$ is the transfer function of output y_1

According to the requirements (Refs. 1 and 2) the design load has to be calculated with

$$y_{1d} = \bar{\lambda}_1 U_\sigma = \bar{\lambda}_1 \frac{U_\sigma}{\sigma_w} \quad (5)$$

U_σ is a design value and is prescribed in the requirements.

The p.d.f. of the load y_1 is

$$p_1(y_1) = \frac{1}{\sqrt{2\pi} \sigma_1} \exp \left\{ -\frac{y_1^2}{2\sigma_1^2} \right\} \quad (6)$$

and it follows that the probability that load y is larger than the design load is

$$P(y_1 > y_{1d}) = \int_{y_{1d}}^\infty p_1(y_1) dy_1 = \frac{1}{2} \left\{ 1 - \operatorname{erf} \left(\frac{U_\sigma / \sigma_w}{\sqrt{2}} \right) \right\} \quad (7)$$

The outputs y_1 and input w are correlated. The correlation coefficient between outputs y_1 and y_j is (see Ref. 3)

$$\begin{aligned} \rho_{1j} &= \frac{R_{1j}(0)}{\sigma_1 \sigma_j} \\ &= \frac{1}{\sigma_1 \sigma_j} \int_0^\infty (H_{1w}(j\omega) H_{jw}^*(j\omega) + H_{1w}^*(j\omega) H_{jw}(j\omega)) \Phi_w(\omega) d\omega \end{aligned} \quad (8)$$

The joint p.d.f. of two loads y_1 and y_2 with correlation coefficient ρ_{12} is

$$P_{12}(y_1, y_2) = \frac{1}{2\pi \sigma_1 \sigma_2 \sqrt{1 - \rho_{12}^2}} \exp \left\{ -\frac{\frac{y_1^2}{\sigma_1^2} - \frac{2\rho_{12} y_1 y_2}{\sigma_1 \sigma_2} + \frac{y_2^2}{\sigma_2^2}}{2(1 - \rho_{12}^2)} \right\} \quad (9)$$

Any combination of loads y_1 and y_2 such that

$$\frac{y_1^2}{\sigma_1^2} - \frac{2\rho_{12} y_1 y_2}{\sigma_1 \sigma_2} + \frac{y_2^2}{\sigma_2^2} = \frac{U_\sigma^2}{\sigma_w^2} (1 - \rho_{12}^2) \quad (10)$$

has the same probability density, namely

$$P_{12}(y_1, y_2) = \frac{1}{2\pi \sigma_1 \sigma_2 \sqrt{1 - \rho_{12}^2}} \exp \left\{ -\frac{U_\sigma^2}{2\sigma_w^2} \right\} \quad (11)$$

It should be noted that Eq. (10) represent an ellipse.

3. DESIGN STRESS AS FUNCTION OF TWO LOADS

It will now be assumed that stress q is a linear function of loads y_1 and y_2 .

$$q = a_1 y_1 + a_2 y_2 \quad (12)$$

The coefficients a_1 and a_2 depend on the dimensions of the structure.

The design value for the stress q can be calculated with

$$q_d = \bar{\lambda}_q U_\sigma \quad (13)$$

in which $\bar{\lambda}_q$ can be expressed as

$$\begin{aligned} \bar{\lambda}_q &= \frac{\sigma_q}{\sigma_w} = \left[\int_0^\infty H_{qw}(j\omega) H_{qw}^*(j\omega) \Phi_w^n(\omega) d\omega \right]^{\frac{1}{2}} \\ &= \left[\int_0^\infty |H_{qw}(\omega)|^2 \Phi_w^n(\omega) d\omega \right]^{\frac{1}{2}} \end{aligned} \quad (14)$$

From Eq. (12) follows

$$H_{qw}(j\omega) = a_1 H_{1w}(j\omega) + a_2 H_{2w}(j\omega) \quad (15)$$

This gives with Eqs. (8) and (14)

$$\begin{aligned} \bar{A}_q^2 &= \frac{\sigma_q^2}{\sigma_w^2} = \int_0^\infty \{ a_1^2 H_{1w}(j\omega) H_{1w}^*(j\omega) + a_1 a_2 H_{1w}(j\omega) H_{2w}^*(j\omega) + \\ &+ a_1 a_2 H_{1w}^*(j\omega) H_{2w}(j\omega) + a_2^2 H_{2w}(j\omega) H_{2w}^*(j\omega) \} \phi_w^D(\omega) d\omega \\ &= (a_1^2 \sigma_1^2 + 2a_1 a_2 \rho_{12} \sigma_1 \sigma_2 + a_2^2 \sigma_2^2) / \sigma_w^2 \end{aligned} \quad (16)$$

It should be noted that stress q is a linear function of the Gaussian processes y_1 . This implies that q also is a Gaussian process with p.d.f.

$$p(q) = \frac{1}{\sqrt{2\pi} \sigma_q} \exp \left\{ -\frac{q^2}{2 \sigma_q^2} \right\} \quad (17)$$

The probability that q is larger than $q_d = \bar{A}_q U_\sigma$ is equal to the probability that load y is larger than $y_{1d} = \bar{A}_q U_\sigma$ (Eq. 7)

$$P(q > q_d) = \frac{1}{2} \left\{ 1 - \operatorname{erf} \left(\frac{U_\sigma \sigma_w}{\sqrt{2}} \right) \right\} \quad (18)$$

The processes $y_1(t)$, $y_2(t)$ and $q(t) = a_1 y_1(t) + a_2 y_2(t)$ are outputs of a system having as input the Gaussian process $w(t)$. It will be clear that if q is equal to its design value q_d , that then y_1 and y_2 can have all values that satisfy

$$a_1 y_1 + a_2 y_2 = q_d \quad (19)$$

It can be shown (see Ref. 3) that the p.d.f. of y_1 under the condition that $q = q_d$, is a Gaussian p.d.f. with mean

$$\bar{y}_1 = \rho_{1q} \sigma_1 \frac{q_d}{\sigma_q} = \rho_{1q} \frac{U_\sigma}{\sigma_w} = \rho_{1q} y_{1d} \quad (20)$$

and standard deviation

$$S_1 = \sigma_1 \sqrt{1 - \rho_{1q}^2} \quad (21)$$

The design load condition, having the highest probability under the condition that q is equal to q_d , is

$$\bar{y}_1 = \rho_{1q} y_{1d} \quad \text{and} \quad \bar{y}_2 = \rho_{2q} y_{2d} \quad (22)$$

The correlation coefficients ρ_{1q} and ρ_{2q} are (Ref. 3)

$$\rho_{1q} = \frac{a_1 \sigma_1 + \rho_{12} a_2 \sigma_2}{\sigma_q} \quad \rho_{2q} = \frac{\rho_{12} a_1 \sigma_1 + a_2 \sigma_2}{\sigma_q} \quad (23)$$

The design load condition as given in Eq. (22) defines the "optimal" design load condition for stress q with coefficients a_1 and a_2 .

The locus of the loads \bar{y}_1 and \bar{y}_2 will now be determined. The loads y_1 and y_2 will be expressed in the non-dimensional form

$$x_1 = \frac{y_1}{y_{1d}} \quad x_2 = \frac{y_2}{y_{2d}} \quad (24)$$

The non-dimensional design loads are

$$\begin{aligned} \bar{x}_1 &= \frac{\bar{y}_1}{y_{1d}} = \rho_{1q} = \frac{n_1 + \rho_{12} n_2}{\sigma_q} \\ \bar{x}_2 &= \frac{\bar{y}_2}{y_{2d}} = \rho_{2q} = \frac{\rho_{12} n_1 + n_2}{\sigma_q} \end{aligned} \quad (25)$$

in which $n_1 = a_1 \sigma_1$
and (see Eq. 16)

$$\sigma_q^2 = n_1^2 + 2 \rho_{12} n_1 n_2 + n_2^2 \quad (26)$$

Eq. (19) becomes with loads \bar{y}_1 and \bar{y}_2

$$\sigma_q = \frac{q_d}{U \sigma / \sigma_w} = n_1 \bar{x}_1 + n_2 \bar{x}_2 \quad (27)$$

Solving Eq. (25) for n_1 and n_2 and inserting the result in Eq. (27) gives the relation between \bar{x}_1 and \bar{x}_2 . The locus of the points (\bar{x}_1, \bar{x}_2) is the ellipse

$$\bar{x}_1^2 + 2 \rho_{12} \bar{x}_1 \bar{x}_2 + \bar{x}_2^2 = 1 - \rho_{12}^2 \quad (28)$$

This equation represents the same ellipse as Eq. (10).

An example is given in figure 2.

Eq. (27) represents the tangent to the ellipse in point (\bar{x}_1, \bar{x}_2) . This point represents the optimal design load condition (Eq. 22).

The distance from the centre of the ellipse to this tangent is

$$D(n_1, n_2) = \frac{\sigma_q}{\sqrt{n_1^2 + n_2^2}} \quad (29)$$

The coefficients n_1 and n_2 , and thus n_1 and n_2 are not known in the design stage. Besides that for various parts of the structure different values of a_1 and a_2 are valid.

All points on the ellipse have the same probability as the optimal design load condition. Suppose that another design load condition is chosen for the calculation of stress q , for example with parameters k_1 and k_2 instead of n_1 and n_2 (see Fig. 2).

$$\begin{aligned} \tilde{x}_1 &= \frac{k_1 + \rho_{12} k_2}{\sigma_k} & \text{or } \tilde{y}_1 &= \frac{k_1 + \rho_{12} k_2}{\sigma_k} \sigma_1 \frac{U \sigma}{\sigma_w} \\ \tilde{x}_2 &= \frac{\rho_{12} k_1 + k_2}{\sigma_k} & \text{or } \tilde{y}_2 &= \frac{\rho_{12} k_1 + k_2}{\sigma_k} \sigma_2 \frac{U \sigma}{\sigma_w} \end{aligned} \quad (30)$$

with

$$\sigma_k^2 = k_1^2 + 2 \rho_{12} k_1 k_2 + k_2^2 \quad (31)$$

The stress that will be obtained with these values of the design load condition is

$$\begin{aligned} q_e &= a_1 \tilde{y}_1 + a_2 \tilde{y}_2 \\ &= \frac{n_1(k_1 + \rho_{12} k_2) + n_2(\rho_{12} k_1 + k_2)}{\sigma_k} \frac{U \sigma}{\sigma_w} \\ &= \sigma_{qe} \frac{U \sigma}{\sigma_w} \end{aligned} \quad (32)$$

The line through the points $(\tilde{x}_1, \tilde{x}_2)$ as defined with the parameter values k_1 and k_2 , and parallel to the tangent as given in Eq. (27) is (see Fig. 2)

$$n_1 \bar{x}_1 + n_2 \bar{x}_2 = \sigma_{qe} \quad (33)$$

The distance from the centre of the ellipse to this line is

$$D(k_1, k_2) = \frac{\sigma_{qe}}{\sqrt{n_1^2 + n_2^2}} \quad (34)$$

It can be shown for $N > 3$ (Ref. 3) and it is easily visible in figure 2, that the estimate σ_{qe} is always smaller than or equal to σ_q , or $q_e \leq q_d$.

From the foregoing can be concluded that combinations of loads y_1 and y_2 can be defined that have an equal probability density. The locus of these design load conditions is an ellipse, that has as a tangent the line representing the relation between the design stress q_d and the loads y_1 and y_2 . Each combination of parameters k_1 and k_2 defines a point on the ellipse and each point on the ellipse defines an estimate $q_e \leq q_d$. One point on the ellipse (the point of contact with the tangent) gives the exact value of q_d .

The locus in the case of N loads in an N -dimensional second order surface, for $N = 3$ an ellipsoid.

4. DESIGN LOAD CONDITIONS

As shown in the previous paragraph any point on the ellipse can be chosen to represent an equal probability design load condition. As in the case of the discrete gust design load conditions, care must be taken to choose meaningful conditions (for example in the discrete gust case, those conditions for which one of the loads attains its maximum or minimum value).

Two sets of design load conditions will be proposed for practical use. The first one, the correlated design load condition is comparable to the discrete gust case, where maximum loads are combined with the loads occurring at the same time. The design load conditions in the discrete gust case will produce relatively low estimates of the design stress if the phase differences between the loads are large. The same will be true for the correlated design load conditions if the correlation coefficients are small. Therefore a second set of design load conditions, the "eigen-vector" loads is proposed.

1. Correlated design load conditions

Each design load condition consists of one design load plus the correlated values of the other loads. This is analogous to the discrete gust case, where each design load condition is composed of one design load plus the values of the other loads at the same time that the first load reaches its maximum value (see Fig. 1).

The two design load conditions can be generated with:

$$\begin{array}{ccc} & \text{condition 1} & \text{condition 2} \\ k_1 & 1 & 0 \\ k_2 & 0 & 1 \end{array} \quad (35)$$

The result is

$$\begin{array}{ll} \bar{y}_{11} = y_{1d} & \bar{y}_{21} = \rho_{12} y_{1d} \\ \bar{y}_{12} = \rho_{12} y_{2d} & \bar{y}_{22} = y_{2d} \end{array} \quad (36)$$

The correlated design load conditions for N loads are

$$\bar{y} = \begin{array}{c|cccc} \text{condition} & 1 & 2 & 3 & \dots\dots N \\ \hline & y_{1d} & \rho_{12} y_{1d} & \rho_{13} y_{1d} & \dots\dots\dots \\ \rho_{12} y_{2d} & & y_{2d} & \rho_{23} y_{2d} & \dots\dots\dots \\ \rho_{13} y_{3d} & & \rho_{23} y_{3d} & y_{3d} & \dots\dots\dots \\ \rho_{14} y_{4d} & & & & \dots\dots\dots \\ \rho_{1N} y_{Nd} & & \rho_{2N} y_{Nd} & & \dots\dots\dots y_{Nd} \end{array} \quad (37)$$

2. Eigen-vector design load conditions

The second set of design load conditions will be defined as the loads that are represented by the end points of the main axes of the ellipse.

These points can be determined using eigen-values and eigen-vectors of the matrix R with the correlation coefficients. This will be shown for the 2-dimensional case.

The eigen-vector κ_1 is defined with the set of equations

$$\kappa_1 + \rho_{12} \kappa_2 + \dots = \lambda \kappa_1 \quad (38a)$$

$$\rho_{12} \kappa_1 + \kappa_2 + \dots = \lambda \kappa_2 \quad (38b)$$

The values of κ define the direction of the main axes.

λ is a scale factor.

This set of equations has a solution only if the determinant is equal to zero.

$$\begin{vmatrix} 1-\lambda & \rho_{12} & \dots \\ \rho_{12} & 1-\lambda & \dots \\ \dots & \dots & \dots \end{vmatrix} = 0 \quad (39)$$

This is an N^{th} order equation in λ , giving N roots or eigen-values λ_1 . For N = 2 follows

$$\lambda_1 = 1 + \rho_{12} \quad \lambda_2 = 1 - \rho_{12} \quad (40)$$

Inserting these solutions in Eq. (38) gives

$$\text{for } \lambda_1: \kappa_{11} = \kappa_{12} \quad (41)$$

$$\text{for } \lambda_2: \kappa_{21} = -\kappa_{22}$$

The normalised eigen-vectors will now be used to define the design load

$$\begin{array}{ll} k_{11} = \frac{\kappa_{11}}{\sqrt{\kappa_{11}^2 + \kappa_{12}^2}} = \frac{1}{\sqrt{2}} & k_{21} = \frac{\kappa_{21}}{\sqrt{\kappa_{21}^2 + \kappa_{22}^2}} = -\frac{1}{\sqrt{2}} \\ k_{12} = \frac{\kappa_{12}}{\sqrt{\kappa_{11}^2 + \kappa_{12}^2}} = \frac{1}{\sqrt{2}} & k_{22} = \frac{\kappa_{22}}{\sqrt{\kappa_{21}^2 + \kappa_{22}^2}} = \frac{1}{\sqrt{2}} \end{array} \quad (42)$$

The design load conditions become (see Eq. 30)

$$\begin{array}{ll} \bar{y}_{11} = \frac{k_{11} + \rho_{12} k_{12}}{\sigma_{k1}} y_{1d} & \bar{y}_{21} = \frac{k_{21} + \rho_{12} k_{22}}{\sigma_{k2}} y_{1d} \\ \bar{y}_{12} = \frac{\rho_{12} k_{11} + k_{12}}{\sigma_{k1}} y_{2d} & \bar{y}_{22} = \frac{\rho_{12} k_{21} + k_{22}}{\sigma_{k2}} y_{2d} \end{array} \quad (43)$$

It can be proven that $\sigma_{k1}^2 = \lambda_1$ (Ref. 3).

For the 2 dimensional case:

$$\begin{aligned}\sigma_{k1}^2 &= k_{11}^2 + 2 \rho_{12} k_{11} k_{12} + k_{12}^2 = 1 + \rho_{12} (= \lambda_1) \\ \sigma_{k2}^2 &= k_{21}^2 + 2 \rho_{12} k_{21} k_{22} + k_{22}^2 = 1 - \rho_{12} (= \lambda_2)\end{aligned}\quad (44)$$

From equations (38a and b) follows

$$\begin{aligned}k_{11} + \rho_{12} k_{12} &= \lambda_1 k_{11} & k_{21} + \rho_{12} k_{22} &= \lambda_2 k_{21} \\ \rho_{12} k_{11} + k_{12} &= \lambda_1 k_{12} & \rho_{12} k_{21} + k_{22} &= \lambda_2 k_{22}\end{aligned}\quad (45)$$

These results inserted in Eq. (43) gives

$$\begin{aligned}\bar{y}_{11} &= \sqrt{\lambda_1} k_{11} y_{1d} & \bar{y}_{21} &= \sqrt{\lambda_2} k_{21} y_{1d} \\ \bar{y}_{12} &= \sqrt{\lambda_1} k_{12} y_{2d} & \bar{y}_{22} &= \sqrt{\lambda_2} k_{22} y_{2d}\end{aligned}\quad (46)$$

or

$$\begin{aligned}\bar{y}_{11} &= \sqrt{\frac{1+\rho_{12}}{2}} y_{1d} & \bar{y}_{21} &= -\sqrt{\frac{1-\rho_{12}}{2}} y_{1d} \\ \bar{y}_{12} &= \sqrt{\frac{1+\rho_{12}}{2}} y_{2d} & \bar{y}_{22} &= \sqrt{\frac{1-\rho_{12}}{2}} y_{2d}\end{aligned}\quad (47)$$

The eigen-vector design load conditions for N loads are with κ as the normalised eigen-vector:

condition	1	2	N
$\bar{y} =$	$\sqrt{\lambda_1} \kappa_{11} y_{1d}$	$\sqrt{\lambda_2} \kappa_{21} y_{1d}$	$\dots \dots \dots \sqrt{\lambda_N} \kappa_{N1} y_{1d}$
	$\sqrt{\lambda_1} \kappa_{12} y_{2d}$	$\sqrt{\lambda_2} \kappa_{22} y_{2d}$	$\dots \dots \dots \sqrt{\lambda_N} \kappa_{N2} y_{2d}$
	$\sqrt{\lambda_1} \kappa_{13} y_{3d}$	$\sqrt{\lambda_2} \kappa_{23} y_{3d}$	$\dots \dots \dots \sqrt{\lambda_N} \kappa_{N3} y_{3d}$
	$\dots \dots \dots$	$\dots \dots \dots$	$\dots \dots \dots$
	$\sqrt{\lambda_1} \kappa_{1N} y_{Nd}$	$\sqrt{\lambda_2} \kappa_{2N} y_{Nd}$	$\dots \dots \dots \sqrt{\lambda_N} \kappa_{NN} y_{Nd}$

(48)

The design load conditions are presented in figure 3. The point opposite to the ones defined above produce the same design load conditions, however with opposite sign.

The design load conditions as defined have special properties. When the design is finished and the dimensions have been defined it is then possible to calculate the correct value of the stress $q = q_d$. Of course the correct value can be calculated also with Eq. (16), using the σ_i and ρ_{ij} values. Assuming, however, that only the design load conditions are available to the stress office, the design-stresses can be calculated with the following rules.

a. Using the estimates q_{ei} of the stress as calculated with the correlated design load conditions. The square of the design-stress q_d is equal to the sum of the products of the i-th estimate and the stress due to the i-th design-load.

$$q_d^2 = \sum a_i y_{id} q_{ei} \quad (49)$$

The estimates q_{ei} in the 2-dimensional case are

$$\begin{aligned}q_{e1} &= a_1 y_{1d} + a_2 \rho_{12} y_{2d} \\ q_{e2} &= a_1 \rho_{12} y_{1d} + a_2 y_{2d}\end{aligned}\quad (50)$$

Inserting this in Eq. (49) and using Eqs. (5), (13) and (16) proves the rule for the 2-dimensional case.

b. Using the estimates of the stress as calculated with the eigen-vector design load conditions

The square of the stress q_d is equal to the sum of the squares of the estimates

$$q_d^2 = \sum q_{ei}^2 \quad (51)$$

The estimates q_{e1} in the 2-dimensional case are

$$q_{e1} = a_1 \sqrt{\frac{1 + \rho_{12}}{2}} y_{1d} + a_2 \sqrt{\frac{1 + \rho_{12}}{2}} y_{2d} \quad (52)$$

$$q_{e1} = -a_1 \sqrt{\frac{1 - \rho_{12}}{2}} y_{1d} + a_2 \sqrt{\frac{1 - \rho_{12}}{2}} y_{2d}$$

Inserting this in Eq. (51) and using Eqs. (5), (13) and (16) proves the rule for the 2-dimensional case.

Proofs for these rules for the N-dimensional case are given in reference 3.

It also is possible to define design load conditions that provide a lower and an upper limit for stress q_d . These conditions are described in Appendix A.

5. DISCUSSION AND CONCLUSIONS

It has been shown that it is possible to generate equal probability design load conditions using P.S.D.-design loads obtained with the Design Envelope criterion, and the correlation coefficients between these loads. The correlation coefficients can be calculated easily together with the \bar{A} -values.

The matrix of correlation coefficients can be used to define an N-dimensional surface. For the 2-dimensional case this surface reduces to an ellipse. Each point on the surface defines an equal probability design load condition. It can be shown (Ref. 3) that such a condition is in equilibrium.

Each design load condition can be used to calculate an estimate for the stress in a point of the structure. Each estimate is lower than the correct value. Only one point on the N-dimensional surface represents a design load condition, that will give the correct value of the stress.

Two sets of N design load conditions are proposed for practical use. They have been chosen such that it can be expected that at least one of the estimates will deviate not too much from the correct value. This however can not be guaranteed. Fortunately the chosen sets of design load conditions both have the property that the correct value of the stress can be calculated, using the estimates. This knowledge can then be used to redefine the dimensions. Note that with the discrete gust method such a check is not possible.

The method also can be used to generate design load conditions for the complete structure, for example the wing. A problem arises if stresses have to be calculated for a section of the structure for which the design values of the loads and the correlation coefficients have not been calculated. It then seems a logical approach to interpolate within a design load condition. This however leads to inconsistent values of both loads and stresses in that section.

The same problem arises in a discrete gust analysis if the design load conditions are defined as the loads occurring at the same time. This problem is discussed in more detail in reference 3. A possible solution is to interpolate between the corresponding design loads and correlation coefficients of the adjoining sections.

A number of hints, that may be useful in the application of the method is given in reference 4. The methods for the determination of equal probability design load conditions can not be used if the loads are obtained with the Mission Analysis. The correlation coefficients in that case are not defined. However it is possible to approximate the equal probability design load conditions. The correlated design load conditions in that case consist of the median value of the loads under the condition that one of the loads exceeds its design value. The derivation and also the application is rather involved. A description is given in reference 3.

The support of the Netherlands Agency for Aerospace Programs (NIVR) for this investigation is gratefully acknowledged.

6. REFERENCES

- [1] Anon.; Federal Aviation Regulations-Part 25 Airworthiness Standards: Transport Category Airplanes, Department of Transportation - Federal Aviation Administration, Washington DC.
- [2] Anon.; Joint Airworthiness Requirements, JAR-25, Large Airplanes, Civil Aviation Authority, Cheltenham.
- [3] R. Noback; The generation of equal probability design load conditions, using P.S.D.-techniques, NLR TR 85014 U, 23-I-1985.
- [4] R. Noback; How to generate equal probability design load conditions, NLR TR 86060 U, 5-XII-1985.

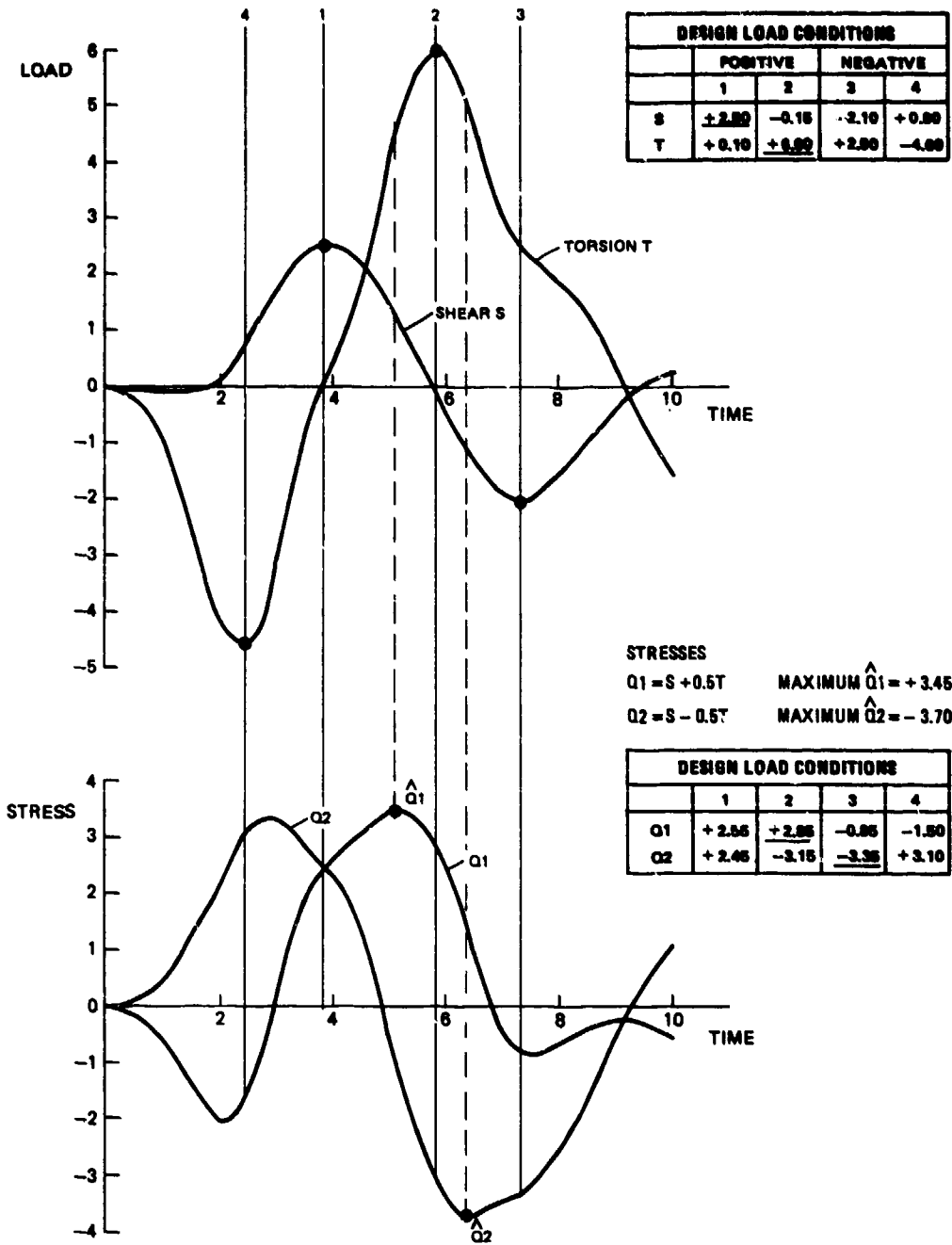


Fig. 1 Example. Stresses as function of shear and torsion

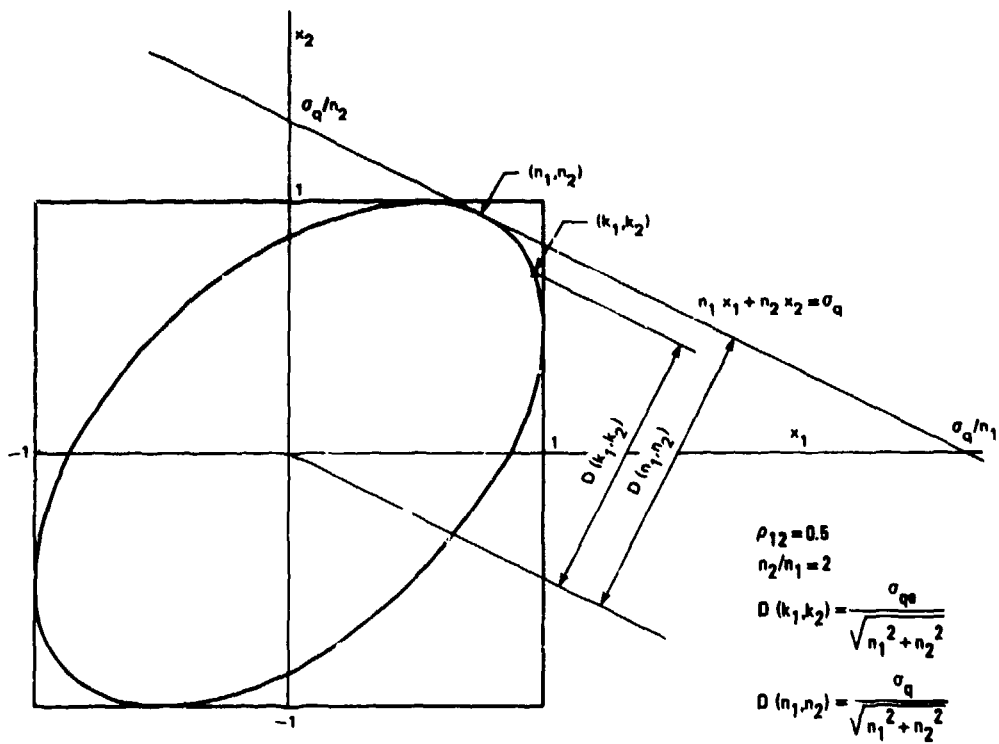


Fig. 2 Equal probability ellipse

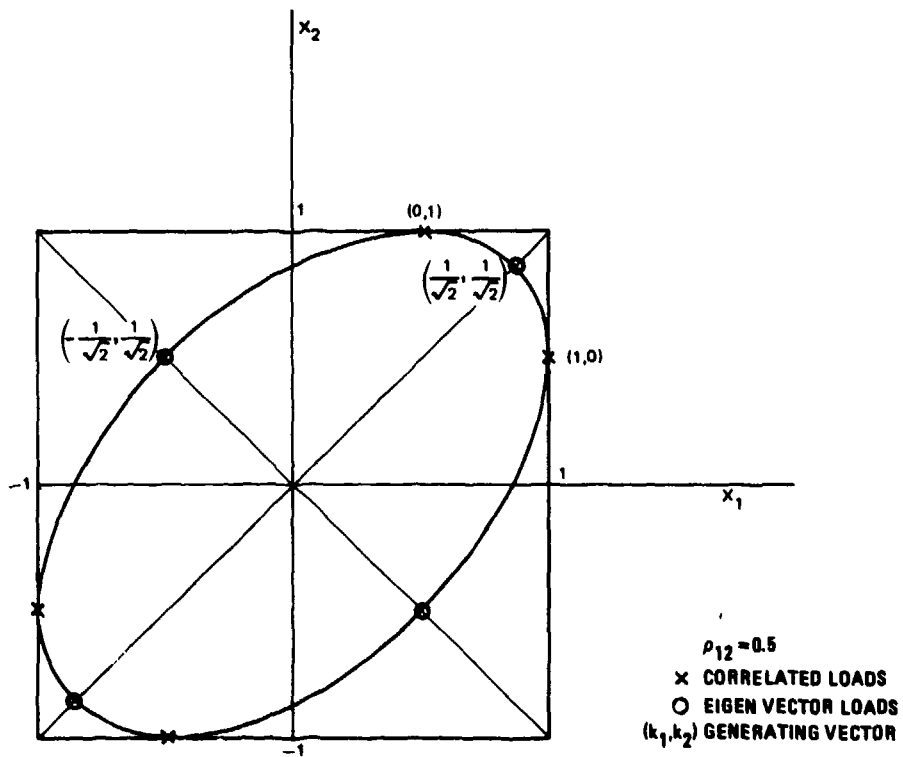


Fig. 3 Design load conditions

APPENDIX A Upper and lower limit design load conditions

One possible set of design load conditions that will produce conservative estimates of the stress, consists of the combinations of positive and negative values of the design loads. The estimate of the stress calculated with these design load conditions (d.l.c.) will be (much) higher than the correct value of the stress q_d .

In the following will be shown that it is possible to define d.l.c. that produce at least one value for the stress larger than q_d , but generally much lower than those obtained with the design loads. The maximum possible error can be established. Using this result, d.l.c. will be defined that give a lower limit for stress q_d .

The proposed conservative d.l.c. are based on the eigen-vector d.l.c. In the case of N loads also N eigen-vector d.l.c. are defined. The conservative d.l.c. in this case consist of N sets, each consisting of 2 to the power $N-1$ d.l.c.

The m -th set is equal to the m -th eigen-vector d.l.c. plus or minus a fraction c of each of the other eigen-vector d.l.c. The k -th d.l.c. of this set can be presented in vector notation with \bar{y}_j as the j -th eigen-vector d.l.c., as

$$y_{mk} = c \sum_{j=1}^{m-1} \pm \bar{y}_j + \bar{y}_m + c \sum_{j=m+1}^N \pm \bar{y}_j \quad (A1)$$

The k -th d.l.c. is defined with one of the possible 2^{N-1} combinations of plus and minus signs.

The stress due to an eigen-vector d.l.c. is

$$q_{ej} = \sum_{i=1}^N a_i \bar{y}_{ji} = a^T \cdot \bar{y}_j \quad (A2)$$

and it follows that the stress due to the d.l.c. of Eq. (A1) is

$$q_{emk} = c \sum_{j=1}^{m-1} \pm q_{ej} + q_{em} + c \sum_{j=m+1}^N \pm q_{ej} \quad (A3)$$

The maximum estimate for the stress, as produced by the m -th set is equal to

$$q_{em} = c \sum_{j=1}^{m-1} |q_{ej}| + |q_{em}| + c \sum_{j=m+1}^N |q_{ej}| \quad (A4)$$

One of the estimates q_{em} will be the largest one. Without loss of generality it can be assumed that it is the estimate of the first set, hence

$$q_{e1} \geq q_{em} \quad m = 2, N \quad (A5)$$

It follows that

$$q_{e1} = |q_{e1}| + c \sum_{j=2}^{m-1} |q_{ej}| + c |q_{em}| + c \sum_{j=m+1}^N |q_{ej}| \geq$$

$$c |q_{e1}| + c \sum_{j=2}^{m-1} |q_{ej}| + |q_{em}| + c \sum_{j=m+1}^N |q_{ej}| = q_{em}$$

or

$$|q_{e1}| \geq |q_{em}| \quad \text{if } c < 1 \quad (A6)$$

It will now be shown that the estimate q_{e1} is a conservative estimate for certain values of c . The square of q_{e1} is

$$q_{e1}^2 = q_{e1}^2 + 2c |q_{e1}| \sum_{j=2}^N |q_{ej}| + c^2 \left(\sum_{j=2}^N |q_{ej}| \right)^2$$

$$= \sum_{j=1}^N q_{ej}^2 - \sum_{j=2}^N q_{ej}^2 + 2c \sum_{j=2}^N (|q_{e1}| - |q_{ej}|) \cdot |q_{ej}| + 2c \sum_{j=2}^N q_{ej}^2$$

$$+ c^2 \sum_{j=2}^N q_{ej}^2 + c^2 \sum_{j=2}^N |q_{ej}| \sum_{i=2}^N |q_{ei}| \quad \text{with } i \neq j \quad (A7)$$

The sum of the squares of the estimates $|q_{e1}|$ of the eigen-vector d.l.c. is equal to the square of stress q_d and it follows that

$$q_{e1}^2 = q_d^2 + E \quad (A8)$$

with

$$E = (2c - 1 + c^2) \sum_{j=2}^N q_{ej}^2 +$$

$$+ 2c \sum_{j=2}^N (|q_{e1}| - |q_{ej}|) \cdot |q_{ej}| + c^2 \sum_{j=2}^N |q_{ej}| \sum_{i=2}^N |q_{ei}| \quad (A9)$$

The relative error is

$$\frac{q_{e1} - q_d}{q_d} = \sqrt{1 + \frac{F}{c^2}} - 1 = \sqrt{1 + F} - 1 \quad (A10)$$

$$\text{with } F = \frac{E}{c^2} = \frac{E}{c^2 q_{e1}^2} \quad (A11)$$

This value should be positive, but as small as possible. The last term of Eq. (A9) is positive. The second term is positive for $c > 0$, because $|q_{e1}| \geq |q_{e2}|$. The first term is zero or positive if

$$2c - 1 + c^2 \geq 0 \quad \text{or } c \geq \sqrt{2} - 1 \quad (A12)$$

This also turns out to be the lowest allowable value of c . Assume that $q_{e1} = 0$, except for $j = 1$ and 2. The third (positive) term of Eq. (A9) is equal to zero and this equation becomes

$$E = (2c - 1 + c^2) q_{e2}^2 + 2c (|q_{e2}| |q_{e1}| - q_{e2}^2) \\ = - (1 - c^2) q_{e2}^2 + 2c |q_{e1}| |q_{e2}| \quad (A13)$$

The ratio $|q_{e2}|/|q_{e1}|$ ranges from zero to one and it follows that E and thus F are positive if c is equal to $\sqrt{2} - 1$.

The maximum value for F is obtained as follows. Assume that the derivatives $\partial F/\partial q_{e_j}$ ($j = 2, N$) are established. Then for symmetry reasons the extreme value if it exists, will occur at $q_{e2} = q_{e3} = \dots = q_{eN}$.

Inserting this result in Eq. (A9) and (A14) and taking the derivative $\partial F/\partial q_{e2}$, taking into account that $c = \sqrt{2} - 1$ it is found that

$$q_{e2} = q_{e3} = \dots = q_{eN} = c q_{e1} \quad (A14)$$

This result inserted in Eq. (A9) and (A11) gives

$$F = (N-1) c^2 \quad (A15)$$

and it follows that

$$0 \leq F \leq (N-1) c^2 \quad (A16)$$

In the table the number of estimates and the maximum possible relative errors are given for some values of N

N	number of estimates		maximum relative error $\sqrt{1+F}-1$
	correlated + eigen-values	conservative $N \cdot 2^{N-1}$	
2	4	4	0.0824
3	6	12	0.1589
4	8	32	0.2307
5	10	80	0.2986
6	12	192	0.3630

The conservative design load conditions as defined in Eq. (A1) with $c = \sqrt{2} - 1$ produce an upper limit for stress q_d . It is now also possible to define a lower limit for stress q_d .

From Eq. (A10) and (A16) follows

$$q_d \leq \bar{q}_e \leq q_d \sqrt{1+F} \quad (A17)$$

\bar{q}_e is the maximum estimate obtained with the upper limit d.l.c.. Eq. (A17) can be written as

$$\frac{q_d}{\sqrt{1+F}} \leq \frac{\bar{q}_e}{\sqrt{1+F}} \leq q_d \quad (A18)$$

and thus

$$\bar{q}_e = \frac{q_d}{\sqrt{1+F}} \leq q_d \leq \bar{q}_e \quad (A19)$$

The lower limit \bar{q}_e for q_d can be obtained with the lower limit d.l.c. (see Eq. A1)

$$\bar{y}_{ml} = \frac{1}{\sqrt{1+F}} y_{ml} \quad (A20)$$

It can be shown that the points representing the lower limit d.l.c. are located on the N -dimensional second order surface representing the locus of the equal probability d.l.c.. The upper and lower limit d.l.c. for the case $N = 2$ are shown in figure A1.

The correct value for q_d can be expressed as a function of the estimates. It can be shown that

A SUMMARY OF METHODS FOR ESTABLISHING AIRFRAME DESIGN LOADS FROM CONTINUOUS GUST DESIGN CRITERIA

Richard N. Moon
Design Specialist Senior
Dynamic Loads
Lockheed Aeronautical Systems Company
P.O. Box 551, Burbank, CA 91520 USA

SUMMARY

Continuous gust design criteria for airframe design are specified in FAR 25, JAR-25 and various United States military specifications. Two forms of criterion, the design envelope approach and the mission analysis, are usually referenced as "an acceptable means of compliance." However, these criteria do not provide methods of applying the statistical results to the design of the structure. Development of such methods is left to the imagination of the airframe manufacturer, subject to the approval of the certifying agency. Some of the methods that are currently used by United States airframe manufacturers are summarized here. Continuous gust design requirements from various certifying agencies are reviewed. A brief discussion is also provided on the methods employed to include the effect of the L-1011 Tristar active-controls wing load alleviation system on the loads due to corrective roll control in turbulence.

INTRODUCTION

This paper is composed of three related sections.

First, a brief review is provided of continuous turbulence requirements specified by various certifying agencies. It is the purpose of this review to provide background material for the reader. Design gust load continuous turbulence psd requirements are quite consistent in their essential aspects among all certifying agencies. Discussion of some of the underlying concepts that contributed to current design gust criteria is included. Much of the discussion reflects the work of Frederic M. Hoblit as presented in a pre-publication version of Reference 1. Mr. Hoblit was the Lockheed-California Company lead engineer on the FAA contract during 1964 - 1966 that resulted in report FAA-ADS-53, which provides the basis for current continuous turbulence gust loads requirements.

The second part of this paper deals with the problem of applying continuous turbulence design criteria to the design and sizing of structure. In short, what do you do with psd statistical parameters after you have them? There has been very little written with respect to practical application. A summary of some of the methods used by United States airframe manufacturers is presented. These methods are dependent on the nature of the airplane to be analyzed (similarity to prior designs and anticipated operation), the criticality of the structure to gust loading, and the complexity of the structure. Different methods are often applied by the same manufacturer in the analysis of different airplane configurations, or for that matter, for different components of the same airplane. Because a mixture of procedures is likely to be used by all companies, these methods are not associated with a single company, but are presented as a composite.

As the use of active controls becomes more prominent in modern aircraft design, the adequacy of the continuous gust design criteria and the associated methods of assuring adequate strength become of concern. The last section of this paper provides a summary of the studies that were performed to include the effects of the Lockheed L-1011 Tristar active control system on the determination of gust loads. The active control system developed for the L-1011 Tristar included a wing load alleviation system. Although wing loads due to gust were significantly reduced, loads due to corrective roll control in turbulence were unaffected and, as a result, became significant. Considerable modification of the standard psd design gust procedures was required to account for this effect.

REVIEW OF CRITERIA

The FAA incorporated explicit continuous turbulence power-spectral gust loads criteria into Appendix G of FAR 25, Reference 2, in September of 1980. These criteria were the result of nearly 20 years of study involving close coordination between the FAA and the manufacturers.

The first attempt to develop a comprehensive set of power-spectral gust loads criteria that had general applications was the study conducted by Lockheed-California Company in 1964 - 1966, under contract to the FAA. This study produced two reports; FAA-ADS-53, "Development of a Power-Spectral Gust Design Procedure for Civil Aircraft," Reference 3, and the companion report from Boeing, FAA-ADS-54, Reference 4. The criteria formulated in FAA-ADS-53 were immediately recognized by the FAA as an "acceptable means of compliance" with the requirements of FAR 25.305(d). At that time the only requirement was that "The dynamic response of the airplane to vertical and lateral continuous turbulence must be taken into account."

FAA-ADS-53 provided the basis for the current Appendix G to FAR 25, and for that matter, it provided the basis for all current continuous turbulence criteria regardless of the certifying agency. The primary difference between the criteria prescribed in FAA-ADS-53 and current criteria are in the specified design gust velocities and their variation with altitude.

European civil regulations as of January 1987 are specified in JAR-25, Reference 5. The continuous gust psd design criteria given here are identical to those given in Appendix G of FAR 25 with one major exception. JAR-25 makes no reference to reduced design gust velocities for airplanes similar to those having extensive satisfactory service experience despite a lower gust velocity capability. This will be discussed later.

The U.S. Air Force and Navy are in the process of updating (simplifying) some of the military specifications. The Air Force Document, for example, is MIL-A-87221(USAF).

However, U.S. Air Force requirements for power-spectral determination of limit design gust loads are still as given in MIL-A-008861A(USAF), Reference 6. This document was first issued in 1971. The specified power-spectral gust criteria are essentially those of FAA-ADS-53 for a mission analysis with design envelope floor. The scale of turbulence values, L , have been reduced at altitudes below 2500 feet and the gust intensity parameter values, b 's, have been correspondingly adjusted. Provision is also made for evaluating mission analysis loads on an ultimate as well as on a limit basis. The same basic criteria were published in SEG-TR-67-28 in 1967, Reference 7. The normalized power spectrum specified for the criteria is the Von Karman representation.

Prior to 1986 the U.S. Navy requirements did not require power-spectral determination of limit design gust loads. However, MIL-A-8861B(AS), Reference 8, issued February 1986 supersedes MIL-

A-8861(ASG) and specifies essentially the same requirements for power-spectral determination of limit design gust loads as MIL-A-008861A(USAF).

Gust fatigue and design load psd requirements for both services utilize the mission analysis approach. Discussion in MIL-A-87221(USAF) does provide for the use of "envelope limit gust" which is similar to the Design Envelope criterion provided in FAA-ADS-53.

Basic Forms of Criterion

As specified in Appendix G of FAR 25, power-spectral gust loads criteria are presented in two basic forms; the design envelope analysis and the mission (flight profile) analysis. Provision is also made for a modification of the design envelope analysis (i.e., reduced design gust velocities) that considers the service experience of existing airplanes.

In the past, two shapes of gust velocity psd were commonly used, the Von Karman and the Dryden. Currently, however, the Von Karman psd representation is specified by FAR 25, JAR-25 and the U.S. military specifications for use in both the design envelope analysis and the mission analysis.

The response of the airplane in vertical and lateral turbulence is characterized by the response parameters \bar{A} and N_0 . \bar{A} is defined as the ratio of root-mean-square, rms, incremental load to root-mean-square gust velocity, expressed as:

$$\bar{A} = \frac{\sigma_y}{\sigma_w} = \left[\frac{\Omega_c \int_0^{\Omega_c} |H_y|^2 \phi_w(\Omega) d\Omega}{\int_0^{\infty} \phi_w(\Omega) d\Omega} \right]^{\frac{1}{2}} \quad \text{Eq. (1)}$$

N_0 is defined as the characteristic frequency of response (the average number of times per second that the response crosses the value zero with positive slope) and is expressed as:

$$N_0 = \frac{V}{2\pi} \frac{\sigma_y}{\sigma_w} = \frac{V}{2\pi} \left[\frac{\Omega_c \int_0^{\Omega_c} \Omega^2 |H_y|^2 \phi_w(\Omega) d\Omega}{\Omega_c \int_0^{\Omega_c} |H_y|^2 \phi_w(\Omega) d\Omega} \right]^{\frac{1}{2}} \quad \text{Eq. (2)}$$

where,

Ω = spatial frequency, radians/ft.

Ω_c = cut-off frequency, an upper limit of integration used in calculations, chosen such that the calculated integral adequately approximates the integral from zero to infinity.

$\phi_w(\Omega)$ is the Von Karman power spectrum for vertical-lateral gust psd's, plotted in Figure 1.

$$\phi_w(\Omega) = \frac{\sigma_w^2 L}{\pi} \frac{1 + \frac{8}{3}(1.339L\Omega)^2}{[1 + (1.339L\Omega)^2]^{\frac{11}{8}}} \quad \text{Eq. (3)}$$

L = scale of turbulence

σ_w = rms gust velocity

Design Envelope Criterion

The design envelope criterion is similar to past discrete gust criteria as well as to current limit design maneuver loads criteria. Operational usage of the aircraft is ignored. Instead the

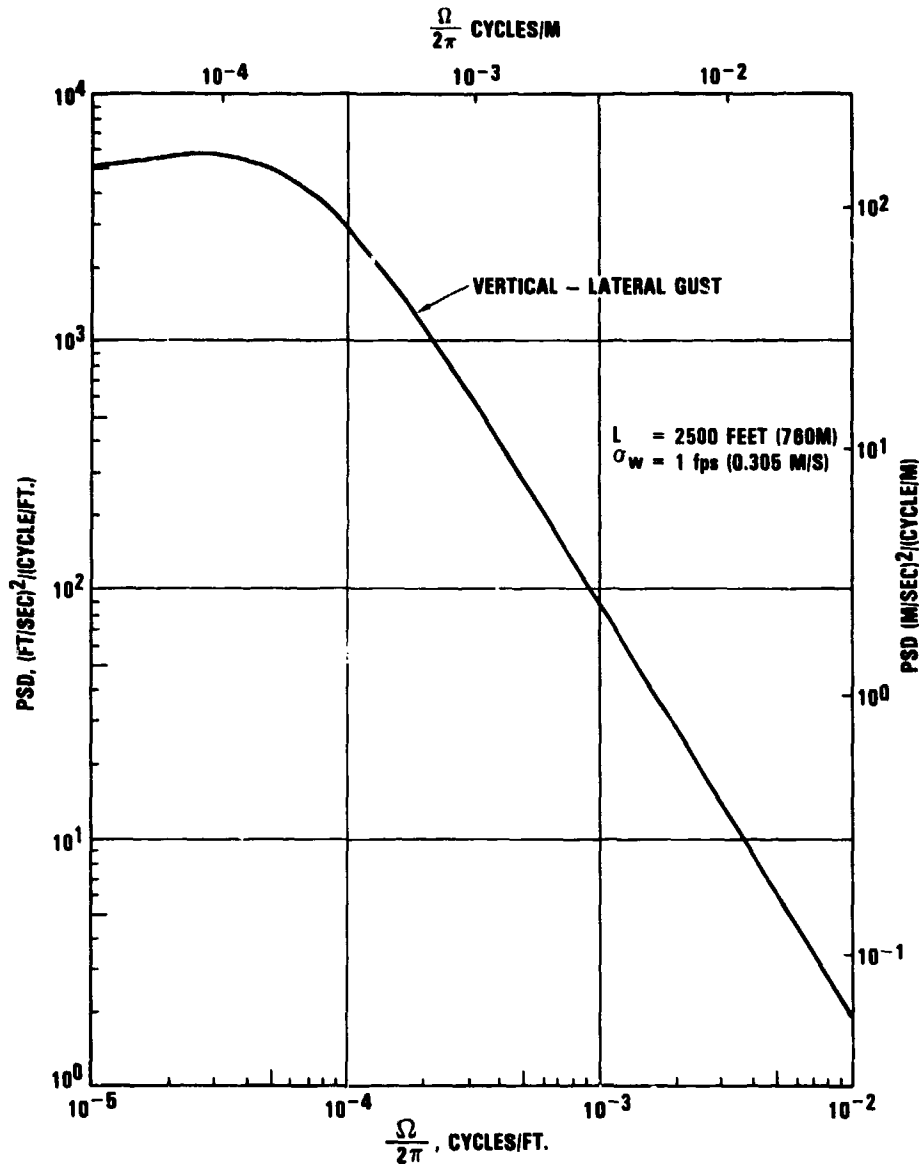


Figure 1. Von Karman Vertical-Lateral Gust PSD's

aircraft response is evaluated for a specified design envelope of speed, altitude, gross weight, fuel weight, and center of gravity, c.g., position. For the load (response) quantities, y , that are of interest, \bar{A} 's are obtained by dynamic analysis. The limit design value of y is given as:

$$y_{\text{design}} = \sigma_y \eta_d = \left(\frac{\sigma_y}{\sigma_w} \sigma_w \right) \eta_d = (\bar{A} \sigma_w) \eta_d = \bar{A} (\sigma_w \eta_d) = \bar{A} U_0 \quad \text{Eq. (4)}$$

where,

σ_w = design rms gust velocity

η_d = design ratio of peak to rms values

\bar{A} is from the dynamic analysis

The quantity U_o is the product of a design rms gust velocity σ_w and a design ratio of peak to rms values, η_d . U_o has the units of velocity and can be thought of as a continuous turbulence design gust velocity. The breakdown between σ_w and η_d is shown here to help in visualizing the criterion; only the product U_o is specified.

U_o can also be expressed as a design value of y/\bar{A} ; that is,

$$\left(\frac{y}{\bar{A}}\right)_{\text{design}} = U_o \quad \text{Eq. (5)}$$

Design values of U_o are specified as a function of altitude, much like the U_{de} values of discrete gust velocity. U_o , however, is a true gust velocity and U_{de} is an equivalent gust velocity. Values of U_o , at speed V_C , are defined as 85 fps true gust velocity from an altitude of 0 to 30,000 ft with a linear reduction to 30 fps at an altitude of 80,000 ft. The variation of design U_o with altitude at V_C is included in the comparison of design velocities given in Figure 2. At speed V_B , U_o is taken as 1.32 times the V_C values and at speed V_D , 0.5 times the V_C values.

Reduced U_o Requirement

Appendix G of FAR 25, Item (b)(3)(i), provides for reduced design values of U_o . Specifically, "Where the Administrator finds that a design is comparable to a similar design with extensive satisfactory service experience, it will be acceptable to select U_o at V_C less than 85 fps, but not less than 75 fps, with linear decrease from that value at 20,000 feet to 30 fps at 80,000 feet." A plot of the variation of U_o with altitude is included in Figure 2. To apply the reduced U_o values requires that:

- 1) Transfer functions of the new design are similar to the prior designs.
- 2) Typical missions of the new airplane are substantially equivalent to that of the similar design.
- 3) The similar design should demonstrate the adequacy of the U_o selected.

This modification to the design envelope criterion came about from an AIA proposal to the FAA after extensive studies of mid-range to long-range transports, such as the L-1011, DC-9 and DC-10, and the Boeing 727, 737, 747, 757, and 767, that showed U_o of 75 fps at V_C was adequate under FAR 25 Appendix G for this type of transport. The higher U_o values specified by the basic design envelope criterion are more appropriate for the lower cruise altitude more-severe types of operation. The more-severe types of operation are represented by short range or commuter operations where cruise altitudes of 20,000 to 30,000 feet are typical. The mid-range to long-range airplanes normally have cruise altitudes in the vicinity of 35,000 feet.

The requirement of similar transfer functions to qualify for use of the modified design velocities does not seem to be particularly relevant. Operation of the airplane is a much more significant consideration. It is logical to assume that the mid- to long-range transports could be classified a single type of airplane having satisfactory service experience; new airplanes in this category should then qualify for use of the reduced U_o design velocities.

It was noted earlier that JAR-25 makes no reference to modification of the U_o design velocities, nor does FAA-ADS-53, which is referenced by JAR-25. Depending on the methods used by an individual manufacturer and the service history of their past airplanes this may or

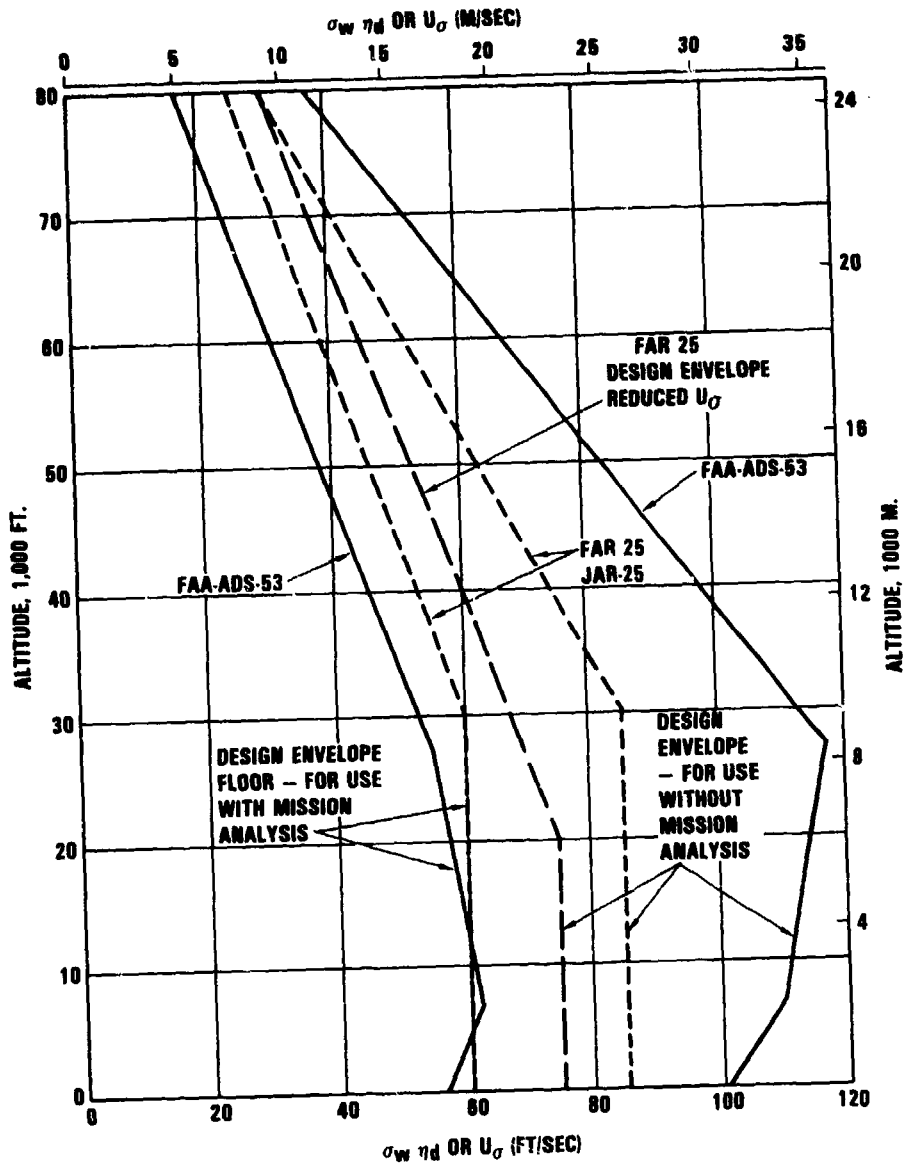


Figure 2. Variation of Design U_σ with Altitude, Criteria Comparison

may not cause some hardship. If the design gust loads for a specific airplane are obtained using the mission analysis criterion, later studies of derivative aircraft can easily be related to the original mission analysis in much the same manner as a design envelope analysis (i.e., by comparison of predominant mission analysis flight conditions). In this instance, lack of the reduced U_σ design envelope criterion should not cause significant problems. Methods are being proposed for JAR-25 evaluation to define a reduction of PSD gust intensity to less than 85 ft/sec.

Mission Analysis Criterion

As originally developed in FAA-ADS-53, the mission analysis approach was a "stand alone" method. It was, however, suggested that the most appropriate criterion would be a combination

of the design envelope approach and the mission analysis approach. Combining these two approaches now constitutes the Mission Analysis Criterion specified in FAR 25, JAR-25 and the various U.S. military specifications.

In addition to a mission profile analysis the Mission Analysis Criterion requires that a design envelope analysis be performed similar to the design envelope criterion, but with reduced U_0 values to provide a design envelope floor. The U_0 values at V_C are specified as 60 fps from 0 to 30,000 feet with a linear reduction to 25 fps between 30,000 feet and 80,000 feet. The V_B and V_D values are still 1.32 and 0.5 times the V_C values, respectively. The variation of U_0 with altitude for use with the mission analysis is also shown in Figure 2.

The mission analysis approach is based on "Rice's Equation", first published in Reference 9.

Rice's equation is:

$$N(y) = N_0 e^{-\frac{1}{2} \left(\frac{y}{\sigma_y} \right)^2} \quad \text{Eq. (6)}$$

This equation yields $N(y)$, the number of crossings of a given y , per unit time, with positive slope. N_0 is the number of zero crossings per unit time with positive slope.

Application of Rice's equation to determine frequency of exceedance as a function of load level requires that the equation be modified to accommodate one or more mission profiles. The mission profiles represent the expected utilization of the airplane. Each profile is divided into a number of mission segments to account for variations over the flight profile of the various parameters affecting \bar{A} and N_0 and the variation with altitude of the expected σ_w exposure. The required modifications to Rice's equation result in the following expression.

$$N(y) = \sum t N_0 \left[P_1 \exp \left(\frac{-|y - y_{1g}|}{b_1 \bar{A}} \right) + P_2 \exp \left(\frac{-|y - y_{1g}|}{b_2 \bar{A}} \right) \right] \quad \text{Eq. (7)}$$

where,

- t = fraction of total mission time in each segment
- y = net value of response quantity
- y_{1g} = value of response quantity in one-g level flight
- Σ denotes summation over all mission segments
- \bar{A} , N_0 = parameters determined by psd dynamic analysis
- P_1 , P_2 , b_1 , b_2 = parameters defining the probability distributions of rms gust velocity. These values are shown in Figures 3 and 4.

This expression provides frequency of exceedance curves from which the limit gust loads are read at a frequency of exceedance of 2×10^{-5} exceedances per hour. The parameters, P_1 , P_2 , b_1 , and b_2 , depend only on altitude. By setting y_{1g} equal to zero, the variable $N(y)/N_0$ can be plotted versus y/\bar{A} to produce the generalized exceedance curves shown in Figure 5. Actual exceedance curves, to be applied about the one-g flight load, can be obtained by multiplying the ordinates by N_0 , and the abscissas by \bar{A} , for the specific load quantity and flight case desired.

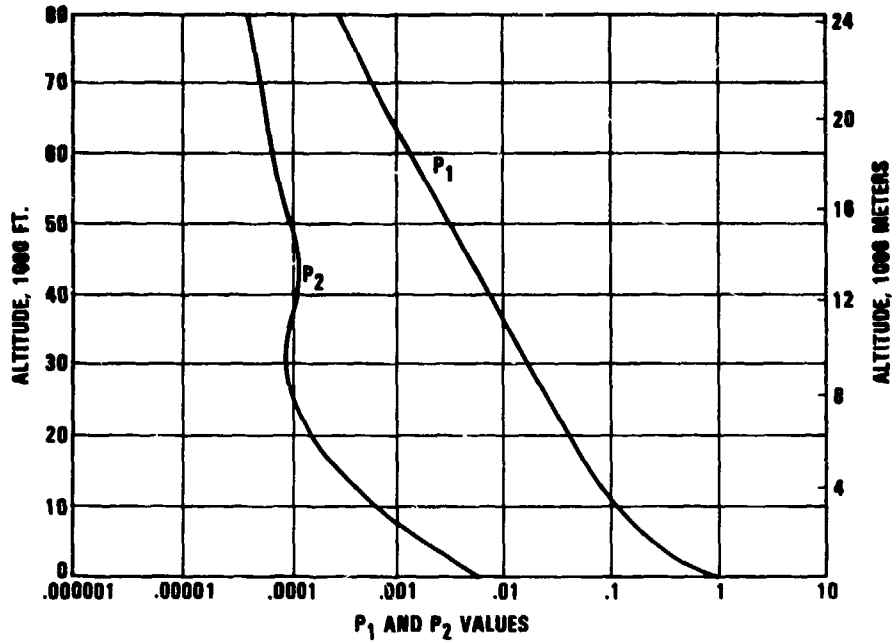


Figure 3. Parameters, P_1 and P_2 , for Defining the Probability Distributions of RMS Gust Velocity

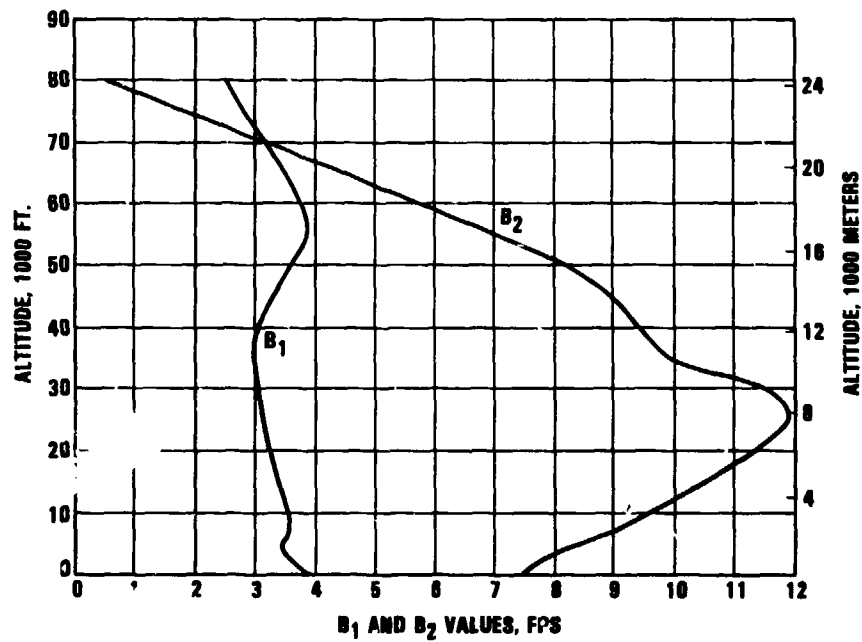


Figure 4. Parameters, b_1 and b_2 , for Defining the Probability Distributions of RMS Gust Velocity

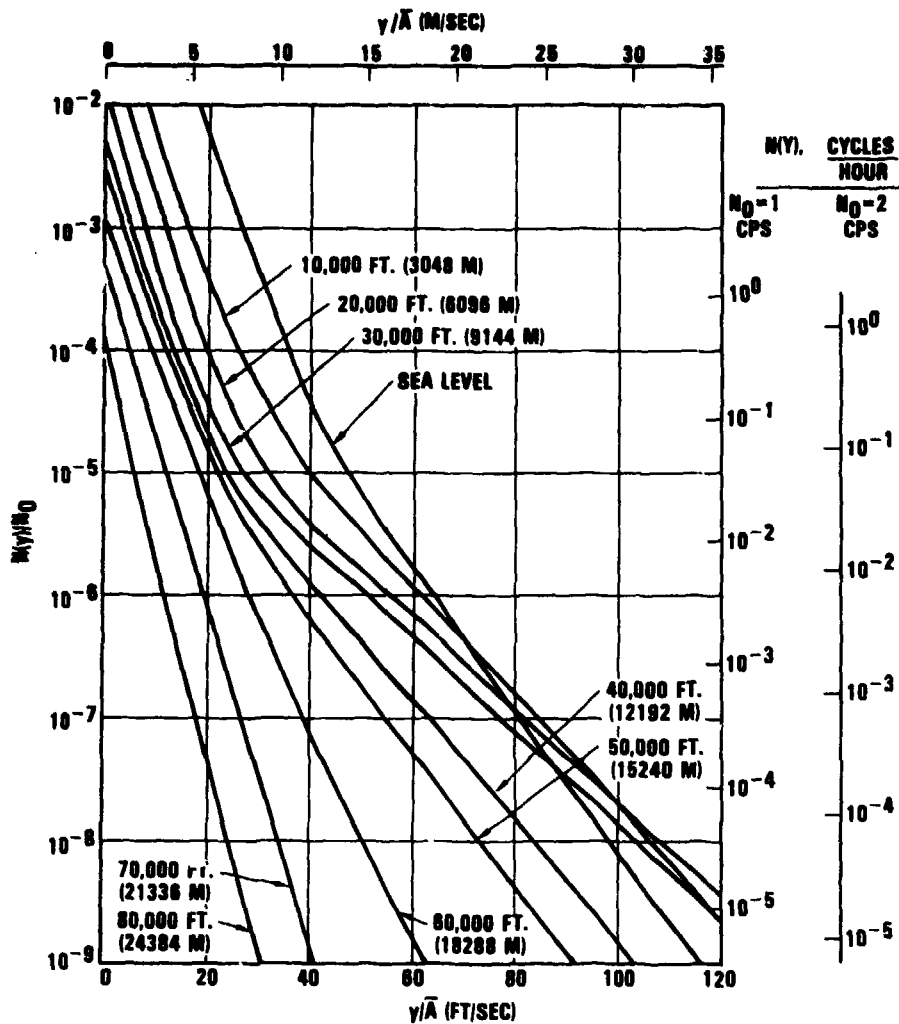


Figure 5. Generalized Exceedance Curves

Mission Profile Generation

The generation of realistic profiles is not a particularly straight forward procedure. It requires ingenuity and judgment to apply information from a number of different areas that includes outside sources. For example, development of realistic profiles for a commercial transport requires knowledge of the target airlines' current and anticipated route structures, probable passenger load factors, and cargo loading practices.

Mission profiles should reflect anticipated operational usage for flight parameters such as speed, payload, flight duration, c.g. location, passenger load factor, etc. A number of different profiles can be generated to reflect significant variations in anticipated usage from one operator to the next. However, the profiles should still reflect the composite of all operations, rather than the most severe.

Design loads obtained from a mission profile analysis are not normally increased simply because utilization by a new operator is moderately more severe than anticipated in the original

mission analysis. In most instances, the effect of a single operator on the frequency of exceedance of limit or ultimate load for the fleet as a whole (all operations) is small enough that no change in loads is required. It is recommended, however, that such changes be qualitatively evaluated.

A number of profiles are normally generated to adequately represent variations in profile distance and duration, cruise altitude and Mach number, payload (both passenger load factor and cargo), fuel, and pilot training or check flights. Plots of a representative mission profile, developed for the L-1011-1, are shown in Figures 6 and 7. Typical segmentation of that profile is shown in Figure 8.

Flaps-extended segments contribute to wing fatigue, flap fatigue, and may affect limit horizontal tail loads, but they do not contribute significantly to wing limit load exceedances. The flaps-extended segments are, therefore, not shown in Figures 6 through 8.

The parameter values to be used in the definition of the mission profiles must be selected with care. This is illustrated in Figure 9. Two samples of airspeed data for the L-1011-1 are shown. In the upper sketch an airspeed of 290 knots based on a simple average is reasonable. However, the airspeed range is so large in the lower sketch that a simple average is not realistic. This is demonstrated by considering the airspeed to be represented by high and low speed segments with the average speed in each segment used for analysis. In this representation the contribution of the low speed segment to the exceedance curve is negligible and the high speed portion contributes half as many cycles as the total distribution but with a considerably higher average speed. The increase in loads due to the higher speed has a greater effect on the exceedance curve than the reduction in cycles. In this case a weighted average should be used.

Mission Analysis or Design Envelope?

The question arises as to which form of criterion, the mission analysis or design envelope, is most applicable for determination of limit design gust loads of a specific airplane. The answer is not always clear; both have advantages and disadvantages.

Historically, before the introduction of power-spectral methods, the design envelope type of analysis was the most common. However, even then, a mission analysis type of evaluation was performed if there were doubts concerning either the ability of a given airplane to withstand the gust loads to which it might be exposed or the applicability of the existing criteria to new aircraft with mission profiles that were considerably different than prior aircraft.

Most airplanes operate well within their placard speeds. NASA VGH data on actual operational usage of similar airplanes shows that the spread between actual and placard speeds is never less than 10 to 15 knots; the gap is often greater. The mission analysis approach will provide adequate loads for airplanes that operate close to their design envelopes most of the time as well as for airplanes that operate well within their design envelopes. The design envelope approach will either over estimate the loads for airplanes that operate well within their design envelopes or under estimate loads for airplanes that operate close to their design envelopes.

On the other hand, the anticipated profiles that must be defined to perform a mission analysis evaluation require considerable judgment. This leads to differences of opinion that can be quite difficult to reconcile. The profiles are then a compromise and the loads obtained are never exactly "right." Use of the design envelope criterion eliminates this type of uncertainty.

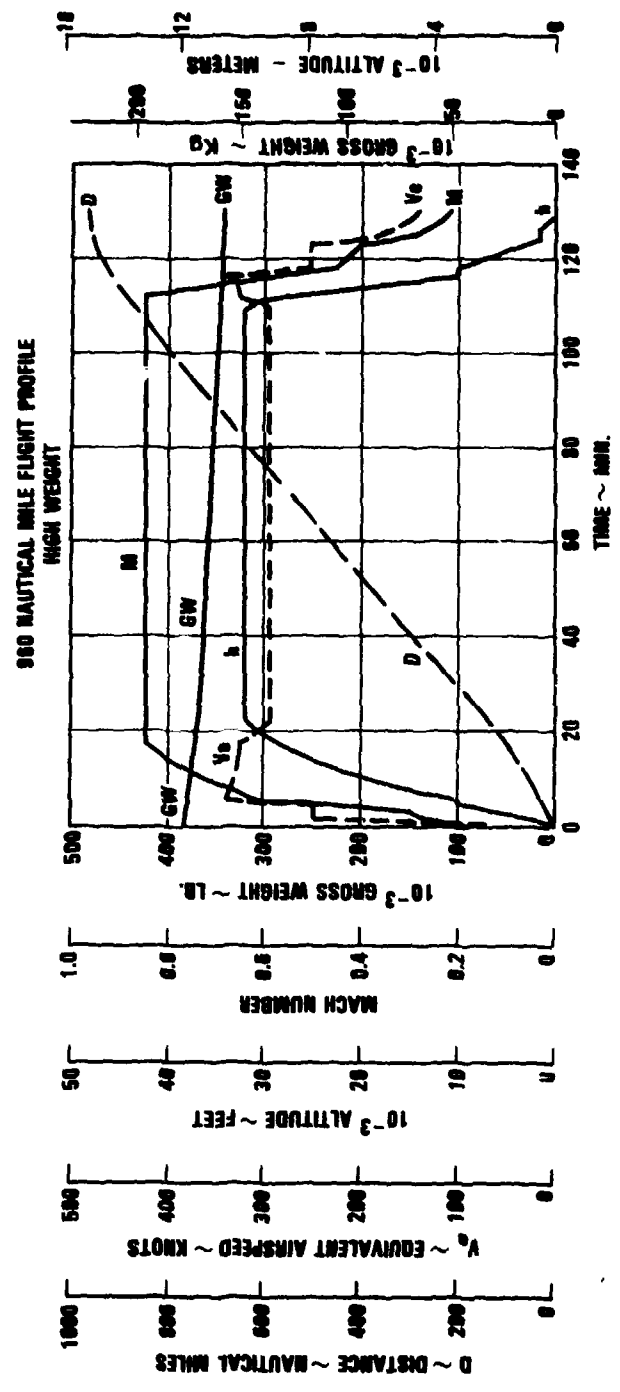


Figure 6. Typical Flight Profile

54

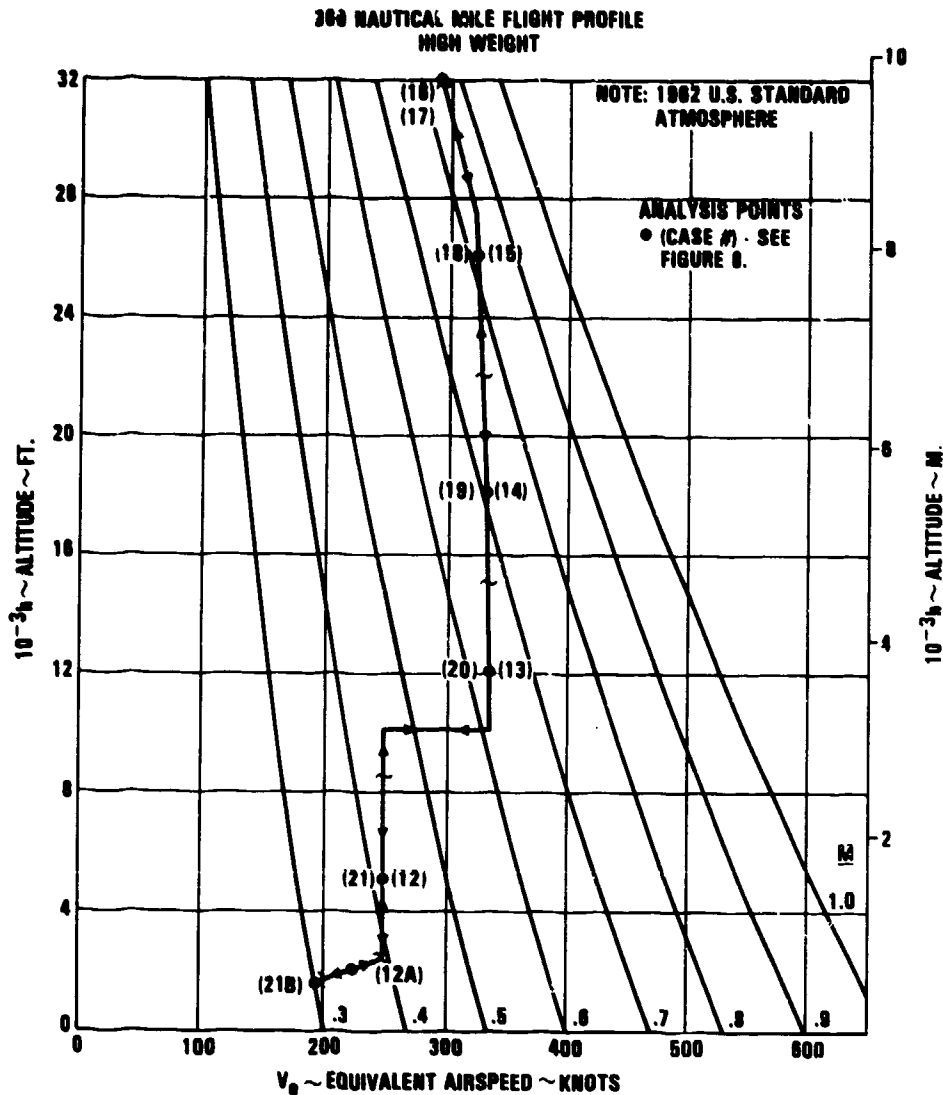


Figure 7. Typical Flight Profile on Speed-altitude Coordinates

In addition, the mission analysis criterion requires that all flight conditions be analyzed and the frequency of exceedance data generated before a single limit design gust load is obtained. Using the design envelope approach, loads can easily be obtained even for preliminary design by analyzing a selected number of flight conditions that are expected to be critical. Additional conditions can be added throughout the design process.

Because a mission analysis is normally required to obtain repeated load spectra for fatigue analysis, use of the design envelope does not eliminate the need to generate mission profiles. In addition, use of the design envelope does NOT guarantee a conservative design. Nor does it guarantee that the airplane can be safely operated at any point within the design envelope. Design gust velocities are based on the satisfactory performance of past airplanes. The design gust velocities are adequate for a new airplane only if it operates in a manner similar to these past airplanes, for example - well within its design envelope.

960 MM PROFILE - HIGH WEIGHT

CASE NO.	GROSS WEIGHT		ALTITUDE, h		MACH NO.	V _{max}	ENGINE POWER SETTING	t ₁ MIN.	V ₁ /t	V ₁ /t LOW WING WEIGHT COMPOSITE	V ₁ /t HIGH WING WEIGHT COMPOSITE
	LB	Kg	FT.	M.							
12A	380,000	172,387	2,000	609	0.353	226	T.O.	2.5	0.01930	0.00249	0.00249
12	379,000	171,913	5,000	1,524	0.415	250	MAX. C	1.5	0.01159	0.00150	0.00150
13	377,000	171,006	12,000	3,658	0.635	335	MAX. C	3.5	0.02703	0.00349	0.00349
14	375,000	170,099	18,000	5,496	0.709	331	MAX. C	4.0	0.03089	0.00398	0.003989
15	372,000	168,736	26,000	7,925	0.822	324	MAX. C	10.5	0.08108	0.01046	0.01046
16	363,000	164,866	32,000	9,754	0.850	293	PLF	43.5	0.33591	0.04333	0.04333
17	360,000	158,759	32,000	9,754	0.850	293	PLF	43.5	0.33591	0.04333	0.04333
18	345,000	156,491	26,000	7,925	0.822	324	FLT. IDLE	7.0	0.03089	0.00398	0.00398
19	344,000	156,037	18,000	5,496	0.709	331	FLT. IDLE	2.0	0.01544	0.00199	0.00199
20	343,000	155,584	12,000	3,658	0.635	335	FLT. IDLE	3.5	0.02703	0.00349	0.00349
21	343,000	155,584	5,000	1,524	C.415	250	FLT. IDLE	5.3	0.04093	0.00528	0.00528
21B	342,840	155,420	1,500	457	0.303	195	A.P.	5.7	0.04401	0.00568	0.00568

t_T = 129.5

Figure 8. Typical Flight Profile Segmentation

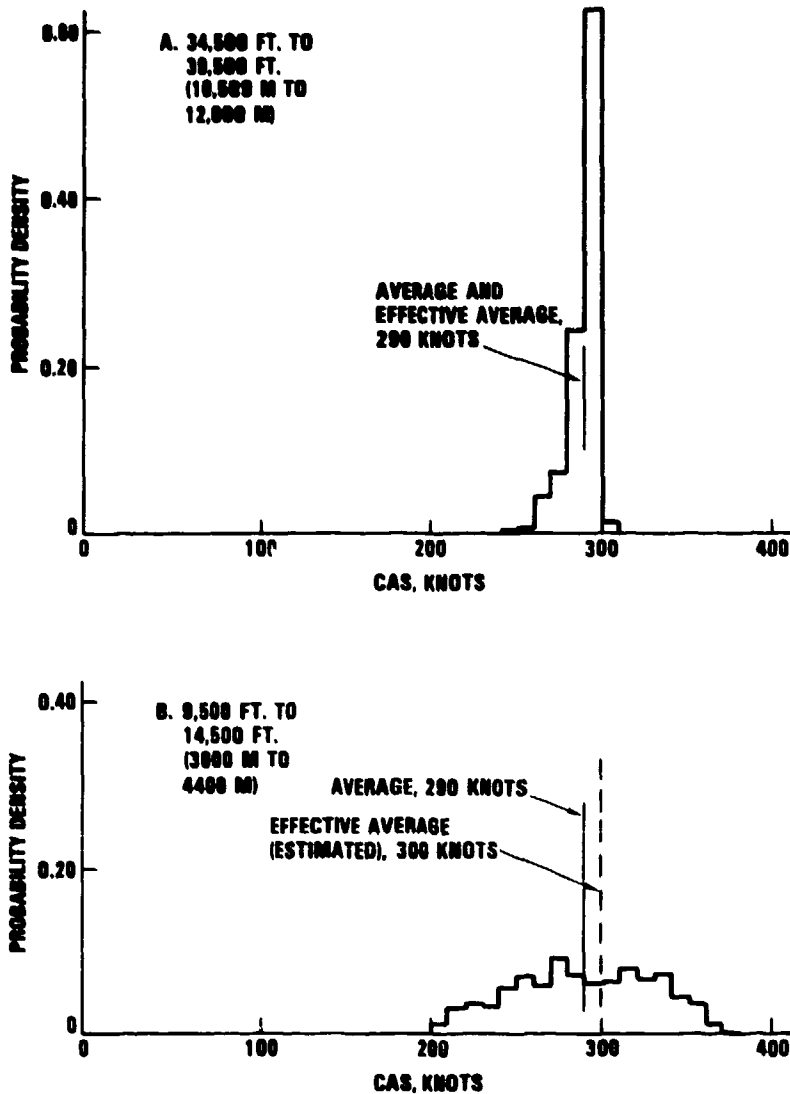


Figure 9. Typical Airspeed Distributions

If the requirements of the certifying agency are not the determining factor, the choice between the mission analysis approach or the design envelope approach is pretty much determined by the anticipated operation of the airplane relative to prior airplanes. If it is basically an existing airplane design, intended to fly in the same manner as past airplanes, the design envelope criterion should be adequate. However, for all other designs, including the use of active controls, the mission analysis approach should be seriously considered.

In spite of the difficulties in defining mission profiles, the Mission Analysis Criterion has always been preferred at the author's company. The other U.S. companies surveyed are applying the Mission Analysis Criterion with increasing frequency. Military specifications specifically require use of the mission analysis approach for gust critical airplanes. The Design Envelope Criterion is used primarily for designing derivatives of existing airplanes or in the design of

airplanes that are similar to past airplanes in both design technology and anticipated operation. It is also used extensively in preliminary design studies.

DESIGN APPLICATIONS

In compliance with either the design envelope or mission analysis criterion, limit design levels of a variety of airplane response quantities can be established. These response quantities may include not only external loads, such as shears, bending moments, and torsions, and translational and rotational accelerations, but also internal loads and stresses acting on the various structural elements. Design limit values of stress in the various structural elements may be obtained from the statistical parameters either by direct computation of the internal stresses or by generating design load conditions that produce the design stress levels when applied to the structure.

In effect, the direct computation of internal stresses involves determining separate power spectra for loads in every element of the structure. For an entire airplane the number of structural elements could number in the thousands. In addition, where the strength of an element such as a wing surface panel involves the interaction of two stresses, for example compression and shear, these stresses must be properly combined (phased) to provide the necessary stress information for design. Because rms stresses obtained in this manner are directly tied to the structure, changes in the stress model require that the internal load rms values be recomputed. Application of this approach has then been limited to local areas of structure with relatively complicated loading patterns, where the gust loads tend to be critical.

The more common approach is to generate design load conditions. A design condition consists of a set of external forces in equilibrium that represents the statistically defined parameters from the psd analysis over specific regions of the airplane. By applying such a set of forces, the stresses in every element of the structure can be determined and the same set of forces can be applied in static tests. These conditions are analyzed by the Stress Department in the same manner as conditions obtained from time history or static loads analyses to determine the internal loads and stresses acting on the structure. Secondary structural changes to the stress model have little effect on the externally applied loads, and such changes can be easily evaluated.

The design procedures that are discussed here are summarized below relative to the approach used - that is, computation of internal stresses or development of design conditions.

<u>DESIGN PROCEDURE</u>	<u>Internal Stress</u>	<u>APPROACH</u>	<u>Design Condition</u>
Matching Conditions			x
Conditional Probability Method			x
Equivalent Discrete Gust			x
Internal Load Method	x		

Some companies apply more than one method. This is done because some procedures require modeling of the airplane that is not available for older derivatives. In addition, some of the more sophisticated methods are applied only to the most complex areas of the structure or to areas that are gust critical or sensitive to gust loading. Conversely, the more easily applied but potentially less accurate procedures are applied in a conservative manner to non-gust-critical structure with relatively simple loading patterns.

All of the airframe manufacturers contributing to this study emphasized that the psd design procedures require close coordination and a high degree of cooperation between the Loads

Department (responsible for providing the loading or stress environment) and the Stress Department (responsible for sizing the various structural elements). In many respects it is an interdisciplinary analysis.

With the exception of the Equivalent Discrete Gust Approach all of the above procedures explicitly consider the problem of phasing.

Phasing

Values of the response quantities obtained by psd analysis are inherently unsigned. Because positive and negative values are equally likely to occur, both must be considered in establishing the design loads. For a mission analysis, separate exceedance curves are obtained for positive and negative net loads (response quantities). For the design envelope analysis, the design net values are computed as:

$$\text{Net load} = \pm U_{\sigma} \bar{A} + L_{1g} \quad \text{Eq. (8)}$$

Because the design values of the various response quantities generally occur at different times, the above design values are "unphased." Design of the structure cannot be determined until proper combinations of these response quantities are defined. This is true even if internal stress quantities are directly computed in the psd analysis.

The phase relationship for any two response quantities is completely defined by their covariance and respective variances, usually represented as correlation coefficients. The method of fictitious structural elements also provides phasing information. The use of correlation coefficients is the more popular procedure; however, fictitious structural elements are occasionally used for special considerations.

Correlation Coefficients

In applying the psd method it is assumed that atmospheric turbulence is a random Gaussian process which acts as an input to the airplane. The airplane is represented as a linear system. The resulting outputs from the psd analysis are then also a Gaussian process. For a Gaussian process the statistical dependency of any two response quantities (outputs) can be represented by a correlation coefficient, ρ_{xy} , given by the following expression, which follows from the equations given in Appendix B of Reference 4.

$$\rho_{xy} = \int_0^{\infty} \frac{1}{\bar{A}_x \bar{A}_y} \Phi(\omega) \left[H_{x\text{real}}(\omega) \cdot H_{y\text{real}}(\omega) + H_{x\text{imag}}(\omega) \cdot H_{y\text{imag}}(\omega) \right] d\omega \quad \text{Eq. (9)}$$

where

- ω - forcing frequencies, the array of frequencies for which the psd analysis was performed
- $\Phi_g(\omega)$ - gust spectrum at each forcing frequency
- \bar{A} - Ratio of the rms of the response quantity to the rms value of the gust velocity, obtained from the psd analysis
- N_0 - characteristic frequency of the response quantity, obtained from the psd analysis
- $TF(\omega)$ - complex transfer function of the response quantity at each forcing frequency

$$TF(\omega) = \underset{\text{real}}{H(\omega)} + i \underset{\text{imag}}{H(\omega)} \quad \text{Eq. (10)}$$

The phasing of any two response quantities is then determined by using the correlation coefficients in the expression for a joint probability density function given in Reference 4, that is:

$$P(x,y) = \frac{1}{2\pi\bar{A}_x\bar{A}_y(1-\rho_{xy}^2)^{1/2}} \exp\left[-\frac{1}{2(1-\rho_{xy}^2)}\left(\frac{x^2}{\bar{A}_x^2} - \frac{2xy\rho_{xy}}{\bar{A}_x\bar{A}_y} + \frac{y^2}{\bar{A}_y^2}\right)\right] \quad \text{Eq. (11)}$$

By assigning various constant values to $P(x,y)$, for a given ρ_{xy} , contours of constant joint probability density are defined. These are ellipses, collapsing to a straight line at $\rho = 1$ or a circle at $\rho = 0$. An ellipse can be defined that is tangent to the design level values of any two specified response quantities. This is referred to as a design ellipse and gives a complete representation of the phased design loads for these two response quantities, Figure 10. By considering only the incremental loads and normalizing these loads to their design values, the variation of the probability density function (i.e., different values of ρ_{xy}) at constant stress levels can be illustrated as shown in Figure 11.

Fictitious Structural Element

Before it was recognized that proper load combinations could be easily obtained through the use of correlation coefficients to define an equal-probability ellipse, load phasing was accomplished using the concept of the fictitious structural element, Reference 3. This method still has some potential advantages relative to the correlation coefficient approach.

The fictitious structural element can directly provide design level values of combined internal loads and stresses. For example, by expressing front or rear beam shear flow as

$$FE = a_s S + a_t M + a_t T \quad \text{Eq. (12)}$$

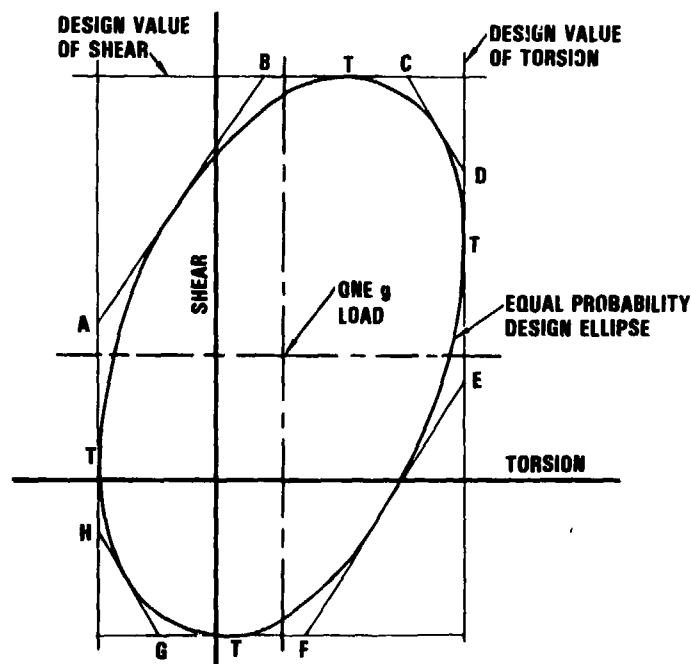


Figure 10. Equal Probability Design Ellipse and Circumscribing Octagon

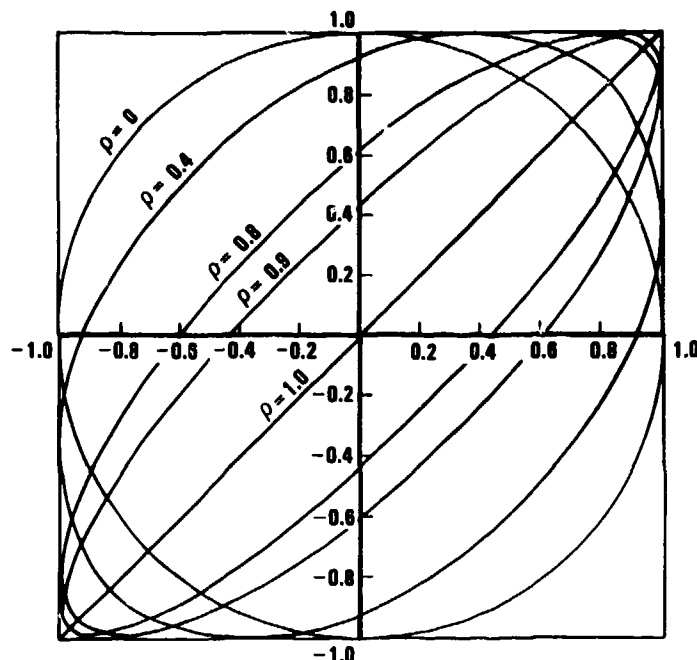


Figure 11. Variation of Probability Density Function, $P(x,y)$,
Maintaining Constant Stress Levels

the frequency response function of "FE" can be determined as a linear function of the frequency response functions of S, M, and T. Its psd, \bar{A} , N_0 , and design value can then be determined. To further illustrate, assume that shear flow is affected only by shear and torsion. The above equation then becomes

$$FE = a_1 S + a_2 T \quad \text{Eq. (13)}$$

which defines a diagonal straight line on shear-torsion coordinates, as shown in Figure 12. This line represents the shear and torsion that result in the design magnitude of the front beam shear flow. No valid combination of shear and torsion can exceed this line. Therefore, in Figure 12, points 2 and 3 could be considered realistic design load combinations, but point 1 is obviously conservative.

The procedure can be applied to any two response quantities, not just front beam shear flow. In addition, arbitrary values of a_1 and a_2 can be selected. This defines a family of diagonal lines each representing the design load or stress in a fictitious structural element. For a design envelope analysis, where the design load is defined as a constant times the rms value, this family of diagonal lines produces the same design ellipse that is obtained using the correlation coefficient approach.

Current psd gust procedures normally apply the correlation coefficient method to establish phasing. However, one potential advantage in using fictitious structural elements is that they can be carried through an entire mission analysis, thereby providing direct load phasing information that includes the effects of differences from segment to segment in one-g flight loads, correlation coefficients, and ratios of (say) design shear to torsion. In general, the result is not an ellipse. This approach is also easily applied to the time history determination of loads and is currently used by at the author's company in the determination of design taxi loads.

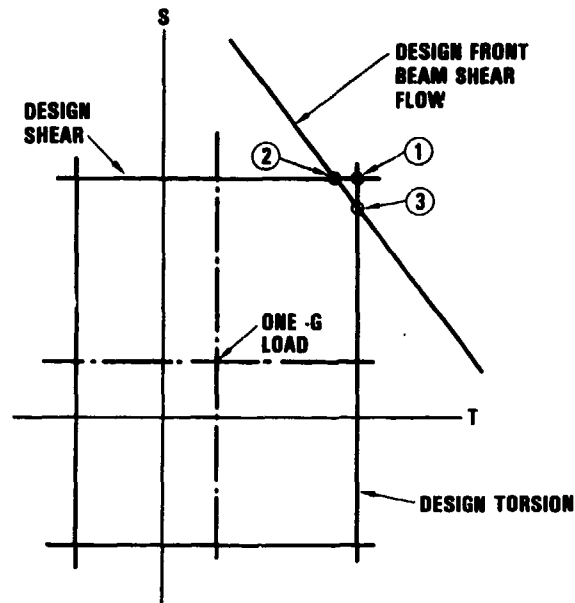


Figure 12. Fictitious Element Shear-Torsion Representation of Front Beam Shear Flow

Matching Condition - Concept

The matching condition procedure or a variation is used by all companies surveyed as one method of generating design conditions. It was first proposed in Reference 3 and further developed in References 10 and 11. In Reference 12, linear optimization techniques were applied to the procedure, which resulted in a batch processing computer program that provided solutions to the matching operation. The matching condition concept is described by the following excerpt from Reference 3.

"The basic concept employed in matching-condition generation is suggested by the fact that, in flying through turbulent air, an airplane responds statically to the low frequency components of the turbulence (long gradient gusts) and it responds dynamically in its various elastic modes to the higher frequency components of the turbulence. The two types of responses - the static and the dynamic - generally have quite different distributions of load throughout the structure. Moreover, each elastic mode will have its own distinctive load distribution. In flight through typical turbulence there is a random interplay among these various distributions. As a result, no single distribution can be expected to reproduce simultaneously the correct stress histories at all points in the structure."

"Accordingly, in generating matching conditions, the approach is to start with a number of 'elementary distributions.' Each of these consists of a set of forces in equilibrium, representing the static response of the airplane or the dynamic response of a particular elastic mode. The elementary distributions, as building blocks, are superimposed in various proportions to give a number of design conditions, which, collectively, envelope the statistically defined shears, bending moments and torsions."

Application of this concept requires a procedure to define each of the following items:

- design load combinations to be matched
- elementary distributions
- contribution of each elementary distribution to a design condition

Design Load Combinations

A design ellipse, obtained by use of either fictitious elements or correlation coefficients, establishes the phase relationship for any two response quantities. To the extent that the critical internal stress required for design of a structural element is a linear function of one or two response quantities, the design ellipse provides sufficient information to define the critical design load combinations.

An infinite number of load combinations is required to define each point on a design ellipse. However, linear combinations of loads can be easily defined that circumscribe the design ellipse and thereby provide a limited number of load combinations that produce a conservative value for the design stress that is a linear function of two inputs. For the matching condition procedure, a design octagon is defined that circumscribes the design ellipse, illustrated in Figure 10 for shear and torsion. Points A through H are defined for the incremental design values of load from the normalized equation that produced Figure 11. The coordinates of points A through H, Figure 10, are then dependent only on the value of the correlation coefficient. The normalized coordinates of points A through H are:

$$\text{Pt. A} = -\text{Pt. E} = (-1.0, -l_a)$$

$$\text{Pt. B} = -\text{Pt. F} = (l_a, 1.0)$$

$$\text{Pt. C} = -\text{Pt. G} = (l_b, 1.0)$$

$$\text{Pt. D} = -\text{Pt. H} = (1.0, l_b)$$

where,

$$l_a = 1.0 - \sqrt{2(1 - \rho_{xy})}$$

$$l_b = -1.0 + \sqrt{2(1 + \rho_{xy})}$$

A set of design load conditions is obtained by matching the phased loads defined at each of the eight points for a number of design octagons defined throughout the structure.

Prior discussions of this procedure given in References 3 and 10 thru 12 have emphasized the use of wing shear-torsion and bending-torsion load combinations. Shear and bending at the various wing locations are in general highly correlated. The elementary distributions inherently reflect this correlation and the design conditions that are developed based on the shear-torsion and bending-torsion load combinations also provide quite rational load combinations of shear and bending. This, of course, is not the case in all areas of the structure.

A procedure is proposed in Reference 13, the "equal probability technique," to define design conditions for load combinations that specifically account for the effect of three (or more) load inputs on the design stress levels. For example, if shear, bending, and torsion all contribute significantly to a design stress, the critical load combinations are defined as a three dimensional ellipsoid, rather than a two dimensional ellipse. In comparing the equal probability technique with the matching condition technique it is stated that the two methods are equivalent for

combinations of two loads, but doubts were expressed concerning the validity of the matching condition approach when three or more load inputs are significant.

The doubts expressed appear to be pointed more toward the definition of proper design load combinations than toward the fundamental matching condition concept. Effective application of the matching condition procedure is dependent on the determination of design load combinations. Unfortunately, procedures that have been applied to define load combinations as input to the matching condition program in the more complex loading areas have not been fully described in past references.

In complex loading areas, such as the interface between wing and fuselage, horizontal or vertical tail and fuselage, or wing engine and wing, a number of additional loads are considered that include selected internal stresses and the forces and moments acting on concentrated mass items. In addition, some areas of the structure require the direct consideration of load phasing between shear and bending.

Information is provided by the Stress Department to assist in selecting additional load combinations that are potentially critical. The information provided includes:

- Stress results for a number of "study" conditions
- Margins of safety for current design conditions
- Unit load distributions for selected internal stresses
- Estimates of relative significance of various external loads in producing specific internal stresses

From this information a number of additional load combinations are defined. For example, in the interface area of the wing and wing engine, load combinations are defined that relate engine forces and moments to each other and to wing shears, bendings and torsions. Load combinations representing three external load inputs are obtained using a concept similar to application of a design octagon. For example, conservative conditions for load combinations of shear, bending and torsion can be defined from the design octagons relating shear-bending, shear-torsion, and bending-torsion. These conditions are:

- Maximum shear with related bending and related to torsion
- Maximum bending with related shear and related torsion
- Maximum torsion with related shear and related bending

This produces 24 load combinations that circumscribe a design ellipsoid in a manner similar to a design octagon circumscribing a design ellipse. A sketch of the concept is given in Figures 13 and 14. These load combinations are slightly more conservative relative to the ellipsoid than those produced by the design octagon relative to a design ellipse. After applying the information provided by the Stress Department very few of these types of load combinations are actually required for design. Simultaneous consideration of more than three load quantities has not been necessary. It is quite possible, however, to define load conditions that include directly phasing the external loads with specific internal stresses.

Elementary Distributions

The mission analysis exceedance curves are surveyed to determine the dominant profile(s) and dominant flight segment(s). Critical design envelope flight conditions are implicitly defined.

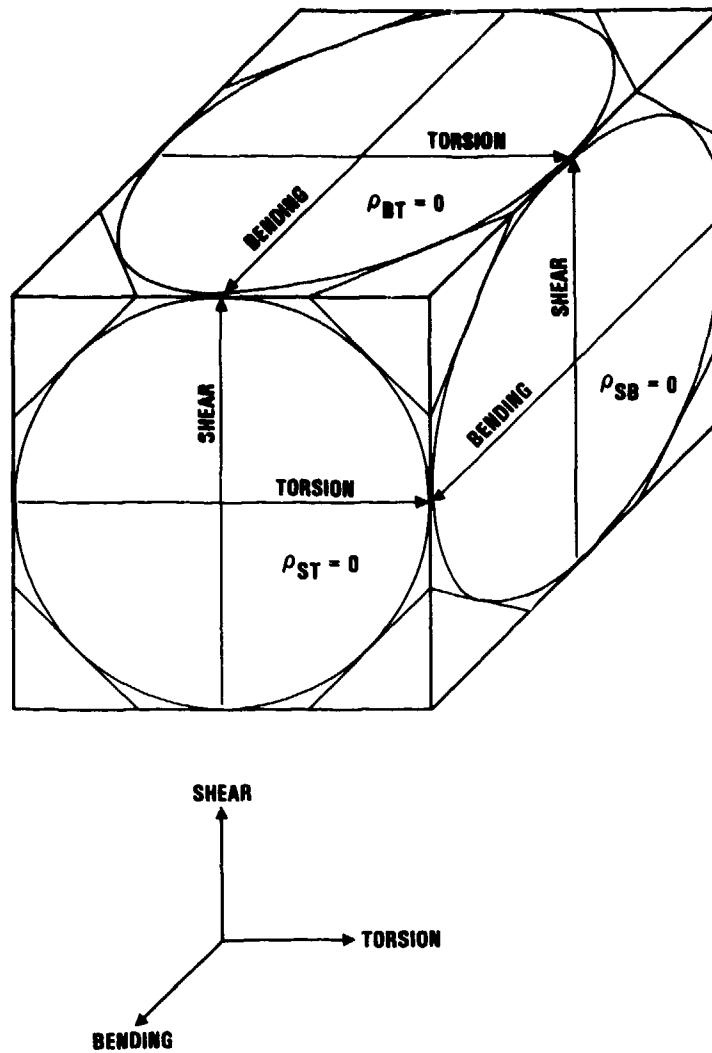


Figure 13. Design Ellipse 3D Projection of Shear-Bending, Shear-Torsion and Bending-Torsion

Elementary distributions are obtained for each critical flight segment or design envelope condition selected. For vertical gust analysis these distributions include:

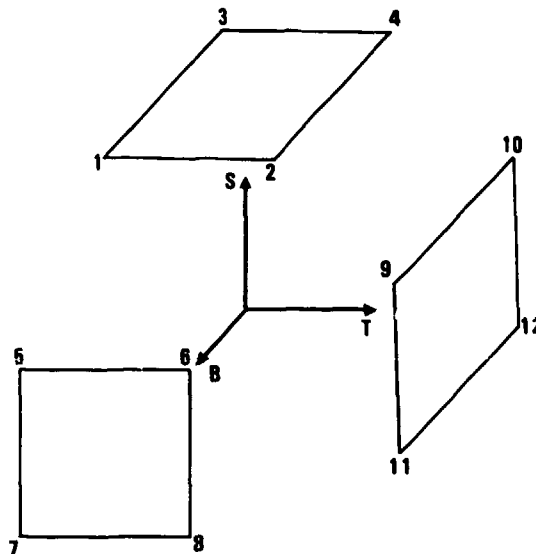
- Static aeroelastic loads due to a one-g static discrete gust. These are effectively the loads due to an arbitrary angle of attack, airloads balanced by plunge and pitch inertia
- Static aeroelastic (or rigid) loads due to a unit pitch rate
- Loads due to unit inboard and outboard aileron angles, balanced by inertia
- Loads due to unit generalized elastic mode acceleration, \ddot{q} , combined with airloads occurring at the associated modal displacement, q

The predominant contribution of an elastic mode to airplane response occurs at its resonant frequency, so the airloads associated with q , calculated on a zero frequency basis, are multiplied by the real part of the lift growth function at the resonant frequency. The loads per q are generally not in equilibrium and are balanced by use of the rigid airplane plunge and pitch

inertia. The aerodynamic term, proportional to modal displacement, is then directly added to the inertia load, proportional to modal acceleration, to form the combined distribution.

In the lateral gust analysis the following elementary distributions are used.

- Static aeroelastic loads per unit sideslip.
- Static aeroelastic loads per unit yaw rate.
- Static aeroelastic loads per unit roll rate.
- Static aeroelastic loads per unit rudder angle.
- Loads due to unit generalized elastic mode acceleration. The airloads due to modal displacement are neglected.



LIST OF COORDINATES

POINT	SHEAR	BENDING	TORSION
1	1.0	l_b	l_a
2	1.0	l_b	l_b
3	1.0	l_a	l_a
4	1.0	l_a	l_b
5	l_b	1.0	l_a
6	l_b	1.0	l_b
7	l_a	1.0	l_a
8	l_a	1.0	l_b
9	l_b	l_b	1.0
10	l_b	l_a	1.0
11	l_a	l_b	1.0
12	l_a	l_a	1.0

Figure 14. Coordinates of Load Combinations That Circumscribe a Design Ellipsoid

Each of the elementary distributions noted above is calculated for each of the critical mission segments or design envelope conditions selected. They are formed initially as panel loads, then integrated to obtain the appropriate loads or response quantities.

Design conditions should reflect rational levels of each contributing elementary distribution. For a design envelope condition the maximum realistic amount of a modal distribution is defined by the \bar{A} value for that distribution times U_g . For a predominant mission segment the maximum value is set equal to the value read from the frequency of exceedance curve for that distribution. This is, however, an approximation and some latitude is allowed.

Generation of Matching Conditions

Each design condition consists of a portion a_1 of distribution E_1 , a_2 of distribution E_2 , etc. A set of coefficients $\{a_i\}$ defines both a complete set of panel loads and integrated loads (response quantities) throughout the airplane. The objective of the matching procedure is then to define sets of coefficients $\{a_i\}$ that match the design load combinations previously discussed. The problem is represented as one of linear optimization of the form:

$$[E \mid I] - \begin{Bmatrix} a \\ s \\ p \end{Bmatrix} = \begin{Bmatrix} \text{Design} \\ \text{Load} \\ \text{Combination} \end{Bmatrix} \quad \text{Eq. (14)}$$

The above expression is developed in Reference 12 and is comprised of both equalities and inequalities. The inequalities are obtained from the equations that define the design octagon boundary lines. Equalities correspond to the equations that define the phased design load combinations for which a design condition is desired. Constraints are applied to the problem such that:

- All loads will lie within their design octagon boundary lines
- The allowable magnitude of any elementary distribution is limited based on psd results
- Each solution, set of $\{a_i\}$ coefficients, contains the minimum number of elementary distributions with the smallest contribution possible to obtain a design condition.

Conditional Probability Method

The Conditional Probability Method is a typical variation of the Matching Condition procedure that is applied by one of the U.S. manufacturers.

Load combinations for a number of response quantities are defined based on the statistical dependency relationships. These load combinations are then matched by manipulating "generic" external force distributions, rather than elementary distributions, to produce design conditions that are applied to stress models to develop internal loads or to work with transformation matrices that relate internal to external loads.

PSD gust analysis flight conditions are selected based on the criterion applied, Mission Analysis or Design Envelope. The phased loads are defined as the expected values of load distribution that will occur when a selected envelope load is a maximum. These distributions are defined

based on the conditional probability density function. Under the condition that y takes on the value y_m , the expression, shown in Reference 13, Appendix A, is:

$$P(x|y = y_m) = \frac{P_{xy}(x, y_m)}{P_y(y_m)} = \frac{1}{\sigma_x \sqrt{2\pi} \sqrt{1 - \rho_{xy}^2}} \exp \left\{ -\frac{x - \frac{\rho_{xy} y_m \sigma_x}{\sigma_y}}{2\sigma_x^2 (1 - \rho_{xy}^2)} \right\} \quad \text{Eq. (15)}$$

The expected value of load x given load y_m is then:

$$x = \frac{\rho_{xy} \sigma_x}{\sigma_y} y_m \quad \text{Eq. (16)}$$

This is equivalent to selecting load combinations corresponding to points "T" on the design ellipse shown in Figure 10.

When the design envelope approach is used, y_m represents a specific load for a specific configuration and flight condition. For the mission analysis, the loads reflect a weighted average of all the individual segments that compose the complete mission. Therefore, the phasing formula is modified by the fraction of total mission time in each segment to account for the phasing associated with each individual mission segment.

When a complete set of external loads in equilibrium is required for use with a finite element stress model, phased external loads are used to define discrete force distributions for application at selected nodes of the model. The number of node points available to apply external forces typically exceeds the number of external loads calculated by PSD gust analysis. The algorithms that define the node external forces assume generic distributions for the undefined degrees of freedom. Different distributions are normally assumed for the aerodynamic as opposed to the inertia forces in the matching process. Three types of phased PSD loads are calculated: net loads, aerodynamic loads, and inertia loads. The matching procedure algorithms are subject to the constraint that the integration of the applied nodal forces must be in equilibrium and must reproduce the phased PSD load combination.

Equivalent Discrete Gust

One of the older concepts of defining external load distributions that represent psd results is that of an equivalent discrete gust. To the best of the author's knowledge, this method has not been used as the primary design procedure by any company in meeting continuous turbulence criteria for commercial transports. This approach should not be confused with the Statistical Discrete Gust (SDG) concept that has been developed by J. G. Jones as a possible alternative to PSD analysis.

The procedure is, basically, to define discrete gust conditions that match the airplane translational and rotational accelerations about the center of gravity as defined by PSD analysis. The resulting time history solutions are assumed to produce properly phased external loading distributions. These conditions are then factored to match specific PSD loads at various locations on the airplane.

For a relatively "stiff" airplane, with minimal dynamic modal response, this procedure produces a rational set of external load distributions. However, for more flexible aircraft, a method of defining the probable external load pattern, similar to that discussed in Reference 14 for SDG application, would seem to be necessary.

The procedure is used primarily during the preliminary design phase to assist in defining those areas of the structure that are potentially critical for gust loading. It can also be used to provide balanced external load distributions for use in various matching procedures.

Internal Load Method

As the name implies, the Internal Load Method directly computes internal load responses in the PSD gust analysis. Unit load coefficients are defined that relate the selected internal stresses to unit external loads applied at each individual structural grid point. The procedure is really no different than the computation of integrated external loads. Usually two internal loads or stresses are sufficient to size a structural panel so the problem of phasing three or more external load quantities is eliminated. Correlation coefficients are applied to define a design ellipse which can then be directly applied by the Stress Department.

As was stated earlier, the number of psd's required to apply this method throughout the airplane is very large. Application of the procedure is normally limited to local areas of structure with complex loading patterns that are also quite sensitive to gust loading.

An internal load method called the Joint Probability Technique is developed in Reference 4. This method is not currently in use and will not be discussed here.

Approach

The general approach to sizing structure from psd results is basically that of a pyramid or hierarchy of increasing complexity.

At the lowest level, areas of the structure that are subjected to potentially critical gust loading are identified by simply comparing the loads or stresses obtained from the psd analysis directly to design envelopes obtained for other types of load conditions, such as maneuver, static and discrete gust, or dynamic landing and taxi conditions. Because of differences in fuselage pressurization, care must be taken when comparing psd results with ground load conditions. The maximum design values of each load or stress are applied without regard to phasing, only the design values are used. This comparison will establish both areas of the structure and the quadrant in which the gust loading is potentially critical. The procedures discussed above are then applied to the extent required to define the design stress levels.

Of these procedures, Matching Conditions, or a variation such as the Conditional Probability, is applied by all of the U.S. manufacturers that were surveyed. The Equivalent Discrete Gust approach is used primarily as a tool to provide additional information on areas of the structure that are potentially sensitive to gust loading and to provide external force distributions for "matching." The Internal Load Method or the use of three dimensional load combinations in the Matching Condition approach are applied only to areas of the structure with complex internal load patterns for which gust loads are actually the critical design condition.

ACTIVE CONTROLS CONSIDERATIONS

The active control system (ACS) developed for the L-1011 extended span configuration involved symmetric motion of the outboard ailerons. This was phased with cg acceleration to relieve static gust and maneuver loads and with wing tip velocity to increase elastic mode damping. Installation of the ACS was intended to offset the load increase due to the increase in wing span, in order to minimize the extent of structural changes.

Loads due to corrective roll control in turbulence were explicitly included in the dynamic gust analysis for the L-1011 airplane configuration with active controls. The following background information contributed to this decision.

Background

Analysis of flight test data from the L-1011 development flight test program in 1971 indicated that the measured wing torsions were much greater than predicted by theory. The ratio of measured to predicted torsions was largest just inboard of the outboard aileron and just inboard of the inboard aileron. At these locations the measured torsions were 1.5 to 3.0 times the theoretical values. Bending moments and shears, however, were more in line with theory. The increased torsions were not coherent with the measured gust velocity, which suggested the presence of other inputs. Although the first wing antisymmetric bending mode appeared to be a contributor, high coherencies between wing torsion and aileron angle indicated that corrective roll control was also a major source of the increase in torsions.

Fortunately there was sufficient strength available in the basic L-1011 airplane to accommodate the measured torsions. The effect of the increased torsions was thereafter included in all derivatives of the L-1011 up to the development of the active controls system by applying an empirical "flight test torsion increment". Because the active controls aircraft represented a significant departure from prior derivatives, a rational approach to account explicitly for the loads due to corrective roll control in turbulence was found to be necessary.

Flight tests were conducted during 1977 and 1978, using the L-1011 flight test airplane, as part of a NASA-Lockheed funded program to evaluate the use of active controls for loads reduction. These tests were made first on the baseline span airplane without active controls and then with the span increased 9 feet by means of wing tip extensions. The results of these tests, reported in Reference 15, showed that the active controls greatly reduced the loads due to gust, L_G , by as much as 50% in the outer wing. But they had no effect on the loads due to roll control. As a result the roll control loads became much more conspicuous. Bending moments and shears as well as torsions were seen to be involved.

Loads due to corrective roll control have always been present when roll control is by means of the outboard ailerons. In the past, these loads have been small relative to loads produced directly by the vertical gusts. As a result, they have been adequately provided for by an implicit conservatism in the design gust velocities (or, in a mission analysis determination of gust loads, in the design frequency of exceedance). But, as noted above, an active-controls wing load alleviation system substantially reduces the vertical gust loads, while leaving the corrective roll control loads unchanged. Consequently, the percentage effect on loads of the corrective roll control increases.

Further, this increase is accentuated by the fact that the two loadings - gust and roll control - add on a root-sum-square basis. For example, if roll control loads, without active controls are 50 percent of the gust loads then:

Without Active Controls

Loads due to vertical gust	- L_G	- 1.0
Loads due to roll control	- L_{RC}	- 0.5
Combined loads	- $L_G + RC = \sqrt{1^2 + 0.5^2}$	- 1.118
Ratio	- $(L_G + RC) / (L_G)$	- 1.118

Although the roll control load is 50% of the vertical gust load, the combined load is increased by only 12 percent. If active controls are used and wing vertical gust loads are reduced by 50% the result is:

With Active Controls

Loads due to vertical gust	= L_G	= 0.5
Loads due to roll control	= L_{RC}	= 0.5
Combined loads	= $L_G + RC = \sqrt{0.5^2 + 0.5^2}$	= .707
Ratio	= $(L_G + RC) / (L_G)$	= 1.414

The increase with active controls is substantial, L_{RC} relative to L_G increases by a factor of 2.0, but the increase in increment in net load due to roll control is a much larger factor of $0.414/0.118 = 3.51$.

From this example it is clear that the increase in gust loads due to corrective roll control must be explicitly considered for any airplane that accomplishes roll control by means of the outboard ailerons and for which an active control system is used to reduce wing loads. In the more general context it can be stated that an active control system can significantly alter the contribution from vertical or lateral gust to combined loads. Special procedures may then be required to accurately predict the resulting gust design load.

The concepts and analysis methods that were used to include corrective roll control effects in the gust design wing loads for the L-1011 Tristar with active controls are summarized below. Based on all available information, which includes operational flight data, flight test data, flight simulator data, and additional theoretical studies, they provided a realistic set of design loads.

Other than for the L-1011, no attempt was made in these studies to explicitly determine when, or whether, or to what extent roll control effects should be included in a dynamic gust loads analysis. Therefore, this discussion is presented primarily to increase awareness of the subtleties involved in the use of an active controls system on the determination of design gust loads.

General Approach

Design gust loads for the basic L-1011 were obtained using the mission analysis approach. The procedure to explicitly include loads due to corrective roll control for the active controls configuration was then defined for mission analysis application.

Results of the basic L-1011 mission analysis showed that the cruise segments were the greatest contributor to wing loading. This was expected, since cruise represents approximately 80 percent of the time in flight. In addition all of the cruise segments exhibit similar wing response characteristics. The cruise segment that contributed most heavily to the wing shear and bending loads at critical wing locations was then selected for explicit roll control analysis. This is referred to as the predominant segment. The effect of other segments, climb and descent, was estimated using a parametric procedure and simplified exceedance curves. Factors were developed to adjust shear, bending and torsion at a number of locations over the wing span. These loads were phased using a combined correlation coefficient method, and design load conditions were developed for stress analysis using the matching condition process.

3-D GUST ANALYSIS

Extensive use was made of a three-dimensional gust analysis computer program that utilizes the work of Dr. Frederick D. Eichenbaum of Lockheed-Georgia Company, References 16, 17 and 18. An existing Lockheed-California one-dimensional program was modified to include the computation of gust input cross spectra and computation of output spectra utilizing these input cross spectra and the computed transfer functions.

The term "three-dimensional" refers to the number of position coordinates upon which the gust velocity is assumed to depend. The most important variation of the gust velocity is along the flight path. This is normally the only variation considered, which results in a "one-dimensional" gust analysis. The three-dimensional analysis considers also, on a statistical basis, the spanwise variation of vertical gust velocity. It also considers, although these are less important, the vertical variation of the vertical gust velocity, and the vertical and lateral variations of the lateral gust velocity. In addition, it combines vertical and lateral inputs into a single analysis.

Basically, the three-dimensional gust analysis consists of three steps:

1. Determination of transfer functions relating the various airplane loads to gust velocities acting on specific streamwise gust strips.
2. Determination of the power spectra of gust velocity on the various strips and cross spectra of gust velocity for all strip pairs. The gust power spectrum on any individual strip is simply the usual one-dimensional gust power spectrum. Three-dimensional effects are brought in by the cross spectra.
3. The transfer functions and the gust velocity spectra and cross spectra are combined to determine response psd's, cross spectra between pairs of response quantities, and cross transfer functions that relate various responses to the gust velocity at a gust probe, for comparisons with flight-measured transfer functions and coherencies. These are then used as in a one-dimensional analysis to provide \hat{A} 's, N_0 's and correlation coefficients.

Steps 2 and 3 were accomplished using Eichenbaum's basic equations as presented in Reference 18. The only simplification was to drop the fore-aft component of turbulence. (Although the fore-aft component may become significant in landing approach, it has only a small effect at the higher airplane speeds that produce the critical gust loads.) These equations not only retained provision for variation of vertical and lateral gust velocities in the y and z directions, but also provided for orientation of the individual lifting surface segments.

The program allowed 20 gust input strips for a half-airplane (15 were used) and included provision for arbitrary dihedral angles and arbitrary locations in the y-z plane. The gust velocity was considered to vary linearly from a maximum at the strip centerline to zero at the adjacent strip centerlines. Computation of the various gust velocity cross spectra was facilitated by applying the planar and nonplanar coherencies tabulated in Reference 18. The arrangement of the gust strips, defined for the L-1011 studies, is shown in Figure 15.

The three-dimensional gust analysis was applied to determine the effect of roll control by the autopilot. It was also used to help select the appropriate autopilot mode. (Some pilots prefer a variation of the CWS (control-wheel-status) such as attitude hold, rather than the turbulence mode, when in turbulence; for the L-1011 the roll control rms aileron angle values, σ_{δ_a} 's were about 10% higher in CWS status than in the turbulence mode.)

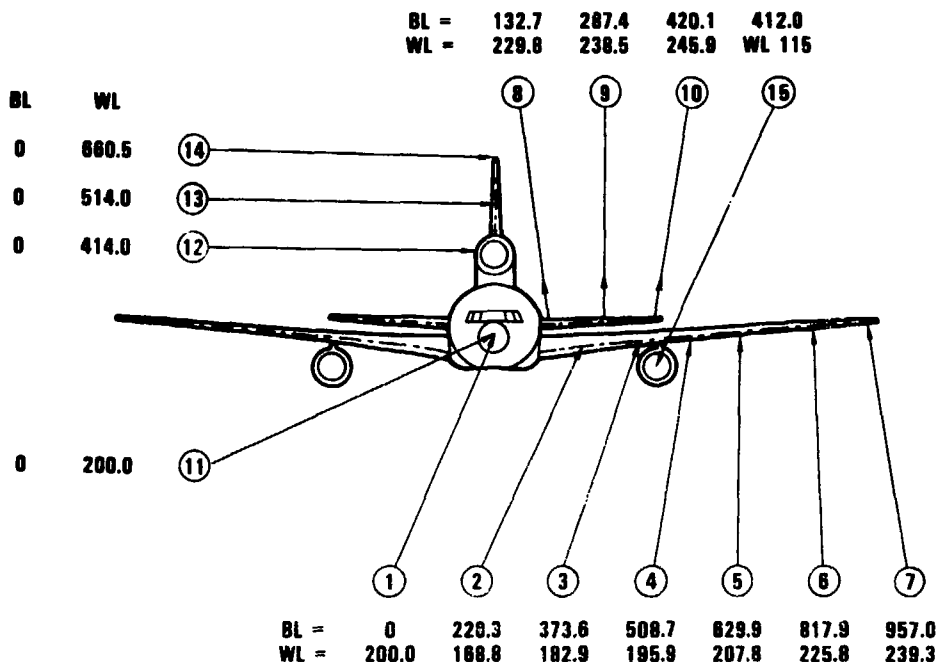


Figure 15. Gust Strip "Centerlines" Used in 3-D Gust Analysis

Loads obtained from the 3-D gust analysis were somewhat lower than the corresponding one-D loads. It was therefore necessary to design to slightly higher gust velocities in order to retain the concept of equivalent strength used in setting the gust criteria design velocities which were determined from a one-D gust analysis. Based on a comparison of several L-1011 cases, it was concluded that the 3-D loads should be increased by a factor of 1.07. It is noted that this factor has much broader applicability than just to the determination of corrective roll effects. If 3-D analysis were to become routine for gust loads determination, the value of this factor would be of primary importance.

In the original design study, 3-D analysis was performed for a predominant mission analysis cruise segment with an altitude of 32,000 feet and Mach Number of .85. Later studies included additional cruise segments and some climb and descent segments. Studies were obtained to determine the effect of ACS-on and off with and without the autopilot, the effect of different autopilot modes, the effect of dihedral, and the effect of the number of structural airframe modes on the computation of stability derivatives.

RMS Aileron Angle

The parameters required to determine loads due to both autopilot and pilot roll control are the rms aileron angle, the aileron angle ρ_{ad} , and, for each response quantity to be analyzed, the ratio of the roll control load component to the rms gust velocity, \bar{A}_{RC} .

The magnitude of corrective roll control aileron angles in turbulence depends upon the turbulence intensity and the flight condition. It is reasonable to expect the rms (root-mean-square) aileron angle, σ_{δ_a} , to vary in proportion to rms gust velocity. A key parameter in the analysis is then the rms aileron angle as a ratio to rms gust velocity, or \bar{A} , which can be expected to vary with flight condition.

In addition the amount of corrective roll control is likely to vary from pilot to pilot, between pilot and autopilot, and from one turbulence encounter to another for the same pilot. As a result, selection of a design \bar{A}_{δ_n} involves judgment in evaluating all of the available data.

Data on the L-1011 rms aileron angle were obtained from a number of sources.

- L-1011 gust response flight tests and flight simulator tests
- L-1011 operational data
- L-1011 3-dimensional gust analysis with autopilot roll control

Data from three flight test programs were available. Seven bursts of from one to four minutes duration were available from the original L-1011 flight test program conducted in 1971. Three bursts were available from the 1977 program and five from the 1978 program. Roll control was by the pilot, except for a limited amount of data from the 1978 tests.

Flight simulator data were available for three different pilots. These data were taken as averages of six 5-minute samples for pilot No. 1 and four each for the other two pilots. This program was conducted in 1978 utilizing the 1977 flight test conditions.

Operational data were obtained from British European Airways (BEA) AIDS tapes. For the original analysis only five samples were available, all from the same flight. The data were questionable and the analysis was quite crude. However, for later studies, 50 additional records were available from British Airways and Gulf Airways, also obtained by means of the AIDS system. Twenty-two of these records were analyzed for the roll control study. As a condition of CAA certification, British Airways continued to obtain such data, of which 17 records were reduced for use in the roll control analysis.

Tabulated values from the AIDS system included CG acceleration with a sampling rate of 8 per second and aileron angle once per second. Rms values of these quantities were calculated from the time histories. Rms gust velocity was then determined from the rms CG acceleration by means of a procedure utilizing an extensive set of curves developed by Lockheed in prior studies, in which the continuous turbulence gust response factor, K_{σ} , was computed and plotted as a function of four dimensionless rigid airplane parameters.

These curves are based on simple theory. The airplane is considered rigid, but is allowed to pitch as well as plunge. The effect of gust penetration on pitch is neglected, and unsteady lift growth is accounted for only with respect to the gust input, not the airplane motions. The Von Karman shape of gust pd is assumed.

The curves were adjusted to agree with results given by the more sophisticated analytical methods used for the L-1011 by back-figuring K_{σ} for a number of mission analysis flight segments. It was found that applying a factor of 1.13 to the plunge-only curve developed from simple theory provided a good representation for the L-1011, Figure 16. The relation of $\sigma_{\Delta n}$ to σ_w is then given as:

$$\bar{A}_{\Delta n} = \frac{\sigma_{\Delta n}}{\sigma_w} = K_{\sigma} \frac{\rho V_T^2 S C_{L_{\alpha}}}{2W} = K_{\sigma} \frac{V_T}{g \delta} \quad \text{Eq. (17)}$$

where

$$\delta = \frac{2W}{\rho S C_{L_{\alpha}}}$$

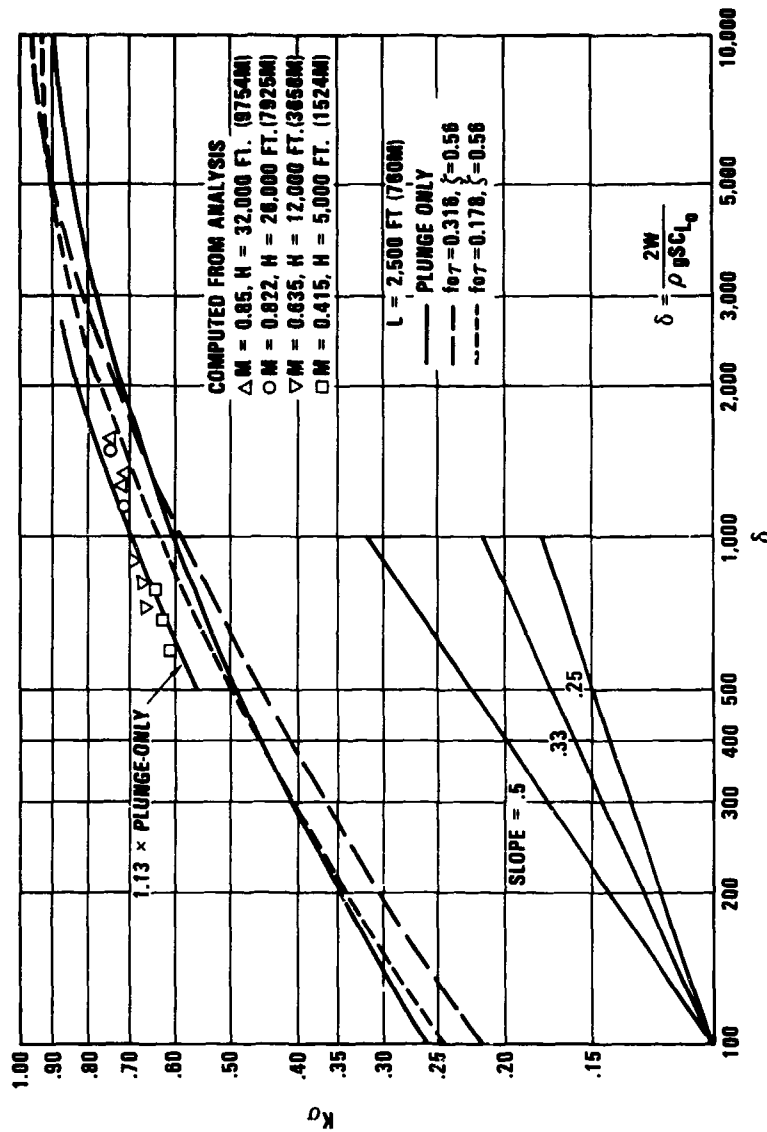


Figure 16. Gust Response Factors Based on Simple Theory

Three-dimensional theoretical data were obtained for evaluation of the autopilot primarily from the predominant mission segment. Because the autopilot is expected to do essentially the same job as the pilot, it should require approximately the same amount of aileron as the pilot to do it. The pilot response, however, is not as likely to be Gaussian.

In all cases, the rms aileron angle was computed and related to the associated rms gust velocity. Both the rms aileron angle and gust velocity were adjusted to give "effective" values corresponding to a reference flight condition.

The use of an effective value allows direct comparison of data from various flight conditions. It is based on the concept that as the flight condition and turbulence vary, the roll control δ_a applied by the pilot will be such as to give a rolling moment proportional to the rolling moment caused by the turbulence. It is believed that the gust induced rolling moments are primarily due to lateral gust working through the rolling moment due to sideslip stability

derivative, $C_{l\beta}$. This parameter is then a key value in obtaining the effective values for σ_w . The reference flight condition was defined as:

h - sea level altitude

V_e - 300 Knots

M - 0.45

W - 350,000 lb

which yields:

$$\sigma_{w_{eff}} = \frac{\sqrt{\rho/\rho_0}}{1} \frac{V_e}{300 \text{ knots}} \frac{C_{l\beta}}{C_{l\beta_{ref}}} \frac{K_\sigma}{K_{\sigma_{ref}}} \frac{\sigma_w}{1} \quad \text{Eq. (18)}$$

and

$$\sigma_{\delta_a_{eff}} = \left(\frac{V_e}{300 \text{ knots}} \right)^2 \frac{C_{l\delta_a}}{C_{l\delta_a_{ref}}} \sigma_{\delta_a} \quad \text{Eq. (19)}$$

where

ρ - density of the atmosphere, ρ_0 - sea level value

V_e - equivalent airspeed

$C_{l\delta_a}$ - rate of change of rolling moment coefficient with aileron angle

$C_{l\beta}$ - rate of change of rolling moment coefficient with sideslip angle

K_σ - ratio of rms sideslip angle produced by continuous turbulence to rms "sharp-edge" gust sideslip angle

The operational data (except for the very early, questionable five data points) is plotted in Figure 17. (The flight test and simulator data points are not shown, but they displayed a similar trend.) The solid line represents $\bar{A}_{\delta_a_{eff}}$ for the autopilot as determined from the 3-D analysis. The dashed line is a least square approximation for the pilot related data. The effective value of \bar{A}_{δ_a} for the autopilot was 0.240 deg/fps and for pilot control 0.210 deg/fps. In the original design study 0.240 was used for both pilot and autopilot. Actual values of \bar{A}_{δ_a} for a given flight condition are then obtained by reverse application of the above parametric relationship.

Aileron Angle PSD and \bar{A}_{RC}

Loads due to autopilot roll control could be obtained directly from the 3-D analysis. However, for pilot roll control, it was necessary to establish an aileron angle psd for computation of the roll-control loads. This was done by examining the psd shapes obtained from various test flights, flight simulator tests, and theoretical (autopilot) cases. Four typical psd shapes were selected, shown in Figure 18. Ratios of rms wing load to rms aileron angle for pertinent wing load quantities were calculated for each psd shape, on the basis of aileron input only. The two most severe sets of loads were then averaged to give a set of ratios for use in design.

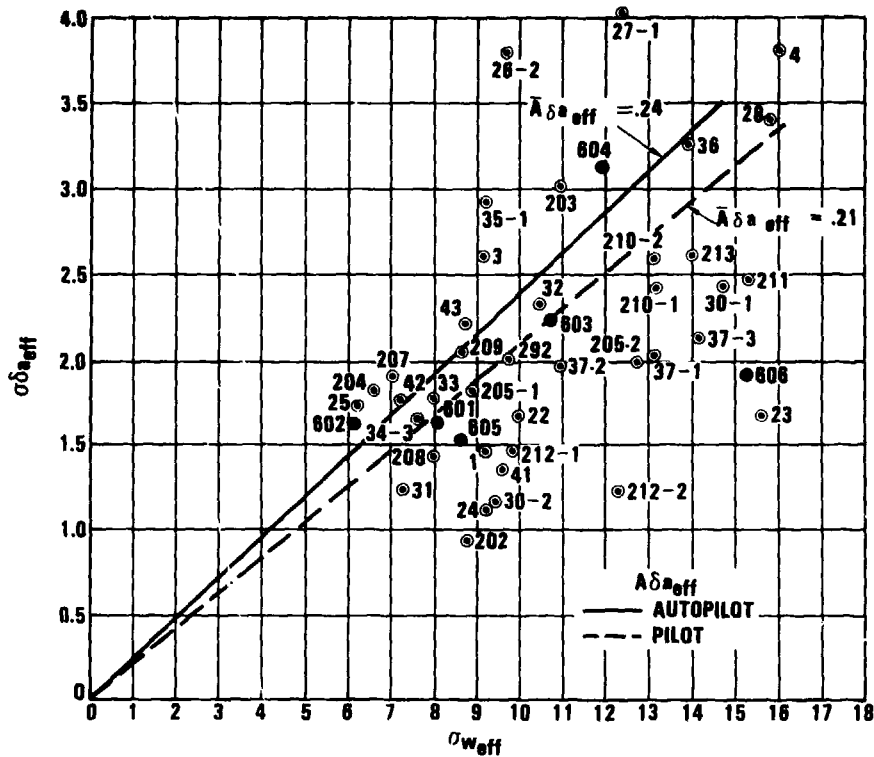


Figure 17. Operational Data on Relation of Effective RMS δ_a to Effective RMS Gust Velocity

Multiplying these ratios by \bar{A}_{δ_a} yields the ratio of the roll control load component to rms gust velocity, \bar{A}_{RC} , that is:

$$\bar{A}_{RC} = \frac{\text{Rms } L_{RC}}{\sigma_w} = \left(\frac{\text{Rms } L_{RC}}{\text{Rms } \delta_a} \right) \left(\frac{\text{Rms } \delta_a}{\sigma_w} \right) = \left(\frac{\text{Rms } L_{RC}}{\text{Rms } \delta_a} \right) \bar{A}_{\delta_a} \quad \text{Eq. (20)}$$

Loads Due to Roll Control, L_{RC}

The roll control component for each load quantity can then be calculated as:

$$L_{RC} = U_o \times \bar{A}_{RC} \quad \text{Eq. (21)}$$

In the original design analysis, roll control effects were explicitly obtained for one predominant mission segment. For this approach, U_o was calculated separately for each load quantity from the expression:

$$U_o = \frac{L_e - L_{1g}}{\bar{A}} \quad \text{Eq. (22)}$$

where

L_e = Limit design value of the load quantity from the mission analysis exceedance curves

L_{1g} = One-g value of the load quantity for this mission segment

\bar{A} = Ratio of rms load to rms gust velocity for this mission segment

For the predominant segment, which was selected based on the contribution of wing shears and bending moments, U_g averaged about 105. This means that in order for design gust loads to be encountered during this mission segment a design gust velocity of 105 fps is required. The U_g value was then limited to 105. Torsions generally required a higher design gust velocity to reach their design levels, indicating that this particular flight segment was not critical for torsion.

Combined Loads - Phasing

The combined loads due to gust and roll control were computed from the following equation:

$$L_{G+RC} = \sqrt{L_G^2 + L_{RC}^2} \quad \text{Eq. (23)}$$

where L_G is the statistically defined gust increment value $L_e - L_{1g}$, factored by the effects of control system saturation and unavailability (reliability).

The effect of the increment in load due to roll control was included in the phasing by adjusting the expression for computing correlation coefficients to account for a second uncorrelated input. For any two load quantities the expression becomes:

$$\rho_{x+u, y+v} = \frac{\rho_{xy}\sigma_x\sigma_y + \rho_{uv}\sigma_u\sigma_v}{\sqrt{\sigma_x^2 + \sigma_u^2} \sqrt{\sigma_y^2 + \sigma_v^2}} \quad \text{Eq. (24)}$$

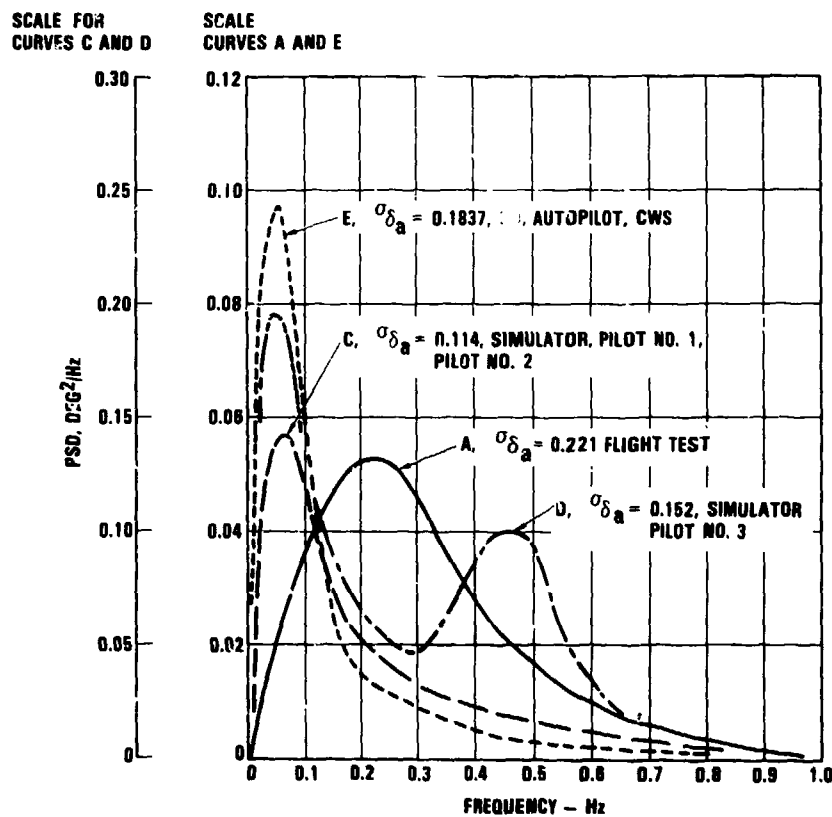


Figure 18. Paired PSD's of Roll Control Aileron Angle

where

ρ = correlation coefficient

σ = \bar{A} , rms value

x, y, u and v denote load quantity and input source, for example, correlations for shear or bending to torsion are defined as shown in the following table. However, the expression is valid for any two load quantities, not just shear or bending to torsion.

	Load Quantity	
	S or B	T
Input Gust	x	y
RC	u	v

The effect of roll control on the correlation of wing bending and torsion is illustrated in Figure 19. The effect on the correlation of wing shear and torsion was similar. The correlation of these loads tended to become more negative, shifting loads on a design shear-torsion or bending torsion envelope from quadrant I toward quadrant II, and broadening the load envelope in general.

Other Segments Factor

Primary emphasis for determining the effect of roll control was placed on the predominant mission analysis segment. However, the climb segments are at lower altitude with a higher equivalent airspeed and tended to yield a higher ratio of L_{RC} to L_G . For these segments the $\bar{A}_{\delta a}$'s were estimated using the parametric approach as:

$$\bar{A}_{\delta a} = \frac{\sqrt{\frac{\rho}{\rho_0} \left(\frac{C_{l\beta}}{C_{l\beta_{ref}}} \right) \left(\frac{K_0}{K_{0_{ref}}} \right)}}{\left(\frac{V_b}{300 \text{ knots}} \right) \left(\frac{C_{l\delta a}}{C_{l\delta a_{ref}}} \right)} \bar{A}_{\delta a_{eff}} \quad \text{Eq. (25)}$$

The effect on loads was then determined by constructing simplified exceedance curves for a limited number of segments within each profile. The exceedance curves for the individual segments were then adjusted to reflect the relative severity of the roll control effects. The sum curves with and without adjustments were then compared. The resulting factor was applied in addition to the $L_G + RC / L_G$ factor obtained based on the predominant segment.

Other Considerations

The effect of control system saturation and reliability should be accounted for in the design loads. It was noted earlier that this was done by applying suitable factors. From prior studies the effect of system unavailability on loads was estimated as a factor of 1.01.

Control system saturation is an entire subject by itself. The methods used to account for saturation of the I-1011 active controls system are reported in an AIAA paper, Reference 19. With respect to roll control a separate study indicated that saturation tended to reduce the increase in loads due to corrective roll control. This effect was not included in the study.

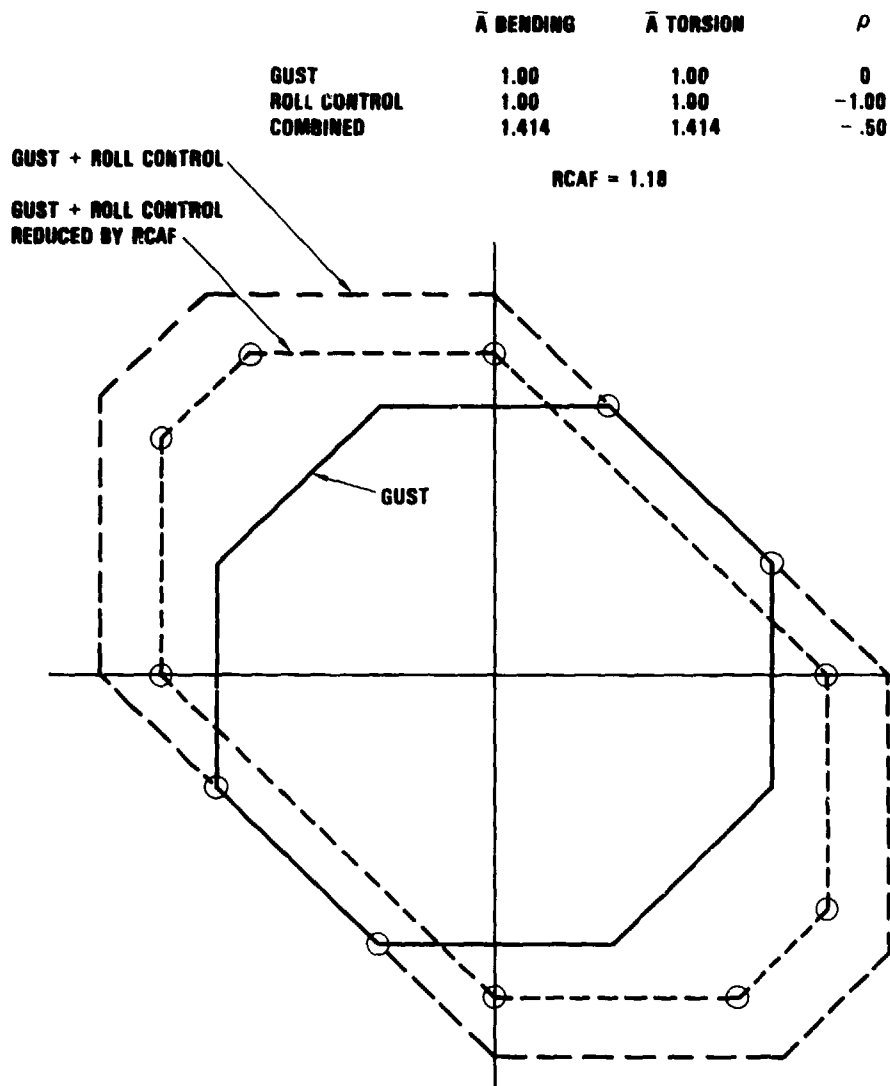


Figure 19. Effect of Roll Control on Bending-Torsion Gust Load Octagons

Roll Control Accountability Factor, RCAF

Continuous turbulence design gust criteria are based on the concept of equivalent strength with past airplanes that have a satisfactory service life. Three reference airplanes were used in establishing the criteria, the Lockheed Model 749 Constellation, the Lockheed Electra (Model 188), and the Boeing Model 720B. Although the Boeing airplane limited the use of outboard ailerons for roll control to the flaps extended configurations, the Lockheed models used outboard ailerons for roll control throughout their flight envelopes. As a result the design gust velocities, U_0 , and the 2×10^{-5} design frequency of exceedance include the effects of roll control by means of the outboard aileron for aircraft without active controls. Therefore, the effect of loads due to corrective roll control is included only to the extent that the percent increase due to roll control

with active controls exceeds the percent increase without active controls for the same airplane, that is:

$$\text{Design Load} = \frac{\text{Load ACS-on with roll control}}{\frac{\text{Load ACS-off with roll control}}{\text{Load ACS-off without roll control}}}$$

In the above expression, the numerator represents various phased load combinations at a given location with the full effect of roll control. The denominator is referred to as the "roll control accountability factor" or "RCAF." This is the factor by which the loads would increase due to roll control if the airplane were designed without an active control system. This effect was included as follows.

First, gust loads were obtained with the active control system present and the full effect of roll control included. These loads were then divided by the "roll control accountability factor." If, for example, roll control increased the gust loads by 66 percent with active controls and 31 percent without, the with-active-control loads would be divided by 1.31. In this example the RCAF is the factor 1.31.

The RCAF was evaluated separately at each wing station. It was found to vary from 1.01 at the wing root to 1.31 at Buttline 833 (85 percent semi-span). This variation is shown in Figure 20. It is seen that the roll control effects are relatively small at the root but become large near the wing tip.

Additional studies were later performed with the intent of developing general procedures separately for use with mission analysis and design envelope analysis that eliminated use of the RCAF. The primary approach has been to identify conservatisms in the methods and data used to obtain the loads due to corrective roll control. It appeared that, with only fairly modest reduction in the roll control loads, perhaps in combination with a very small reduction in design gust velocities, the net loads (gust plus roll control) might be sufficiently reduced so that the RCAF would not be necessary. Although these studies have shown some promise, they have not yet yielded a design procedure that is ready for general application.

As a result only the original design procedure has been presented here; more work remains to be done before a more general procedure is ready to use.

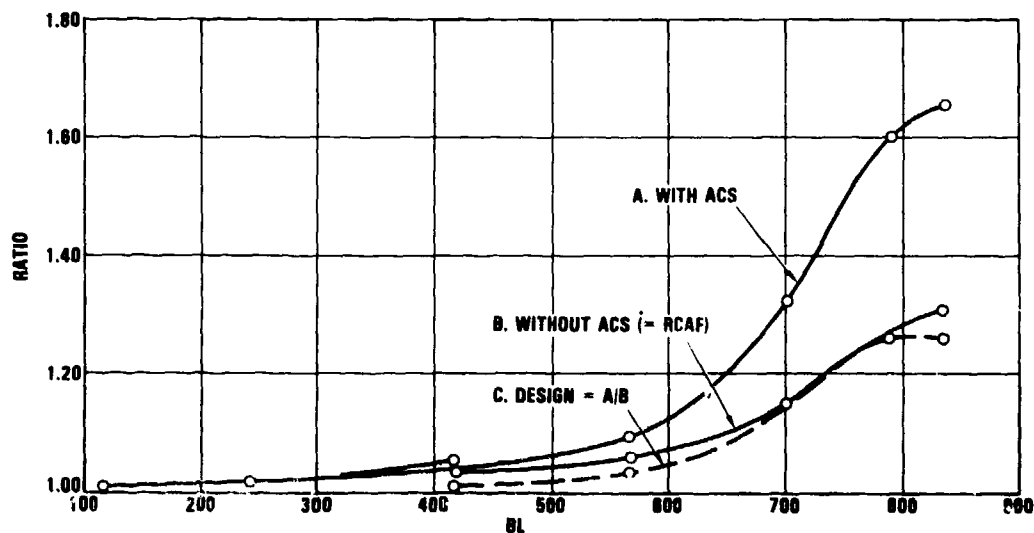


Figure 20. Spanwise Variation of $L_G + RC / L_G$ for Wing Bending

SUMMARY COMMENTS

Both the Mission Analysis and Design Envelope criteria were developed from the concept of equivalent strength with past airplanes that have a satisfactory service life. If an airplane is operated in a manner that is considerably different than these past airplanes, the design gust loads on the new airplane will be different depending on which of the two criteria is used. It is important to understand the differences in criteria to assure that the criterion selected for analysis will indeed give realistic loads for the new airplane.

The most common method of determining internal loads and stresses for the design and sizing of structure from the psd results is that of "Matching Conditions" or variations of this approach. The selection of load combinations to be matched and the use of rational external force distributions in the development of the design conditions are of primary importance. The general approach is to identify areas of the structure that are potentially critical for gust loading based on a conservative comparison of the PSD gust loads with other types of conditions. The more complex analysis procedures are then applied to these areas of the structure.

Application of the psd continuous gust design criteria to airplanes designed with active controls and gust load alleviation systems presents a challenge. This is an area where considerable analysis, development effort, and possibly new methods will be required in the coming years. The use of three-dimensional gust analysis procedures is likely to be beneficial.

ACKNOWLEDGEMENTS

The author is grateful to Richard M. Heimbaugh of Douglas Aircraft Company and Joe J. Nishikawa of Boeing Commercial Airplane Company for their assistance in supplying information on methods of applying continuous gust design criteria to the design and sizing of structure.

The study of loads due to corrective roll control presented here was conducted by Frederic M. Hoblit before his retirement from Lockheed-California Company. The author is grateful for the support and advice provided by Mr. Hoblit during the preparation of this paper.

REFERENCES

1. Hoblit, F. M., "Gust Loads on Aircraft: Concepts and Applications." American Institute of Aeronautics and Astronautics Education Series, scheduled for publication: May 1988.
2. "Federal Aviation Regulations - Part 25 - Airworthiness Standards: Transport Category Airplanes." Department of Transportation, Jan. 1984 Rev., Federal Aviation Administration, Washington D.C.
3. Hoblit, F. M., Paul, N., Shelton, J. D., and Ashford, F. E., "Development of a Power Spectral Gust Design Procedure for Civil Aircraft," FAA-ADS-53, Jan. 1966, Federal Aviation Agency, Washington D. C.
4. Fuller, J. R., Richmond, L. D., Larkins, P. C., and Russell, S. W., "Contributions to the Development of a Power-Spectral Gust Design Procedure for Civil Aircraft," FAA-ADS-54, Jan. 1966, Federal Aviation Agency, Washington D. C.
5. Joint Airworthiness Requirements, JAR-25 Large Airplanes, Civil Aviation Authority, Cheltenham, 1986 Rev.
6. MIL-A-008861A(USAF), "Military Specifications - Airplane Strength and Rigidity Flight Loads," 31 March 1971
7. Austin, W. H. Jr., "Development of Improved Gust Load Criteria for United States Airforce Aircraft," SEG-TR-67-28, 1967
8. MIL-8861B(AS), "Military Specifications - Airplane Strength and Rigidity Flight Loads," 7 Feb. 1986
9. Rice, S. O., "Mathematical Analysis of Random Noise," Bell System Technical Journal, Vol. XXIII, No. 3, July 1944, pp 282 - 332. In Wax, Nelson: Selected papers on Noise and Stochastic Processes, Dover Publications, New York, 1954.
10. Stauffer, W. A. and Hoblit, F. M., "Dynamic Gust, Landing, and Taxi Loads Determination in the Design of the L-1011," Journal of Aircraft. Vol. 10. No. 8, pp. 459 - 467, August 1973.
11. Stauffer, W. A., Lewolt, J. G., and Hoblit, F. M., Application of Advanced Methods to the Determination of the Lockheed L-1011 Tristar," AIAA Paper No. 72-775, 1972.
12. Moon, R. N., "Application of Linear Optimization Theory to Development of Design Load Conditions from Statistical Analyses," AIAA/ASME 20th Structures and Structural Dynamics Conference, Paper No. 79-0740, 1979.
13. Noback, R., "The Generation of Equal Probability Design Load Conditions, Using P.S.D. - Techniques," NLR TR 85014 U, National Aerospace Laboratory NLR, Amsterdam, The Netherlands, Jan 1985.
14. Jones, J. G., "On the Development of Structural Design Load Conditions from Statistical Analyses of Aircraft Response to Turbulence," Royal Aircraft Establishment Technical Memorandum FS(F) 504, London, February 1983.
15. NASA CR 159097, "Accelerated Development and Flight Evaluation of Active Controls Concepts for Subsonic Transport Aircraft - Vol. I, Load Alleviation/Extended Span Development and Flight Tests," September 1979.
16. Eichenbaum, F. D., "A General Theory of Aircraft Response to Three-Dimensional Turbulence," Journal of Aircraft, Vol. 3, No. 5, pp. 353-360, May 1971.
17. Eichenbaum, F. D., "Response of Aircraft to Three-Dimensional Random Turbulence," AFFDL-TR-72-28, October 1972.
18. Eichenbaum, F. D., "Evaluation of 3-D Turbulence Techniques for Designing Aircraft," AFFDL-TR-74-151, March 1975.
19. Gould, J. D., "Effect of Active Control System Nonlinearities on the L-1011-3(ACS) Design Gust Loads," AIAA Paper No. 85-0755, AIAA/ASME/ASCE/AHS 26th Structures, Structural Dynamics, and Materials Conference, Orlando, FL, April 15-17, 1985.

COMPARISON OF THE INFLUENCE OF DIFFERENT GUST MODELS ON STRUCTURAL DESIGN

by

Manfred Molzow
 Chief Structural Dynamics
 Messerschmitt-Bölkow-Blohm GmbH
 Civil and Transport Aircraft Division
 P.O. Box 950109, 2103 Hamburg 95
 Federal Republic of Germany

Abstract:

Depending on the country of certification different gust models and means of compliance of the airworthiness requirements have to be covered in structural design of civil transport aircraft.

The influence on aircraft design from

- gust models
- A/C modelling
- control systems/laws

is demonstrated on example of a short to medium range transport aircraft.

Recommendations for future harmonized approaches in gust methods and modelling will be given.

A b b r e v i a t i o n s

AA	Airworthiness Authority
A/C	Aircraft
CAA	Civil Aviation Authority
DGAC	Direction Generale de l'Aviation civile
FAA	Federal Aviation Agency
LBA	Luftfahrtbundesamt
RLD	Rijksluchtvaartdienst
STPA	Service Technique des Programmes Aeronautiques
FAR 25	Federal Airworthiness Requirements (US)
JAR 25	Joint Airworthiness Requirements (Europe)
NV	National Variant
AC	Advisory Circular
SC	Special Condition
IM	Interpretative Material
EDP	Electronic Data Processing
EFCS	Electrical Flight Control System
FBW	Fly By Wire
LAS	Load Alleviation System
CT	Continuous Turbulence
MA	Mission Analysis
DEA	Design Envelope Analysis
SDEA	Supplementary DEA
DG	Discrete Gust
DTG	Discrete Tuned Gust

MoC	Means of Compliance	
TAS	True Airspeed	
EAS	Equivalent Airspeed	
U _d	Derived Gustvelocity (fps, EAS)	
U _e	Gustvelocity (fps, TAS) in CT	
\dot{c}	Gustgradient	
QF	quasi flexible	
FF	full flexible	
NZc	Loadfactor	
V _c	Crusing speed	
$\dot{\theta}$	rate of attitude	
ϕ	Bank angle	
$\dot{\phi}$	bank angle	Indices:
$\ddot{\phi}$	rate of bank angle	c commanded
r	roll velocity	
β	sideslip angle	

1.0 Introduction

Different from military fighters the large transport aircraft up to relatively large grossweights are designed by gusts in big parts of their structural components.

Being so, the component weight and the overall standard of safety during flying in gusts will depend on

- Gust Models
- A/C Modelling
- Systems Introduction

used in static design work. But the manufacturer is not free in the choice of models, neither in

Gusts

nor in

Aircraft

He is rather guided by existing regulations or their related and by authorities accepted means of compliance.

Although flying around in the same atmosphere all over the world, different countries require through their airworthiness authorities different Gust and A/C models.

AA normally defend their since centuries nearly unchanged position by stating:

THE EXISTING LEVEL OF SAFETY MUST NOT BE ERODED

Nobody will and can oppose to that, the question is:

WHEN IS EROSION STARTING?

The author believes, based on discussions with several AA in this field that sometimes the improvements against the past in

- more and more sophisticated investigations of gusts in relation to masses, c.G., massdistributions, Mach, altitude and dynamic pressure using extensively EDP
- physical and numerical methods
- correction of data by ground and/or flight tests
- extensive service experience with former designs
- weather radar and improved weather forecast by satellites
- extensive use of qualified equipment and systems on board

is not adequately taken into account in this judgement.

Therefore, while accepting the requirement for a high safety standard, there is on the other hand the danger

TO PENALIZE A/C DESIGNS BY UNNECESSARY CONSERVATISMS

The truth will be - as always - a very narrow path. Therefore very openminded discussions will be needed, to get real progress in this field. But let us first review the today's situation.

2.0 Comparison of Requirements and Interpretations

2.1 Gust Requirements

The requirement situation for large transport A/C and the different interpretations represented by the following national airworthiness authorities will be reflected (Fig 1) .

COUNTRY	REGULATION	AA
Germany	JAR 25	LBA
France	JAR 25	STPA/DGAC
Great Britain	JAR 25 + NV	CAA
NETHERLANDS	JAR 25 + NV	RLD
USA	FAR 25	FAA

Fig. 1. Airworthiness Requirements and AA in different countries

NV stands for national variant and means that in this country additional to the basic rule a special gust-requirement exists. Also in the case where the requirement basis is similar, different means of compliance and interpretations from one country to another might be valid, as later will be shown. (Fig. 2)

Gust Requirements					
Gust Model	Basic JAR 25		Nat. Variants		FAR 25
	Ude		GB	NL	
Pratt		100 %			Formula
		Quasi Pratt (1 - cos) 12.5 c - const.			
	A/C	Q.F.			or
Discrete Gust	Ude	90 %	90 %		100 %
		(1 cos) 12.5 c - const.	(1 cos) fused	Req. Gust for Wing	(1 cos) 12.5 c - const.
	A/C	F.F.	F.F.	Q.F.	Q.F.
Continuous Turbulence	U ₀ *	75 fps Mission or Design Envelope Analysis			75 fps (78 fps) Mission or Design Envelope Analysis
	A/C	F.F.			F.F.

Fig. 2. Gust requirements in different regulations

* Floor Level for Supplementary DEA, $U_0 = 60$ fps

2.2 Aircraft Modeling

Besides the already existing differences in gust requirements as shown in chapter 2.1, different A/C models are required by the forementioned AA.

These differences are mainly

- how flexibility
- if and how unsteady aerodynamic forces

are taken into account.

Whilst in the requirements exists a clear statement how flexibility has to be considered, it is normally left to the manufacturer how unsteady lift is introduced.

So all AA are in agreement that in CT-investigations

- dynamic response for
- the full flexible A/C taking into account steady and unsteady lift

have to be considered.

The question how many modes and frequencies and which unsteady lift theory will be taken to have an optimal representation of the A/C lies in the hands of the manufacturer.

The situation is different in the required discrete gust models. The QF-approach, A/C regarded as frozen under deformation, is accepted (see figure 2) from

- FAA for Pratt-Formula and the (1-cos) gust.
- RLD for their N.V. of the negative gust.
- Basic JAR 25 as "Quasi Pratt", but in combination with a FF discrete (1-cos) gust.

For DTG the CAA and for the DG with 90% Ude all other European authorities require the FF-A/C.

The term "Quasi Pratt" is used here for a complete A/C response calculation of a (1-cos) gust, but suppressing the effect of the flex modes and frequencies.

2.3 Effect of Control Systems and Control Laws

In history the only systems effect came in by

- autopilots
- autostabilizers
- yawdampers.

Normally for design the A/C was conservatively regarded without these systems and the effect had only to be demonstrated by a supporting study.

This situation has changed since modern transports have EFCS (FBW) with Control Laws and sometimes Load Alleviation Systems.

It is self-evident that AA in this situation will request that

- systems have to be introduced in the A/C modelling

to prevent that the loads situation does not become worse than for the conventional A/C.

Accepting this, the interest of the manufacturer is that

- systems effects are taken into account also there, where it means benefits for the structure

and that this is adequately accepted by AA.

Naturally the problem starts with the different opinions represented by AA and industry about the meaning of

adequately.

The existing requirements do not cover this area at all.

The FAA gives in its Advisory Circular

AC 25.672
"Active Flight Controls"

some advice.

The JAA have together with European industry in the frame of an actual A/C design established a special condition to JAR 25

SC - A 2.1.1.

together with interpretative material

IM - A 2.1.1.

"Certification Criteria for an A/C designed with systems interacting with structural Performance"

The European paper goes further, as can already be seen by the heading, and covers - to the opinion of the author - the problem more appropriate.

Both papers are derived from actual necessities in the different countries and will need - having now more experience - a critical review, update and generalisation. A lot of conservatism is in the early papers, taking into account the lack of experience and the fear of the AA to erode safety.

In between the term "adequate" needs a revised interpretation, not to destroy the attraction of these new systems, which also brought an improvement in handling for the manufacturer by insisting on old unjustified conservatisms.

Fig. 3 to 6 give for control systems of modern transport A/C in schematic sketches.

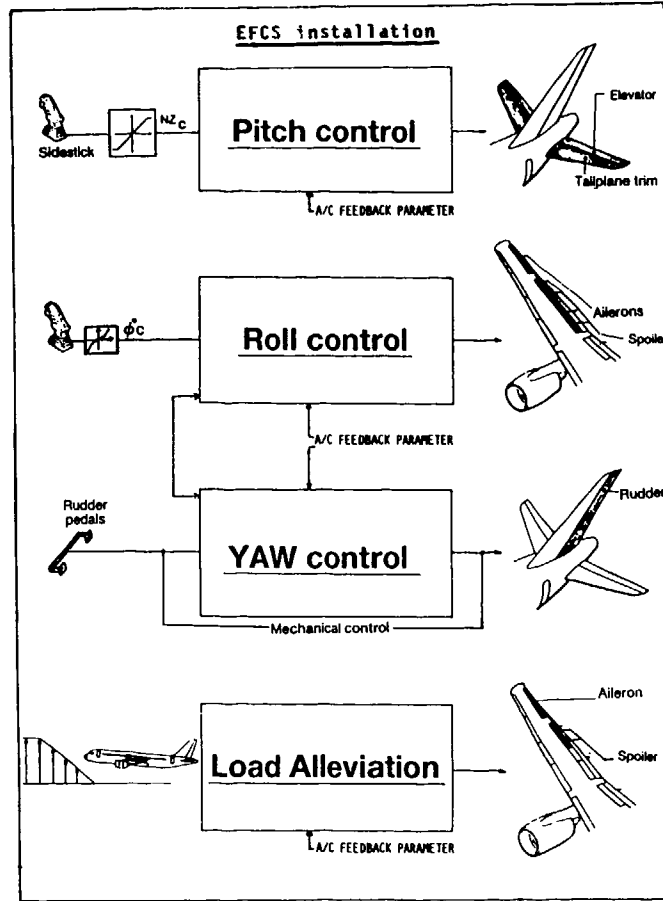


FIG. 3 CONTROL LAW REALISATION FOR LOADS

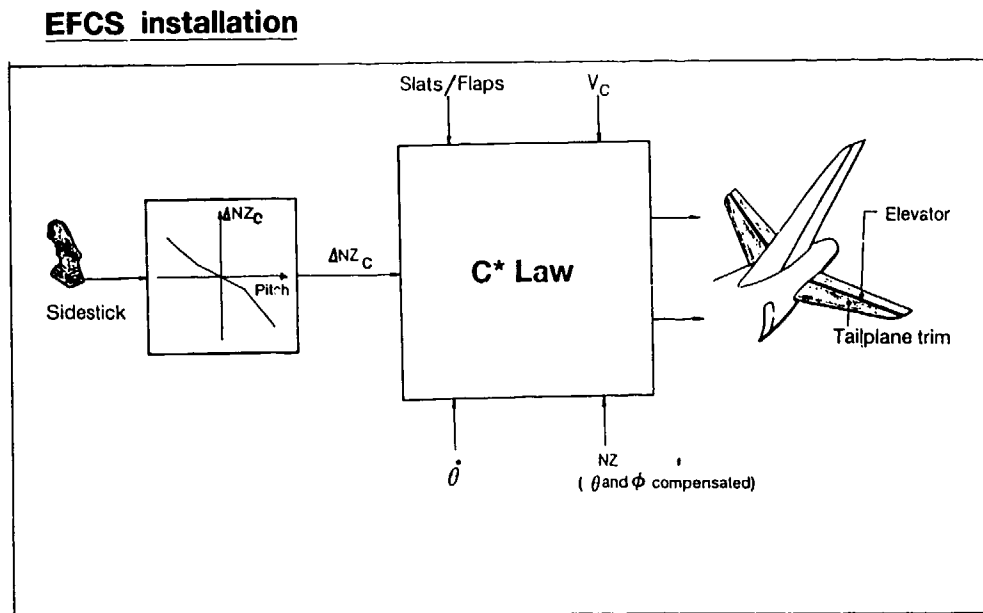


FIG. 4 CONTROL LAW REALISATION FOR LOADS - PITCH AXIS

EFCS installation

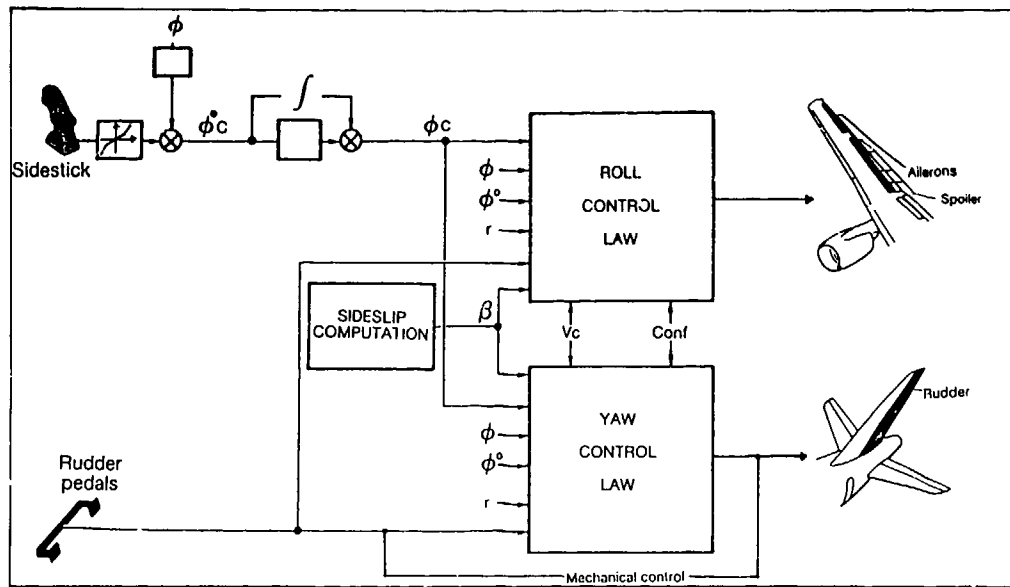


FIG. 5 CONTROL LAW REALISATION FOR LOADS - YAW + ROLL AXES

EFCS installation

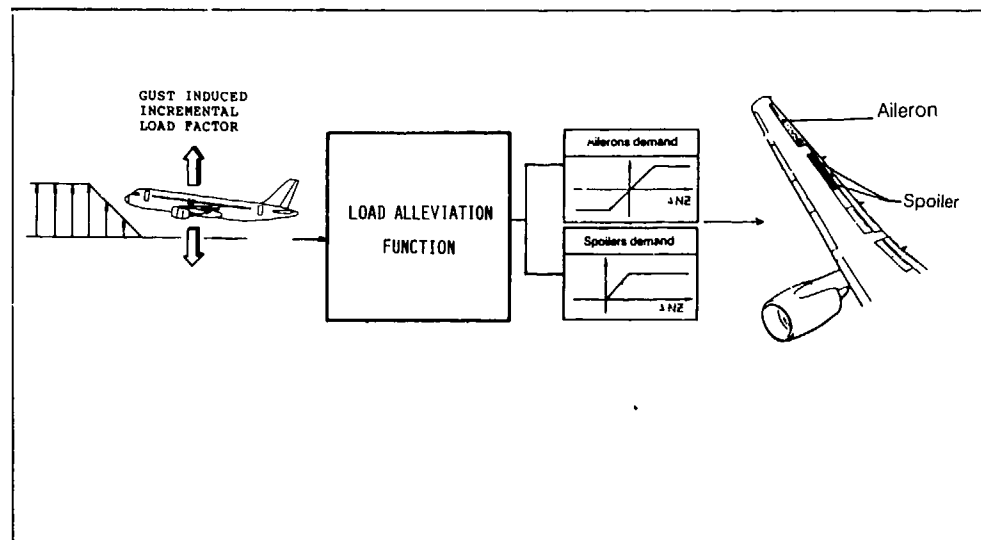


FIG. 6 CONTROL LAW REALISATION FOR LOADS - LOAD ALLEVIATION

3.0 Influence of Requirements on Static Design Load Levels

The influence of the different national requirements and its means of compliance on the static design load level of a large transport A/C, which is designed in major parts by gusts, is demonstrated in the following figures.

As representative quantities were chosen,

for Vertical Gust

- wing bending
- tail bending

for Lateral Gust

- fuselage bending
- fin bending

Further the influence of introduction of control systems, control laws and load alleviation on the Vertical and Lateral Gust Load Level is shown.

3.1 Vertical Gust

The following gustmodels and MOC are compared:

- Vertical Gust Load Level due to European/American requirements (Fig. 7 and 8)
All system effects inclusive load alleviation are included.

CT (85 fps. TAS) - reference level
with
CT (75 fps. TAS)
DG + DTG / 100% resp. 90% Ude/FF
DG / 100% Ude / QF

For the wing (Fig. 7) it is found that the DG and DTG-Level with the European interpretation to be calculated FF gives a load level even higher than the JAA load level due to CT (85 fps).

The FAA approach with the chance of CT (75 fps) in special cases and the DG interpreted QF gives a marked lower load level.

For the tailplane the highest gust load level is found also for the JAA gust interpretation with the DG interpreted QF next, both higher than CT.

- Vertical Gust Load Level due to British National Variant
(Fig. 9 and 10)
Systems as before.

DG / 90% Ude/FF - reference level
with
DTG / shaping law with max. 90% Ude/FF

Fig. 9 and 10 show the effect of the gust shaping due to the UK-National Variant. It is found that at wing and tailplane depending on the spanwise station the National Variant produces the higher load level. This means that at components, where CT is below DG, the DTG will give the design case.

- Vertical Gust Load Level, effect of pitch control law and load alleviation
(Fig. 11 and 12)
DG / 90% Ude/FF pitch control law and LAS incl reference level

with
DG / 90% Ude FF pitch control law included
DG / 90% Ude FF no systems included.

For the wing (Fig. 11) it is found that the introduction of the pitch control law gives the same level as the conventional A/C. This is different for the tailplane where the pitch control law introduction leads to an increase of tailplane loads in relation to all "systems introduced" where the conventional A/C leads to an underestimation.

FIG. 7 : WING BENDING MOMENT RATIO (JAA/FAA)

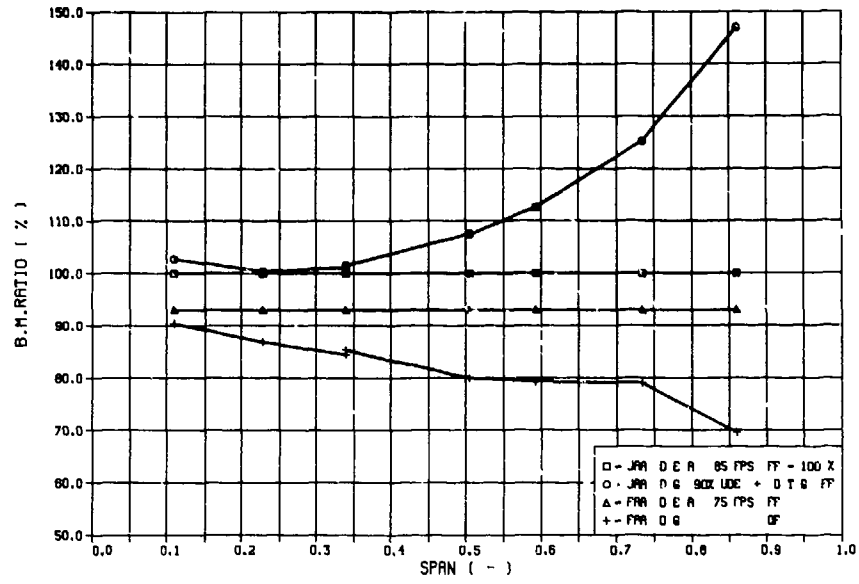


FIG. 8 : TAIL BENDING MOMENT RATIO (JAA/FAA)

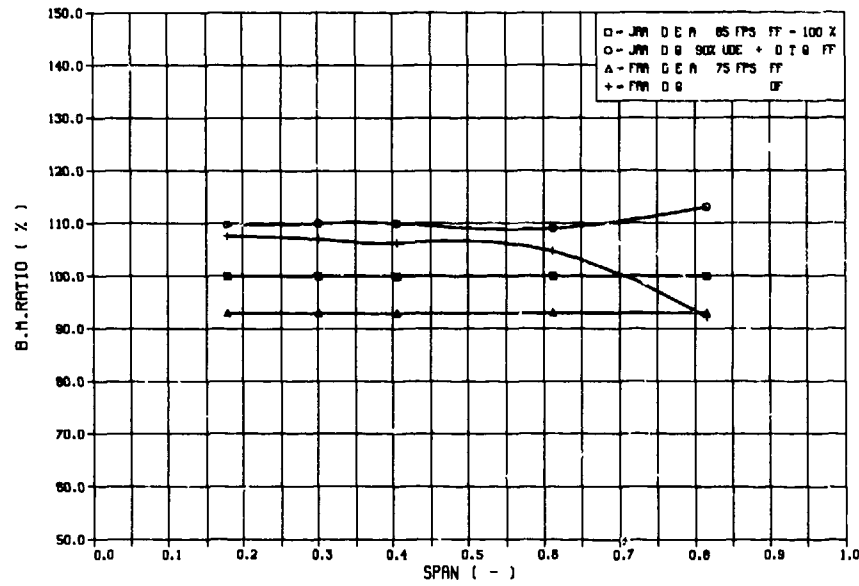


FIG. 9 : WING BENDING MOMENT RATIO (W)

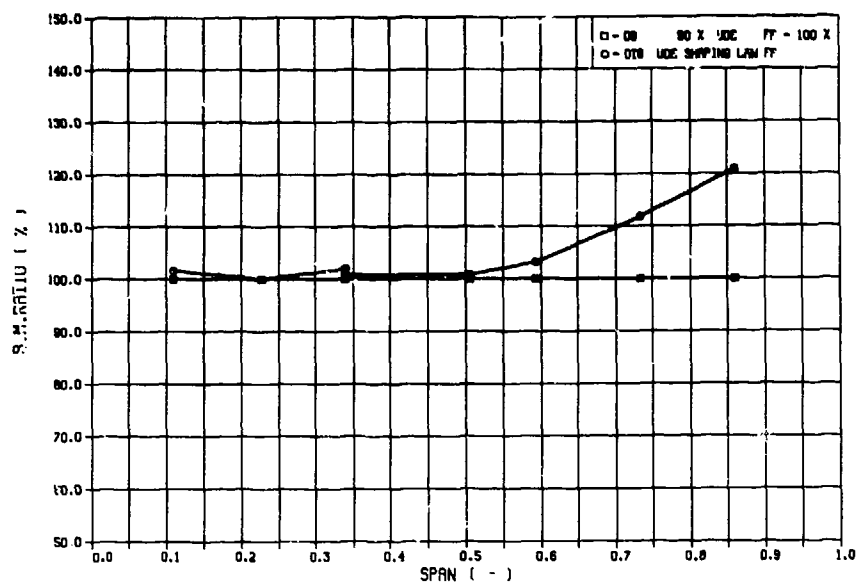


FIG.10 : TAIL BENDING MOMENT RATIO (W)

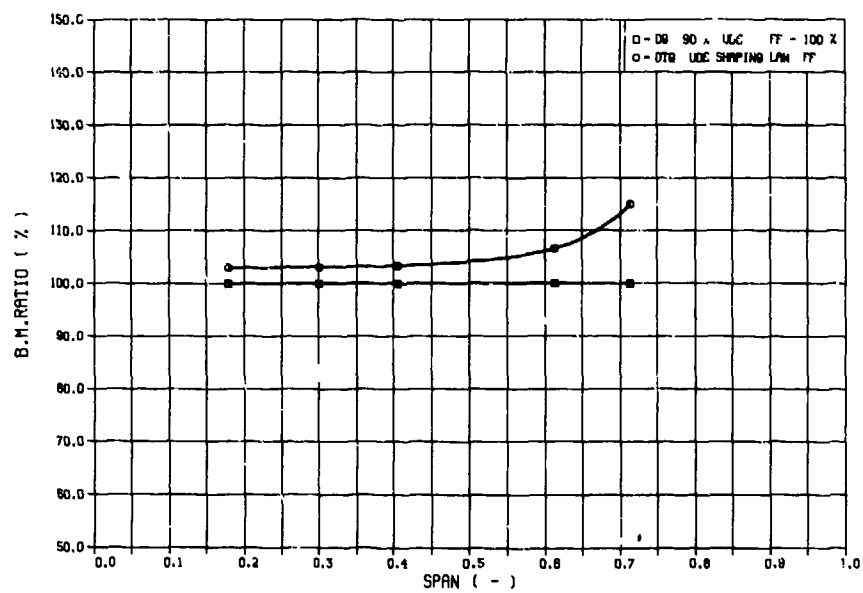


FIG.11 : WING BENDING MOMENT RATIO (SYSTEMS)

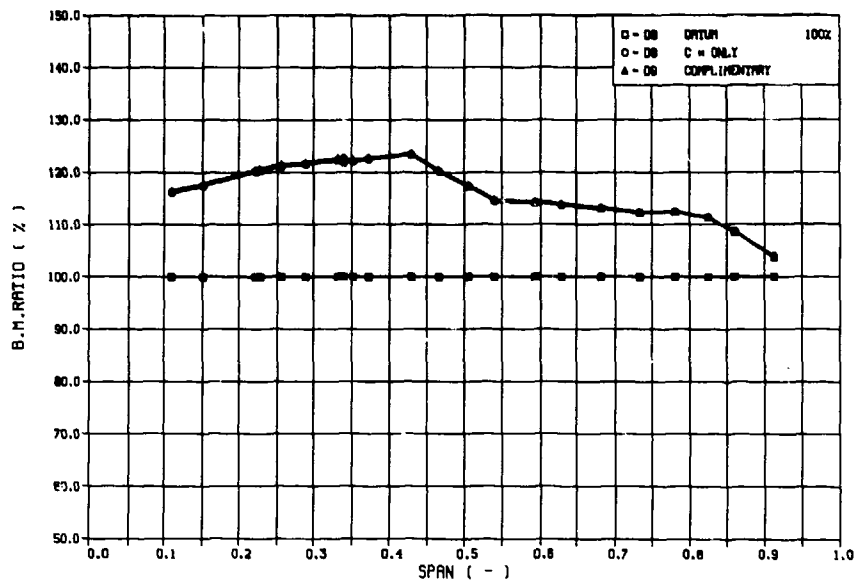
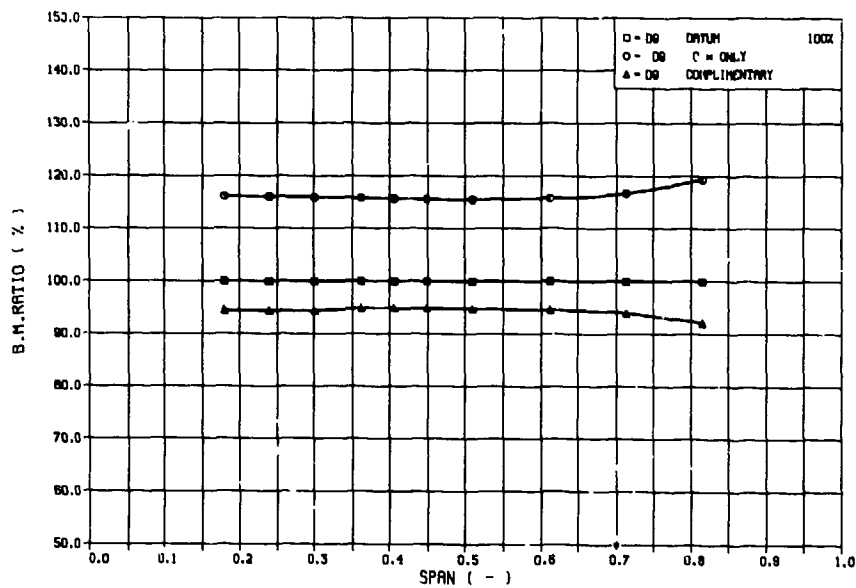


FIG.12 : TAIL BENDING MOMENT RATIO (SYSTEMS)



3.2 Lateral Gust

The following gustmodels and MOC are compared:

- Lateral Gust Load Level due to European/American requirements (Fig. 13 and 14) The influence of systems and control laws was not introduced.
 CT (85 fps, TAS) - reference level
 with
 CT (70 fps, TAS)
 DG + DTG / 100% resp. 90% Ude/FF
 DG / 100% Ude/QF

The JAR 25 requirement basis inclusive the NV and its usual MOC lead to a higher load level as well in continuous turbulence as in discrete gust than FAR 25 and its usual interpretations.

- Lateral Gust Load Level due to British National Variant (Fig. 15 and 16). The influence of systems and control laws was not introduced.

DC / 100% Ude / FF - reference level
 with
 DTG / shaping law with max 90% Ude / FF
 This NV gives a higher to equal load level for the fuselage and a lower one than discrete for the fin. In this design the CT-level is dominating all components in lateral gust which must not always be the case.

- Lateral Gust Load Level, effect of systems and control laws (Fig. 17 and 18)
 CT (85 fps, TAS) without EFCS - reference level
 with
 CT (85 fps, TAS) with EFCS, 100% operating

The introduction of systems, especially yawdamper function and lateral control laws leads in general to reductions of gust loads because of its damping effect of the dutch roll. It is obvious that if this level is taken for design, system failure cases have to be investigated. IM-A2.1.1 defines a safety factor as function of failure probability of occurrence to calculate ultimate load. (Fig. 19 and 20) These figures illustrate the high importance of a reliable system on structural weight.

FIG.13 : FN BENDING MOMENT RATIO (JAA/FAA)

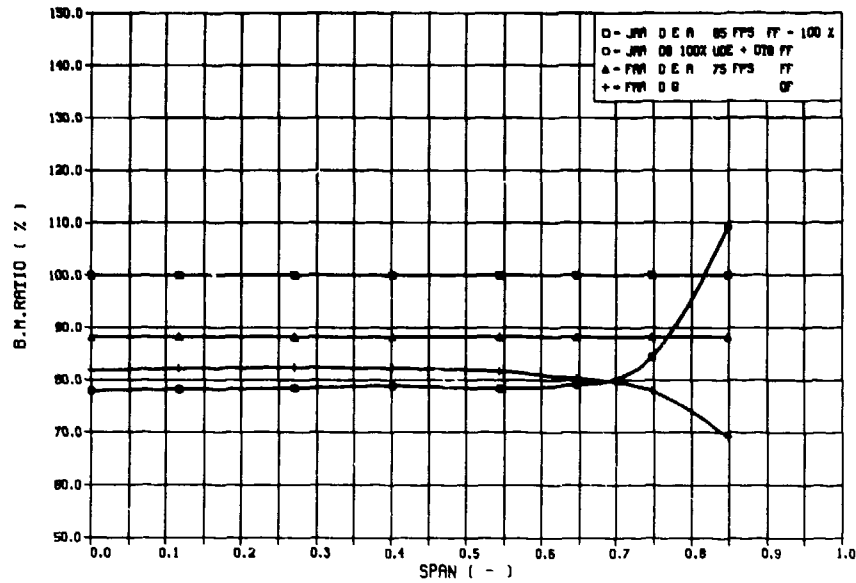


FIG.14 : FUSELAGE BENDING MOMENT RATIO (JAA/FAA)

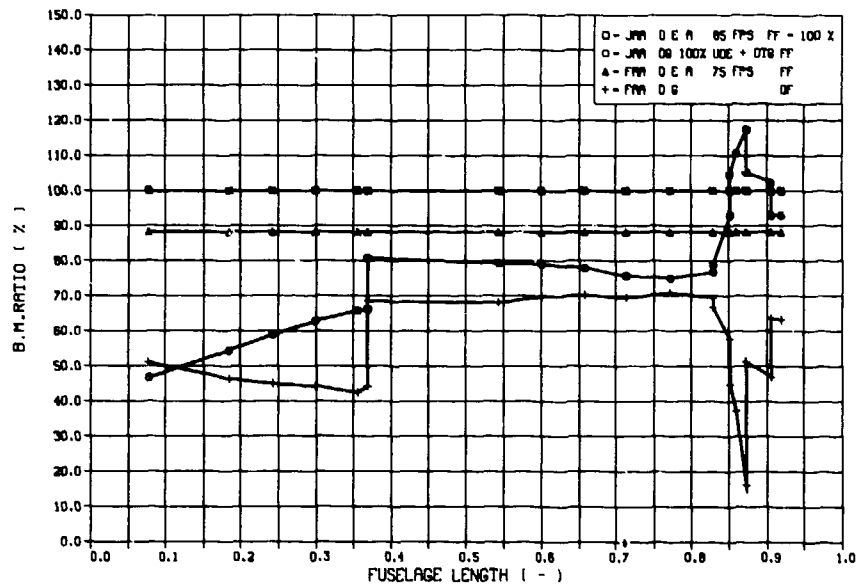


FIG.15 : FIN BENDING MOMENT RATIO (NV)

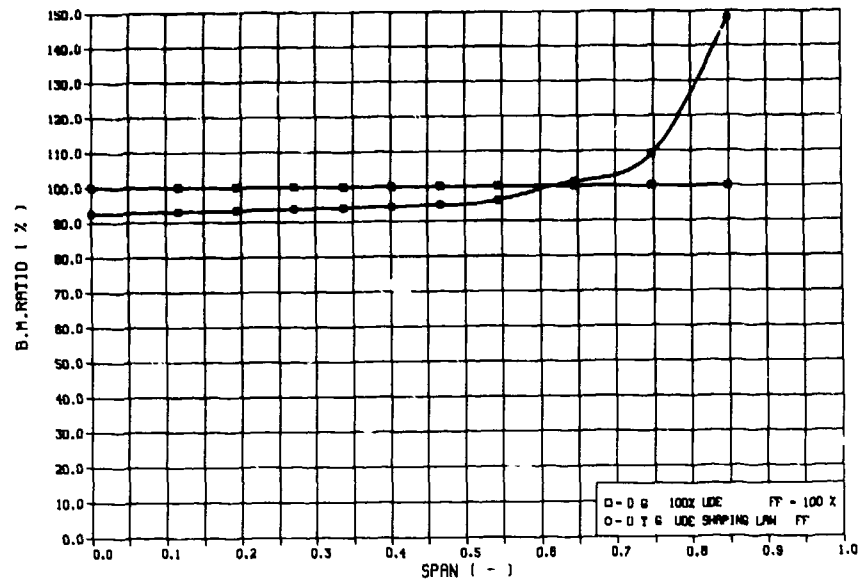


FIG.16 : FUSELAGE BENDING MOMENT RATIO (NV)

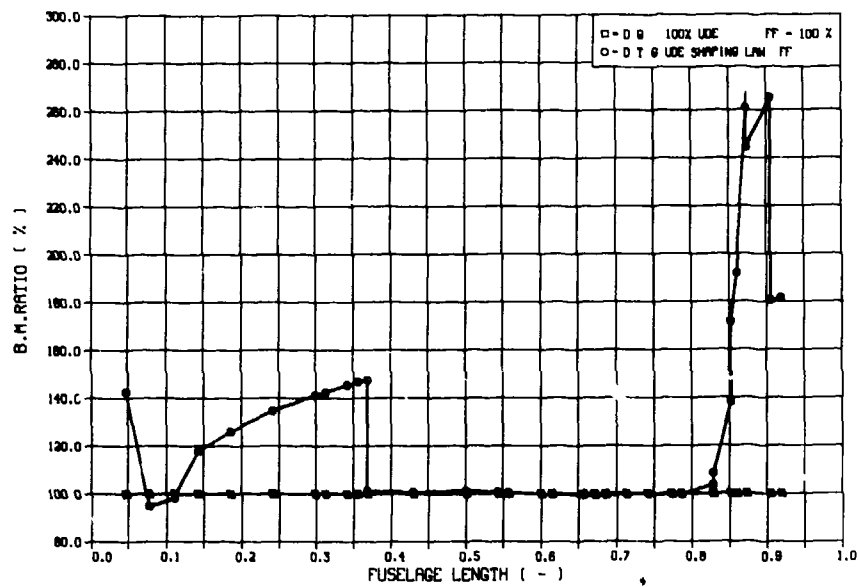


FIG.17 : FN BENDING MOMENT RATIO (SYSTEMS)

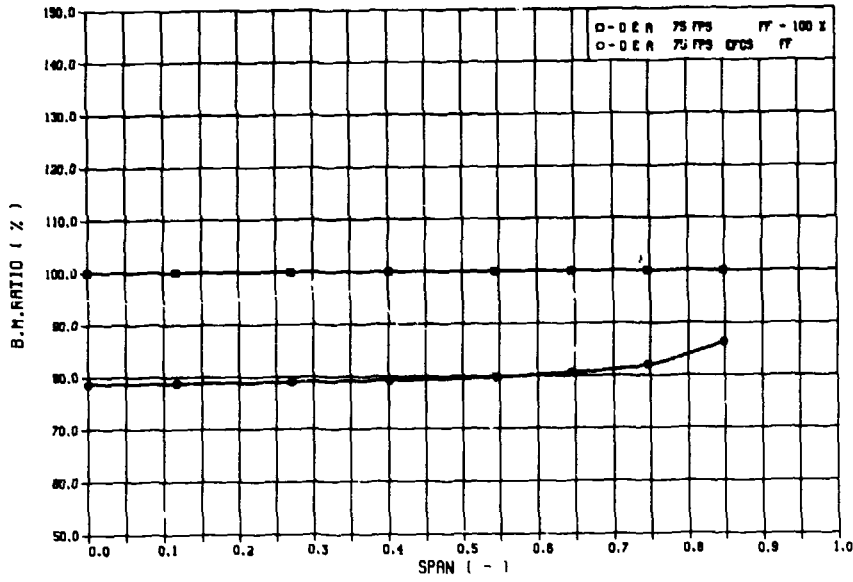
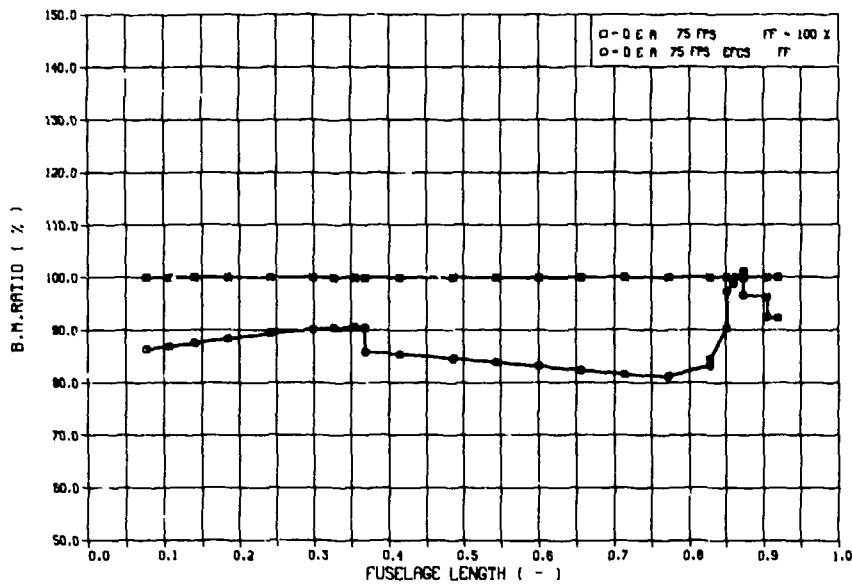


FIG.18 : FUSELAGE BENDING MOMENT RATIO (SYSTEMS)



4.0 CONCLUSIONS

The shown situation can be regarded as representative for a major gust load designed transport A/C.

It was shown that more severe gust requirements or interpretations in Europe lead to higher gust design loads.

It is doubtful whether this is necessary to guarantee an acceptable level of safety. But there is no doubt that this situation distorts the international competition.

The objections of AAs to this statement will be that also Import- A/C entering the European market will have to cover these requirements.

Although this is true it cannot satisfy a manufacturer that own A/C designs, flying in the same atmosphere as those of a competitor, have to cover different severe gust requirements, depending on the country of certification.

A critical review of the total gust requirement situation is therefore requested, ending up in a harmonization of the conditions to be covered, independent from the country of certification.

We must refrain from the former artificial load conditions, coming as near as possible to the real physical conditions.

New statistical material for better representation of the atmosphere is needed, only this will guarantee a good level of safety and will at the same time give us the chance to use all the benefits we can get also in the structures field from introduction of modern electronic systems, to improve overall economics.

Industry, Laboratories and Authorities are requested to take over this task in the interest of all of us.

Acknowledgement

The author likes to thank all those members of his staff, who supported him in establishing this document.

**MEASURED AND PREDICTED RESPONSES OF THE NORD 260 AIRCRAFT
TO THE LOW ALTITUDE ATMOSPHERIC TURBULENCE**

by

J.L. Meurzac and F. Poirion
ONERA
9 ave de la Division Leclerc
92320 Châtillon
France

Summary : A program of in-situ measures using the Nord 260 plane equipped with accelerometers has allowed to compare the predicted and the measured responses of the flexible aircraft to the turbulence. It shows a good agreement between the two sets of results and it emphasizes the better modeling of the turbulence using the isotropic model rather than the cylindrical one.

INTRODUCTION

A flying program using the plane Nord 260 has allowed to compare the experimental and the calculated responses of the flexible airplane to the low altitude atmospheric turbulence. The results of these comparisons give a good fitting between calculated and measured transfers, spectral densities and coherence, once the adequate turbulence length scale and standart deviation have been found.

Those comparisons show also that the responses calculated by using an isotropic model in order to represent the atmospheric turbulence are much more closer to the experimental responses than those obtained using a cylindrical model, which shows the more realistic behavior of the isotropic model.

After recalling in a first part how the responses are calculated, we show by drawing the curves representing the transfers, the spectral density and the coherence, the comparison between the experiment and the calculus

I Theoretical responses to the turbulence

I.1. Non stationary forces due to the turbulence

The non-stationary pressure created by the atmospheric turbulence at point M and time t on a flexible aircraft is given by the relation :

$$(1) \quad \Delta \mathcal{P}(M, t) = \int_S G(M, M', t) * \alpha(M', t) dM'$$

where $G(M, M', t)$ represents the Green function of the problem calculated by the doublet lattice method [1], and $\alpha(M', t)$ is the local angle of attack induced at point M' and time t by the turbulence, S being the wing surface

The generalized non-stationary forces relative to the displacement field $H(M)$ are then given by :

$$(2) \quad \mathcal{F}_H(t) = \int_S \Delta \mathcal{P}(M, t) H(M) dM$$

In the modal basis of the plane, the vector q of the generalized coordinates is given by the relation

$$(3) \quad q(t) = a * F(t)$$

where a is the impulsional response and F is the vector of the generalized forces components. We denote $A = \hat{A}$ the admittance matrix.

Knowing the vector $h(M)$ of the displacements $(h_i(M))$ of the eigen modes at point M , we can deduce the vertical displacement Z at that point using the relation

$$(4) \quad Z(M,t) = \sum_i h_i(M) q_i(t)$$

In order to achieve the calculus it is necessary to know the expression of the local angle of attack $\alpha(M,t)$ in function of the turbulence. This expression will be different according to the model chosen to represent the atmospheric turbulence.

1.2. Cylindrical turbulence

The cylindrical model is a simplified model of the atmospheric turbulence which suppose that it is constant spanwise and which is entirely defined as soon as its value at a single point M_0 is known.

More precisely, for an airplane flying along the x direction at speed V , the local angle of attack $\alpha(M,t)$ induced by the turbulent field $W(M,t)$ is given by :

$$(5) \quad \alpha(M,t) = W(M,t) / V = W(M, t - (x_0 - x)/V) / V$$

where $M(x_0)$ is the point where the turbulence is measured and which is located at the nose of the plane.

Denoting $\hat{\Delta P}(M,\omega)$ the Fourier transform of the non-stationary pressure $\Delta P(M,t)$ at point M , we get easily :

$$(6) \quad \hat{\Delta P}(M,\omega) = \hat{w}(M,\omega) / V \int_S \hat{p}(M,M',\omega) \exp(-j\omega(x_0 - x_{M'}) / V) dM'$$

Therefore we see that the pressure is obtained by a linear filtering of the cylindrical turbulence, the frequency response being given by the previous integral.

In the same way the non-stationary forces and therefore also the vertical displacement $Z(M,t)$ are obtained by a linear filtering of the cylindrical turbulence and we consider the frequency response that we shall call transfer at point M by :

$$(7) \quad T_{WZ}(M,\omega) = \hat{Z}(M,\omega) / \hat{W}(M_0,\omega) = 1/V h^T \hat{A} \hat{F}$$

We can then construct :

$$\Phi_{ZZ}(M,\omega) = |T_{WZ}(M,\omega)|^2 \Phi_{WW}(\omega)$$

and the coherence :

$$\gamma^2(M,\omega) = |\Phi_{WZ}(M,\omega)|^2 / \Phi_{WW}(\omega) \Phi_{ZZ}(M,\omega)$$

1.3. Isotropic turbulence

The vertical atmospheric turbulence is modeled by a second order stationary continuous and zero mean gaussian process which is isotropic and homogeneous. In this context, the

local angle of attack is given by the relation

$$(8) \quad \alpha(M,t) = w(M,t) / V,$$

and the non-stationary pressures and the responses of the aircraft are not given any more by a linear filtering of the turbulence at the single point M_0 .

In order to get the transfer, we are going to construct directly the spectral density $\Phi_{ZZ}(M,\omega)$ of the response Z at point M and the interspectral density between the turbulence measured at the reference point M_0 and the response Z at point M , $\Phi_{ZW}(M_0,M,\omega)$.

To calculate the generalized forces, the surface S is discretized. We denote, $G(t) = (G_{ij}(t)) = (g_{ij}(M_i, M_j, t))$ the matrix of the discretized kernel $G_{ij}(t)$, $H = (h_i(M_j))$ the matrix which columns contain the displacement of the mode i at point M_j of the lattice, $W(t)$ the vector which components are the value of the turbulence at time t and at the points of the lattice M_j .

The vertical displacement at point M , $Z(M,t)$ is therefore given by the relation

$$(9) \quad Z(M,t) = h^T(M) A * (H G * W/V)(t)$$

The process Z is thus obtained by the composition of two linear filtering of the process W/V , the first impulse response being $HG(t)$, the second one being $h^T(M)A(t)$. The general theory of second order processes [4] show then that the process Z is a second order, zero mean continuous gaussian process which is stationary, the spectral measure of which being given by the formula:

$$(10) \quad \Phi_{ZZ}(M,\omega) = h^T(M) \hat{A}(\omega) H \hat{G}(\omega) S_{W/V}(\omega) \hat{G}^*(\omega) H^* \hat{A}^*(\omega) \bar{h}(M)$$

The quantity $S_{W/V}(\omega)$ is the matrix spectral measure of the process W/V which elements are defined by:

$$(11) \quad S_{W/V}(\omega) = [S_{W/V}(M_i, M_j, \omega)]_{i,j}$$

where $S_{W/V}(M_i, M_j, \omega)$ represents the transverse spectral measure of the process W/V at the two points M_i and M_j .

In the same way, the cross-spectral density between the response Z and the turbulence W/V at the measure point M_0 is given by:

$$(12) \quad \Phi_{ZW}(M_0, M, \omega) = h^T(M) \hat{A}(\omega) H G(\omega) S_{W_0/V}(\omega)$$

where

$$(13) \quad S_{W_0/V}(\omega) = [S_{W_0/V}(M_0, M_j, \omega)]_j$$

represents the column of the transverse spectral measure at point M_0 .

In order to be able to define completely expression (10) and (12), we still have to write down the transverse spectral measure $S_{W/V}(M', M, \omega)$ between two points M and M' .

This quantity has been calculated in reference [3]:

$$(14) \quad S_{W/V}(M, M', \omega) = \exp(-i(x-x')) C(\omega, \eta) \Phi_{WM}(\omega) = \sigma_{W/V}(\omega) \Phi_{WM}(\omega)$$

$$(15) \quad C(\omega, \eta) = 2/\Gamma(p+1/2) ((\eta/2)^{p+1/2} K_{p+1/2}(\eta) - 2 B(\eta/2)^{p+3/2} K^{p-1/2}(\eta))$$

$$\eta = \rho/a \sqrt{(\omega a)^2/V^2 + 1}$$

$$\rho = \sqrt{(y-y')^2 + (z-z')^2}$$

$$a = L\sqrt{\pi} \Gamma(p) / \Gamma(p+1/2)$$

$$B = (1 - (1 + (\omega a)^2/V^2) ((z-z')/\rho)^2)^{-1} (1 + 2(p+1) (\omega a)^2/V^2)^{-1}$$

101

L being the turbulence length scale, K_p the Bessel function of order p.

$\Phi_{ww}(\omega)$ is the spectral density of the vertical turbulence :

$$(16) \quad \Phi_{ww}(\omega) = \sigma_w^2 L / \sqrt{2\pi} (1 + 2(p+1)(a\omega)^2/V^2) (1 + (a\omega)^2/V^2)^{-p-3/2}$$

The Karman's model is obtained when $p = 1/3$.

We can then construct a pseudo transfer T_{zz} between the response Z and the process of the vertical turbulence :

$$(17) \quad \Phi_{zz}(M, \omega) = |T_{zz}(M, \omega)|^2 \Phi_{ww}(\omega)$$

where

$$(18) \quad |T_{zz}(M, \omega)|^2 = h^*(M) \hat{A}(\omega) H \hat{G}(\omega) \sigma_{w/v}(\omega) \hat{G}^*(\omega) H^* \hat{A}^*(\omega) \bar{h}(M)$$

In the same way, using relation (12), we can construct the pseudo transfer T_{wz} :

$$(19) \quad \Phi_{wz}(M, \omega) = T_{wz}(M, \omega) \Phi_{ww}(\omega)$$

and the pseudo coherence

$$\gamma^2(M, \omega) = |\Phi_{w/vz}(M, \omega)|^2 / \Phi_{ww}(\omega) \Phi_{zz}(M, \omega)$$

I.4. Turbulence length scale

The quantities $C(\omega, \eta)$ and $\Phi_{ww}(\omega)$ depend of the turbulence length scale L and of the standart deviation σ_w^2 .

If we want to compare the theoretical plane's responses to the measured ones, it is necessary to estimate correctly these two parameters which characterize the turbulence state during the in flight measures. In order to do that, using the measured spectral density, we do the ratio of two values of the spectrum (16) for two different frequencies and we obtain a relation which depends only of the length scale L. We get L using an numerical iterative scheme.

Then we get easily the standart deviation. This method is however limited by the scattering of the experimental spectrum values but it gives a rough estimate that it is possible to improve.

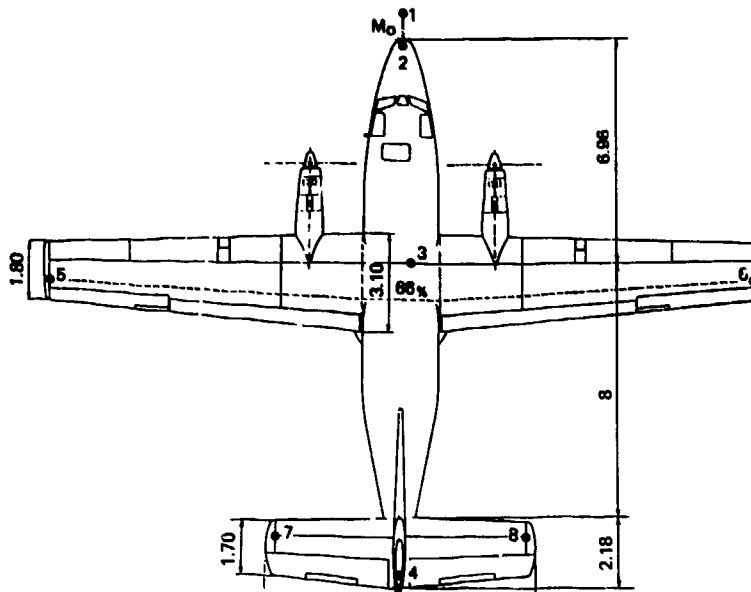
II In flight measures for the Nord 260.

II.1. Modal Basis

The modal basis contain two rigid modes of pitching and plunging and twelve flexible modes obtained during ground vibrations measures [2] and which characteristics are given below :

frequencies Hz	1	4.52	6.32	8.03	9.5	10.41	11.95	13.30	15.59	16.17	23.3	27.8
generalized mass	6.4	201	559	692	6.7	135	345	431	1.2	1070	88.2	256
structural damping	.35	.009	.014	.011	.034	.027	.016	.017	.025	.022	.015	.018

II.2. Positions of the accelerometers



III Comparison measure and theory

We use a length scale of 75 m for the turbulence which give a value of .78 for the standart deviation.

Figure 1 shows the comparison of the experimental and theoretical spectrum. The inertial area is well represented.

From now on we shall only look at the acceleration $Z(M,t)$ of the vertical displacement. Figures 2 and 3 show for two different accelerometers how the theoretical response compare when either the isotropic or the cylindrical model is used. We can see a rather big difference for the two results, especially in the flexible modes area. Such a difference had not been found for the responses of the Mirage III, this last airplane having a much smaller aspect ratio than the Nord 260 which can be considered as a large aspect ratio plane.

The 5 last figures show the comparison between the theoretical response using the isotropic model and the experimental response for 5 different accelerometers. We see the good agreement of the results except for the figure 7 which involve accelerometers located at the wings's tip. This is due maybe to bad measures at these points.

The results for the transfers are not much modified when the value of the turbulence length scale varies. This is not the case for the power spectral densities.

Of course the agreement is not perfect between the experimental and theoretical results : the turbulence is already anisotropic at the altitude of 150 m where the measures were made and there is always some noise wich add up to the turbulence excitation.

References

- [1] HUTIN, P.M. ; CHOPIN, S. Etude d'un code de calcul des forces aérodynamiques instationnaires sur un avion complet tenant compte des interactions entre les différents éléments. RTS2/9074 RY 002R 1979
- [2] LUBRINA, P. Essai de vibrations au sol de l'avion Nord 260
- [3] MEURZEC, J.L ; TRETOUT, R.. Etude d'une loi de contrôle en turbulence sur un ensemble delta-canard souple RTS 21/5108ry 042 R 1985
- [4] SOIZE, C. Eléments mathématiques de la théorie déterministe du signal Cours de l'ENSTA n° 739

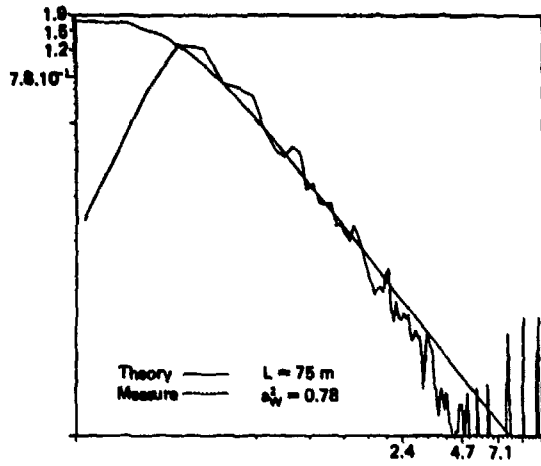


Fig. 1 - Comparison of the theoretical and measured turbulence spectrum.

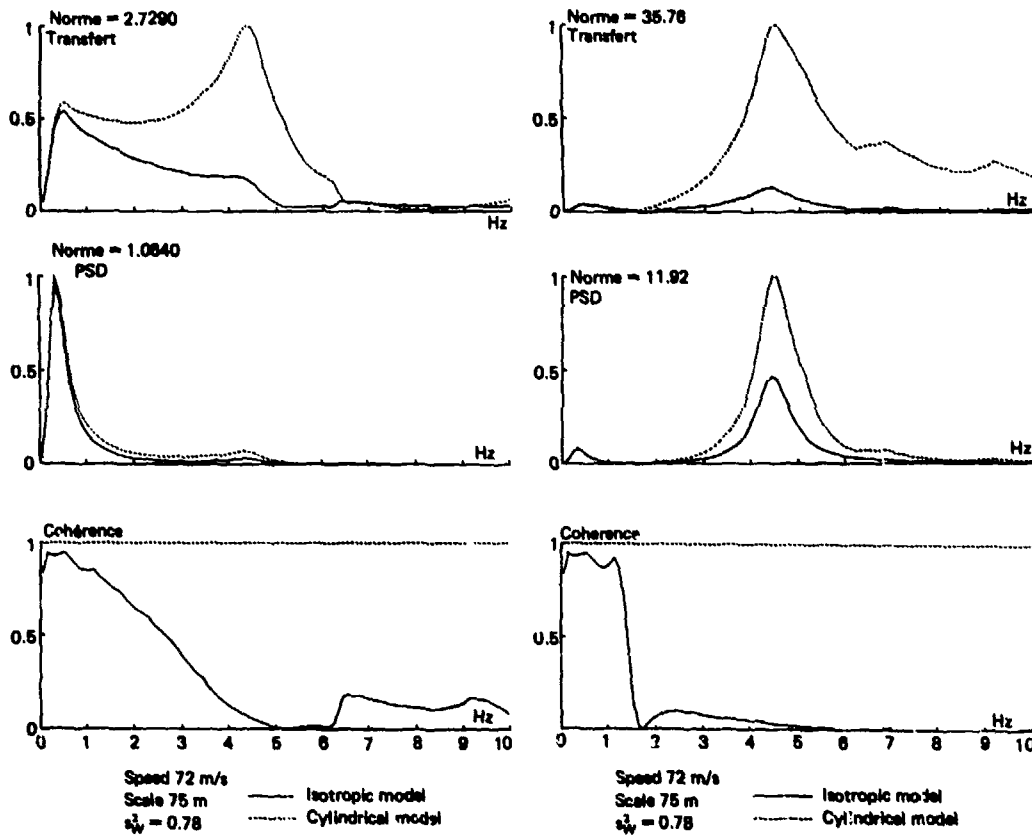


Fig. 2 - Comparison of the theoretical responses at accelerometer 3 using a cylindrical and isotropic model.

Fig. 3 - Comparison of the theoretical responses at accelerometer 5 + 6 using a cylindrical and isotropic model.

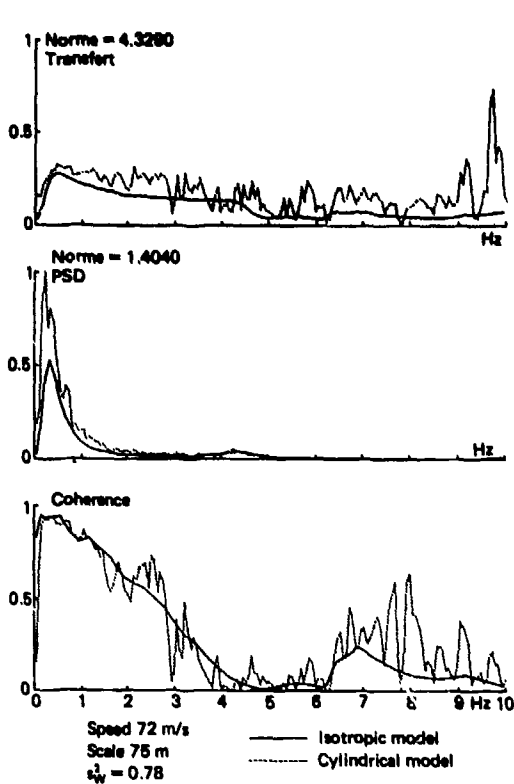


Fig. 4 - Comparison of the experimental and theoretical vertical response accelerometer 2.

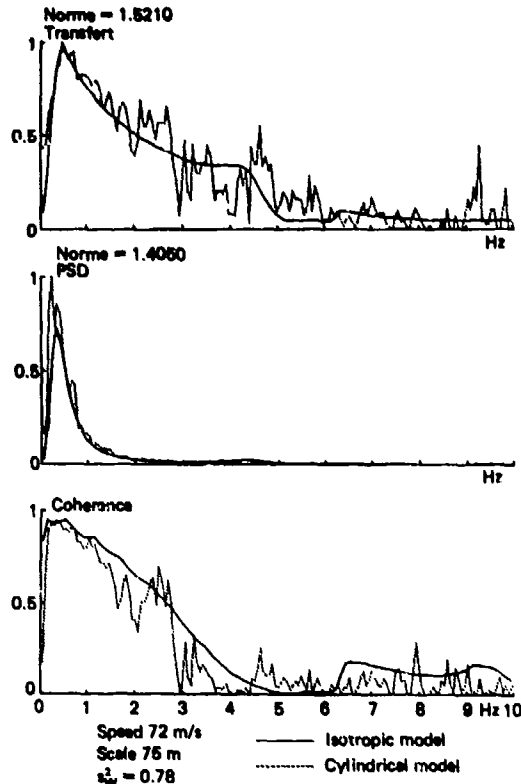


Fig. 5 - Comparison of the experimental and theoretical vertical response accelerometer 3.

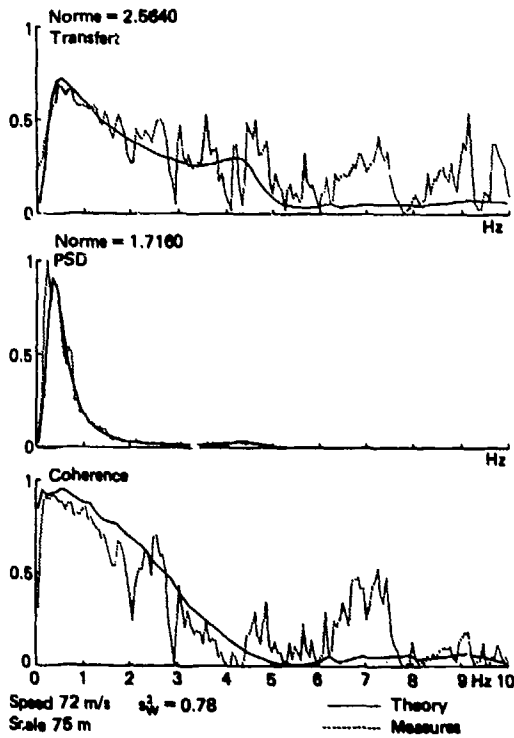


Fig. 6 - Comparison of the experimental and theoretical vertical response accelerometer 4.

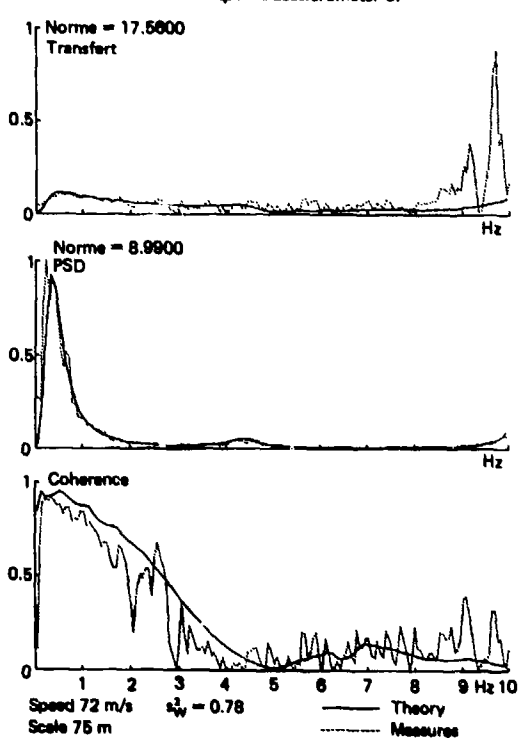


Fig. 7 - Comparison of the experimental and theoretical vertical response accelerometer - $\frac{1}{2}$ (5 + 6).

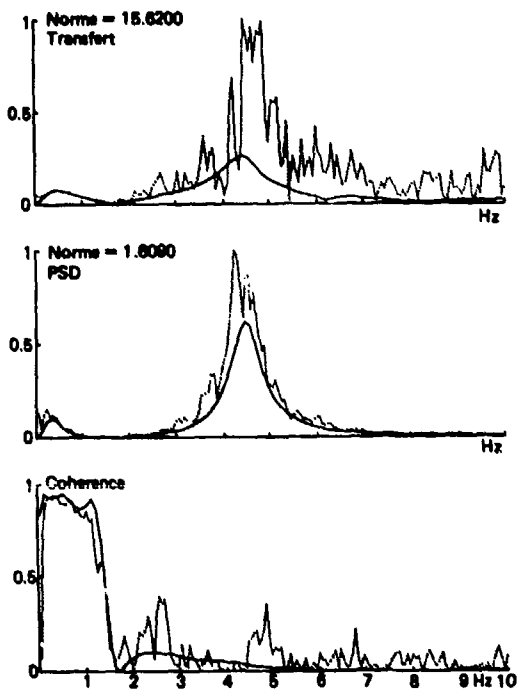


Fig. 8 - Comparison of the experimental and theoretical vertical response accelerometer (7 + 8).

Speed 72 m/s
Scale 75 m
 $\sigma_w^2 = 0.78$

— Theory
..... Measures

A REVIEW OF MEASURED GUST RESPONSES IN THE LIGHT OF MODERN ANALYSIS METHODS

by

V. Card
Principal Airworthiness Surveyor
Civil Aviation Authority
Airworthiness Division
Brabazon House
Redhill RH1 1SQ
UK

1.0 INTRODUCTION

In the past various gust load formulas have been developed for the calculation of design gust loads on aircraft. Since it was first published in 1954 (Ref 1), the alleviation factor approach of Pratt and Walker has gained almost universal acceptance and for many years has been a familiar part of the airworthiness requirements for both civil and military aircraft.

The original concept of the "Pratt formula" was to predict the peak accelerations due to discrete gusts on a given aircraft for flight through a discrete gust of the same shape and amplitude. Thus the derived gust velocity is not so much an absolute physical quantity, but is rather more a gust-load transfer factor defined within the terms of the formula. As such the method is most accurate when restricted to use on aircraft with very similar characteristics. Less confidence must be attached to predicted gust loads on aircraft which are unconventional when compared to the data collecting aircraft.

Fortunately, as in many other fields of aeronautical science, the methods of calculating design gust loads have been constantly improved over the past 30 years. Rational and accurate analysis procedures are now common amongst all the major aircraft manufacturers. These have allowed all the important features of new aircraft to be modelled and thus have ensured that differences in gust response characteristics are fully accounted for in the design process. This is fully in accord with a fundamental principle of airworthiness requirements which demands that load intensities and distributions should closely represent actual conditions or else they must be shown to be conservative. In general, however, only one set of design gust velocities is prescribed and these are based upon equivalent values derived using the simple formula.

This would be reasonable if all the elements of the modern gust analysis were only applicable to modern aircraft and if the effects on the previous generation of aircraft were insignificant. However, this is patently not the case. The alleviation factor formula approach leans heavily on many simplifying assumptions which were introduced purely to facilitate the solution of the equations of motion. That is not to say that all the elements of the equations of motion which were eliminated by Pratt and Walker and other researchers were negligible but rather that their inclusion would have led to an overly arduous analysis task.

The degree to which current assumptions concerning the modelling of aircraft response to discrete gusts could have affected earlier conclusions upon gust statistics derived from measured acceleration data is the subject of this paper. The work described was done by British Aerospace, Weybridge under a research contract sponsored by the Civil Aviation Authority of the United Kingdom.

The opinions expressed in this paper are solely those of the Author.

2.0 INVESTIGATION OF THE EFFECTS OF MODELLING REFINEMENTS UPON PREDICTED ACCELERATION RESPONSES.

The design gust velocities in current gust load requirements are based, for the most part, on statistical data collected on U.S. transport aircraft prior to 1950 and supported by further data collected on European transport aircraft prior to 1960. Gust velocity probabilities were derived from exceedance counts of centre-of-gravity acceleration using a simple gust alleviation factor approach based upon the aircraft mass parameter. Gust velocities derived in this way can be confidently used for design, providing that the aircraft under consideration has similar response characteristics to the data collecting aircraft. Where this is not the case a more realistic picture of the distribution of true gust velocity should be sought. Ideally, design methods and design requirements should be complementary; together producing the required safety objective without undue economic penalty.

Gust load analysis methods have developed steadily over recent years to keep in step with developments in aircraft technology. The effects of flexibility, wing sweep, high speed aerodynamics, transport delays, interference between lifting surfaces, configuration changes (flaps, slats spoilers etc) and autopilot are now routinely included in the design analysis wherever appropriate. Some of these features are also

relevant to the data collecting aircraft, but were excluded from the data reduction process to facilitate a solution of the equations of motion. In order to determine the effects that these features could have had on the gust statistics data, therefore, it was necessary first to understand how each element of a modern analysis would have influenced the conclusions of earlier research studies, had such analytical tools been available at the time.

Examination of Reference 1 shows nine different aircraft types were used to collect V-G data during the period 1933-1950. Of these two aircraft which figure prominently have been selected as worthy of renewed investigation. - Type E and Type J. These aircraft were selected as being representative of the class of aircraft for which the Prett formula is expected to be most effective.

They are also aircraft types for which reasonable estimates of wing mass and stiffness data exist in published literature (Ref 2). Using this data it was possible to set up mathematical models which would give a reasonable engineering representation of the gust response characteristics of each type in accordance with present day theory.

Early European accelerometer data was collected on a large number of different aircraft types. Of these one (Type V) was selected as fairly typical. It was also advantageous to study an aircraft on which reliable design data was available. This allowed a detailed and accurate mathematical model of the aircraft to be formulated and checked against full scale test results. Published data on this aircraft (Ref 3) has an added refinement of a height band breakdown, requiring investigation of gust load factors at greater altitudes than were needed for the U.S. aircraft.

3.0 AIRCRAFT THEORETICAL MODELS

Mathematical models of the aircraft under review were developed using the latest analytical techniques from previously published mass and stiffness data. Rigid aerodynamic load distributions were calculated for each lifting surface using a combination of vortex lattice and slender body theory. In areas where detailed information was not available engineering judgement was exercised to provide a working approximation of the missing data. Owing to these assumptions it cannot be claimed that the final theoretical model gave an exact representation of each aircraft. However, it should be assumed that the models do possess the inherent gust response characteristics representative of the class of aircraft under study. As such each can be seen as indicative of the relative trends in gust factors and gust loads to be associated with each change in modelling technique.

With the model of the Type V aircraft, of course, this is not the case. This mathematical representation was based upon validated design data, with the structural modes confirmed by the results of full scale stiffness tests, and ground and flight vibration tests, with aerodynamic data supported by wind tunnel test measurements.

A comparison of the major design features of each type of aircraft studied is given in Table 1. In each case the aircraft response equations were established in a way which permitted an individual variation in some aspect of modelling technique. At each stage the responses to a range of "1-cosine" shaped gusts were calculated to determine the change in incremental acceleration at the centre-of-gravity.

The modelling assumptions inherent in the Prett formula approach to response analysis are summarised in Table 2, together with brief details of the improvements embodied in current state-of-the-art modelling procedures. Analysis of some typical results obtained for each class of aeroplane are summarised in Figures 1-3. These figures show how the predicted incremental c.g. acceleration can vary depending upon the assumptions made concerning each physical characteristic of the aircraft included in the equations of motion.

Each block in the diagram represents the maximum predicted centre-of-gravity acceleration in response to a "1-cosine" shaped gust. Reading from left to right represents the introduction of a selected improvement in modelling technique. The far right of the figure faithfully represents the complete design procedure in accordance with current UK practice. In each case the datum value shown is that which would be obtained from the basic rigid Prett formula solution. It can be seen that the general trend is towards a higher response as the mathematical model is progressively refined.

The final result confirms that the simple alleviation factor approach will seriously underestimate the true acceleration which would be caused by any discrete gust of a given magnitude. Conversely, derived gust velocities based upon these simple models will, in turn, be over-estimates of the true gust velocity.

4.0 IMPLICATION FOR AIRCRAFT DESIGN LOADS

In addition to the calculation of aircraft accelerations in the various cases, estimates of the values of some important load parameters were also derived so that the effects of the various modelling refinements upon design loads could be checked. The overall trends for Wing Root Bending Moment for each class of aircraft investigated are summarised in Figures 4-6. The results confirm that modern analysis techniques are quite conservative when compared with the Prett formula approach and these have led to a gradual but significant increase in the severity of the design criterion. These hidden strength increases must be assessed in the light of current safety objectives to ensure that the intended airworthiness targets are met without undue economic penalty.

5.0 REASSESSMENT OF GUST FREQUENCY DISTRIBUTION

The maximum value of centre-of-gravity acceleration that results from an encounter with a vertical gust is largely dependent upon weight, speed, altitude and centre-of-gravity position. The first three of those parameters were fully accounted for by Pratt and Walker in their assessment of operational gust statistics (Ref 1). As only the heave degree-of-freedom was considered at that time, the position of the centre-of-gravity was immaterial. This recent work has also confirmed that the severity of the response to a gust is also very dependent upon the gust gradient distance. This is demonstrated in Figures 7-9, which present calculated responses of each class of aircraft used in the current study to a range of discrete gusts of varying wavelength. The tuning effect is clearly evident even for these relatively rigid aircraft where the dynamic effects of wing flexibility would be expected to be much lower than on a modern high aspect ratio wing, particularly one with pylon mounted engines.

As all the early gust response data was collected using standard V-G recorders, no information on gradient distance is available. Early researchers circumvented this problem by arbitrarily assuming all gusts to be of equal wavelength for each aircraft type, although varying from type to type owing to the fixed chord length ratio. The sensitivity of the data collecting aircraft to gusts of different wavelengths can be introduced into the assessment procedure, however, providing that a probability of occurrence can be established for each gust length.

Alternatively, research by Jones into the statistical nature of discrete gusts has shown (Refs 4-5) that families of ramp gusts, whose amplitudes vary as "wavelength to the power one-third", have an equal probability of occurrence. This physical characteristic has been demonstrated in turbulence analysis studies carried out by British Aerospace at Weybridge (Ref 6) for single ramps and combinations of ramps with a smooth "1-cosine" profile. Adoption of this feature of equiprobability to more familiar symmetric discrete gust (Figure 10) will allow a family of "1-cosine" gusts to be defined, each member of which will be as likely to occur as any other. Furthermore if the 25 chord is chosen as the datum for definition of the amplitude scaling law as in Figure 11, then a tuned gust of equal probability to the 25 chord gust can be found. Thus factors for conversion of acceleration to derived gust velocity can be established which incorporate the concept of variable gust lengths, whilst maintaining the same level of probability inherent in the earlier analyses of Pratt, Walker, Bullen and others.

The effects of the application of the discrete gust power law on the peak acceleration can be seen in Figures 12-14 which provide a direct comparison with the constant amplitude gust responses of Figures 7-9.

The development of acceleration to gust velocity conversion factors appropriate to the latest modelling assumptions, and a comparison with the Pratt datum result is summarised in Figures (15-17). These factors are based upon representative flexible aircraft models which for the aircraft type V will give the true correspondence between gust velocity and acceleration at the mean cruising conditions. For the US aircraft the factors represent a reasonable estimate of the likely correspondence due to uncertainties in the model data.

The prime use of the revised gust factors described above has been in the evaluation of more realistic derived gust velocities appropriate to a large part of the American V-G data collected prior to 1950 and the part of the V-G-H data measured on European aircraft between 1953-1958. Calculated values of derived gust velocity had previously been fitted with theoretical extreme value distributions (Ref 7) in order to smooth out irregularities in the data and to provide a consistent basis for extrapolation. For this investigation therefore it was necessary only to apply the relevant gust conversion factors to the given frequency distributions. This has a powerful effect upon the gust probabilities as shown in Figures 18-19.

It is emphasised that the new result is a product only of revised assumptions concerning the response of the aircraft to the gust. These assumptions were made in the light of accepted modern techniques of mathematical modelling and of recent theories of the nature of the atmosphere. Other assumptions pertinent to the operation of the data collecting aircraft, such as estimates of mean operating weights, speeds and altitudes have not formed part of this investigation and have been accepted as soundly based.

6.0 AIRWORTHINESS CONSIDERATIONS

British Civil Airworthiness Requirements were revised in December 1964 in an attempt to anticipate the needs of turbine engine operations. The gust probabilities assumed at that time were extrapolated from pre-1958 operational data and the target limit gust velocity was set at a value that would be met once in 30,000 hours. It was assumed that the gust occurrence rate would not vary with time so that experience from 30,000 hours of turbine powered operation could be equated directly to 30,000 hours of piston powered operations. The minimum requirement of 50ft/sec EAS at 20,000 feet reducing to 25ft/sec at 50,000 feet therefore reflected the maximum gust experienced in 30,000 hours at 250 mph assuming a dynamic stress factor of 1.0. The constant gust velocity below 20,000 feet represented a relative increased probability of meeting the design gust but this was balanced by the decreased exposure times associated with climb and descent.

From 1964 the ECAR discrete gust design velocities have reflected those contained within U.S. Federal Aviation Regulations. That is not to say that the requirements themselves are identical since the FAR 25 discrete gust requirements specifies a fixed gradient distance of 12.5 wing mean chords. In the United Kingdom there is concern over the need to take account of aircraft dynamic response in the calculation of design gust loads. To this end the concept of varying gust gradient distance to find the most critical responses on different parts of the aircraft has been introduced. Although for many aircraft the 12.5 chord gradient is close to being the most critical for response quantities such as

wing root bending moment, most aircraft have important responses affecting structural loads which tune to other gradient distances.

Thus, while, from a point of view of structure weight the 12.5 chord gust gradient is near to being the most important, this is not the case for all aircraft nor is it the case for all parts on any aircraft. Future developments, such as the application of active controls or other advance configurations can be more sensitive to discrete gust effects than past designs and it therefore becomes more imperative to consider more than one gradient distance.

As previously shown gust velocities developed from simple response models are severe when used with a fully rational dynamic analysis. The CAA has recognised this fact and in its National Variant to JAR 25 has introduced a reduced gust velocity for use in conjunction with a dynamic analysis. It can be seen in Figure 20 that the reduction recognises two important considerations. Firstly, that modern analytical methods would support lower probabilities of "true" gust velocity than the simple alleviation factor approach. Secondly, that the reliability of modern jet transport has led to greater expectations of operational safety than were thought possible when the turbine engine aircraft were first introduced. An airworthiness objective of one encounter with the limit gust in 50,000 flying hours is now thought to be appropriate.

7.0 CONCLUSIONS

- 1) In the past simplified models of aircraft used to assess operational gust statistics have led to conservative estimates of derived gust exceedances.
- 2) Modern refinements in aircraft modelling techniques have gradually introduced conservatism in the process of calculating gust loads. Gust statistics reviewed in the light of these modern analytical methods support the CAA view that gust velocities developed for use with simple rigid aircraft models are too severe for use with a modern dynamic analysis.
- 3) Even in the light of improved safety targets, a 10 per cent reduction in design gust velocity can be readily justified. Further reductions may be justified on the basis of mission analysis considerations, or by investigation of more recent acceleration statistics collected by the current generation of transport aircraft. In the latter case it will be essential to account for all relevant features of the subject aircraft in the derivation of gust velocities so as to obtain a true picture of the gust statistics.

REFERENCES

1. A Revised Gust Load Formula and a Re-evaluation of V-G Data Taken on Civil Transport Airplanes from 1933 to 1950. NACA Report 1206 (1954). K.G.Pratt W.G.Walker.
2. Structural Response to Discrete and Continuous Gusts of an Airplane Having Wing Bending Flexibility and a Correlation of Calculated and Flight Results. J.C.Houbolt, E.E.Kordes.
3. A Review of Counting Accelerometer Data on Aircraft Gust Loads. RAE TR66234 July 1966.N.I.Bullen.
4. A Theory for Extreme Gust Loads on an Aircraft Based on the Representation of the Atmosphere as a Self-Similar Intermittent Random Process. RAE Technical Report 68030 (1968) J.G.Jones.
5. Statistical Discrete Gust Theory for Aircraft Loads. A Progress Report RAE Technical Report 73167 (1973) J.G.Jones.
6. The Development of the Jones Statistical Discrete Gust Method for the Prediction of Aircraft Gust Loads. BAE (Weybridge) Report V10/D/M/257. November 1976. V.Card.
7. The Application of the Statistical Theory of Extreme Values to Gust-Load Problems.NACA Report 991 (1950). H.Press

RE-ASSESSMENT OF OPERATIONAL GUST VELOCITIES**COMPARISON OF SIGNIFICANT DESIGN FEATURES
OF THE DATA COLLECTING AIRCRAFT**

	AIRCRAFT E	AIRCRAFT J	AIRCRAFT U
Wing Area	987 sq.ft	864 sq.ft	963 sq.ft
Wing mean chord	10.39 ft	9.27 ft	10.28 ft
Aspect ratio	9.1	10.1	9.2
Maximum RW	25200 lb	39900 lb	50500 lb
Maximum fuel weight	4000 lb	4900 lb	15600 lb
Typical speed	210 mph	260 mph	310 mph
Typical altitude	5000 ft	5000 ft	20000 ft
Estimated wing modal frequencies	4.5 hz 10.2 hz 16.4 hz 32.8 hz	3.7 hz 7.8 hz 10.7 hz 26.3 hz	2.2 hz 3.9 hz 4.6 hz 7.1 hz

TABLE 1

SCOPE OF THE INVESTIGATION

PRATT ASSUMPTION	CURRENT MODELLING TECHNIQUE
The aircraft lift curve slope is based on wing area, and is estimated from the formula $a = \frac{6\pi}{A+2}$	All surfaces contribute to the aircraft normal force coefficient. Accurate load distributions are derived from three-dimensional theory supported by wind tunnel measurements.
All parts of the aircraft penetrate the gust together	Sweep effects and separation between lifting surfaces are included.
Kussner and Wagner functions are for infinite aspect ratio.	Unsteady lift functions appropriate for each surface are derived from three-dimensional theory.
The aircraft responds in heave only.	All significant freedoms are allowed, including control and autopilot equations where appropriate.
The aircraft responds as a rigid body.	The full effects of flexibility are included. The shapes and frequencies of the major structural modes are confirmed by full-scale vibration tests.
The aircraft is a concentrated mass.	The aircraft mass is correctly distributed. Centre-of-gravity, payload and fuel are varied to find the worst case.
The gust gradient distance is fixed at 12.5 chords.	The gust gradient distance is varied to find the peak response. (U.K. only)

TABLE 2

**EFFECTS OF CHANGES IN MODELLING ASSUMPTIONS
UPON CALCULATED AIRCRAFT RESPONSES TO DISCRETE GUSTS**

FIGURE 1

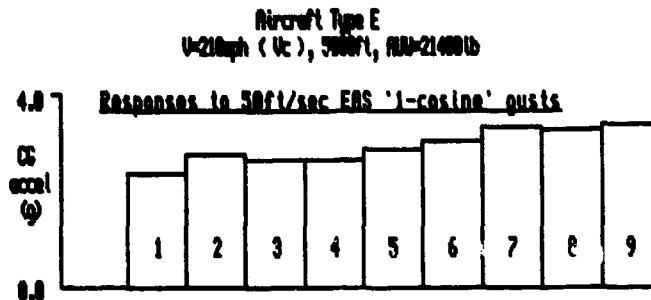


FIGURE 2

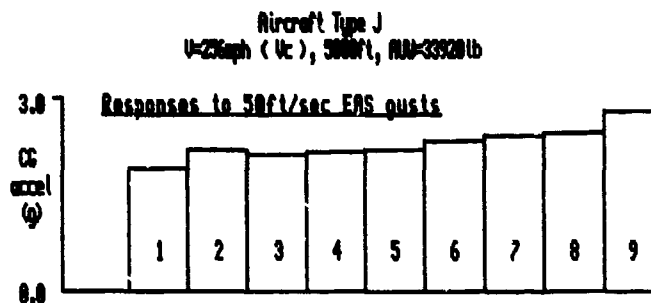
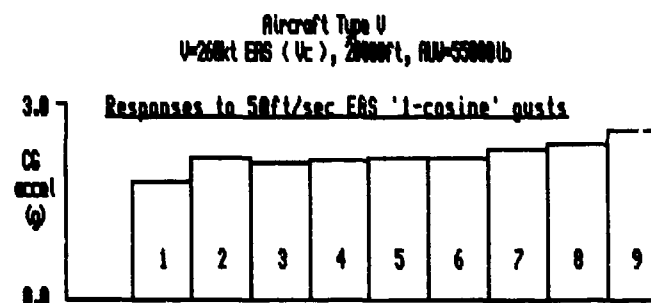


FIGURE 3



- 1: Pratt datum solution for 12.5c gust (ref. NACA 1286).
- 2: Pratt solution for a 12.5c gust, including fuselage and tail lift.
- 3: Howe only solution, including delay between surfaces.
- 4: Howe only solution, including the effects of tapering chords.
- 5: Howe only solution, including changes to lift growth functions.
- 6: Howe and pitch solution for a 12.5c gust.
- 7: Howe and pitch solution for a tuned gust.
- 8: Flexible aircraft solution for a 12.5c gust.
- 9: Flexible aircraft solution for a tuned gust.

**EFFECTS OF CHANGES IN MODELLING ASSUMPTIONS
UPON CALCULATED AIRCRAFT RESPONSES TO DISCRETE GUSTS**

FIGURE 4

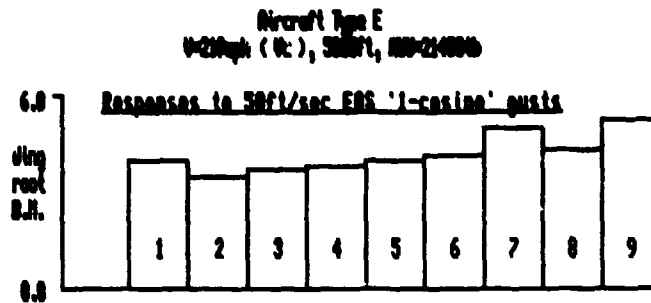


FIGURE 5

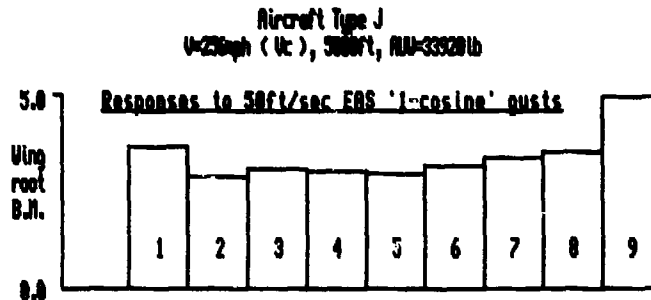
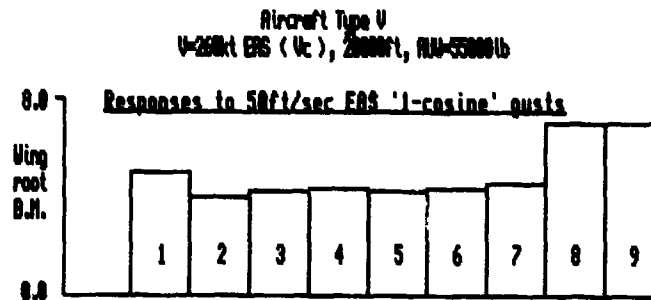


FIGURE 6

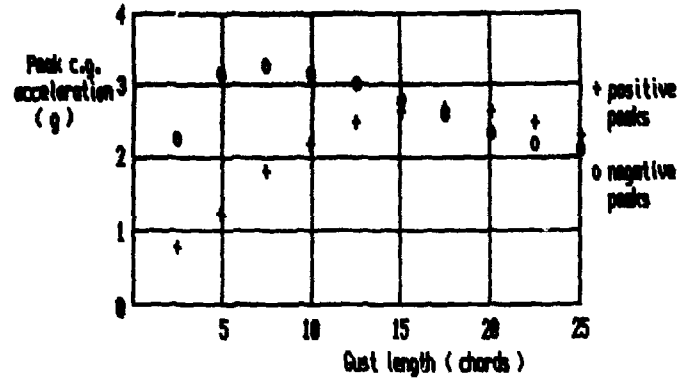


- 1: Pratt datum solution for 12.5c gust (ref. NACA 1286).
- 2: Pratt solution for a 12.5c gust, including fuselage and tail lift.
- 3: Naive only solution, including delays between surfaces.
- 4: Naive only solution, including the effects of tapering chords.
- 5: Naive only solution, including changes to lift growth functions.
- 6: Naive and pitch solution for a 12.5c gust.
- 7: Naive and pitch solution for a tuned gust.
- 8: Flexible aircraft solution for a 12.5c gust.
- 9: Flexible aircraft solution for a tuned gust.

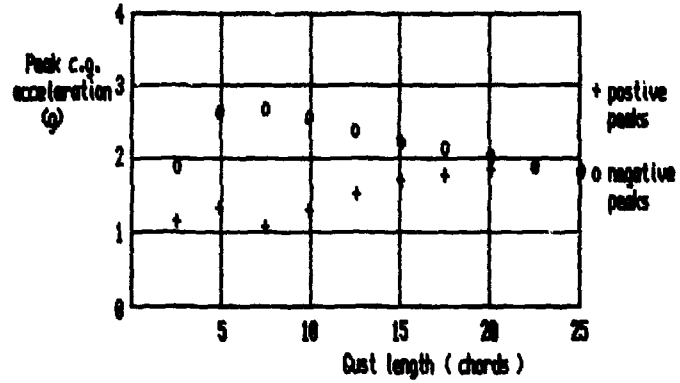
**GUST RESPONSE CHARACTERISTICS OF THE
DATA COLLECTING AIRCRAFT**

Variation of the peak response with gust length

Aircraft Type E, 210 mph (Uc), 5000 ft
RW = 21400 lb, Min fuel, Rear c.g.



Aircraft Type J, 235 mph, 3000 ft
RW = 33900 lb, 60% fuel, Rear c.g.



Aircraft Type U, 260 KTS, 2000 ft
RW = 53000 lb, 75% fuel, Forward c.g.

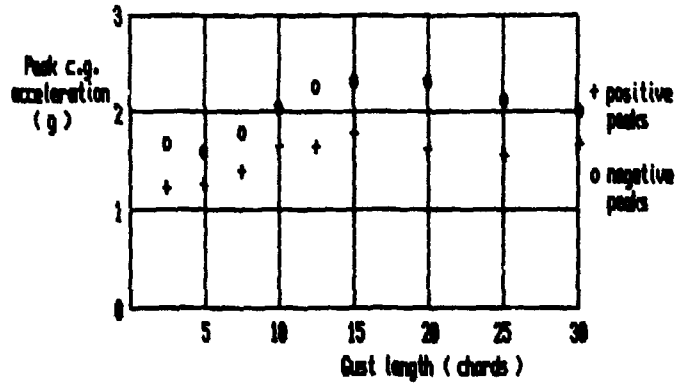
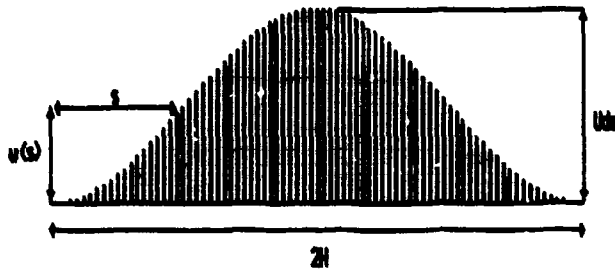
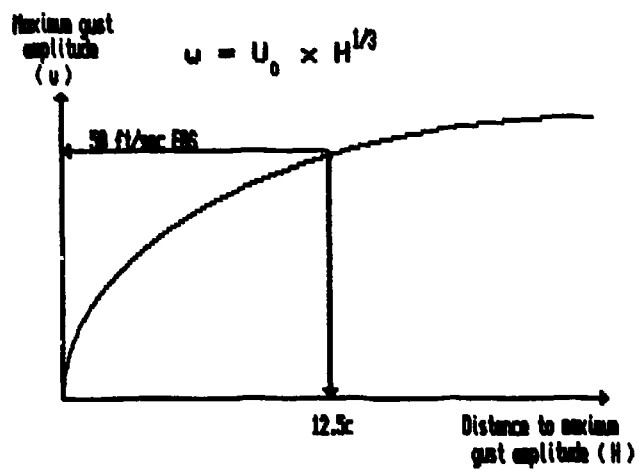


FIGURE 10

THE DISCRETE GUST

$$v = \frac{U_0 h}{2} \left[1 - \cos \frac{\pi s}{H} \right]$$

FIGURE 11

DISCRETE GUST AMPLITUDE POWER LAW

GUST RESPONSE CHARACTERISTICS OF THE
DATA COLLECTING AIRCRAFT

Variation of the peak response with gust length
for an equiprobable gust family

Aircraft Type E, 250 mph (Uc), 5000 ft
RW = 21400 lb, RW fuel, Rear c.g.

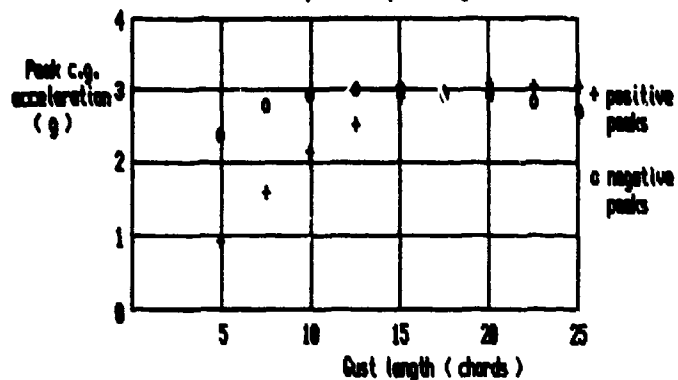


FIGURE 12

Aircraft Type J, 255 mph (Uc), 5000 ft
RW = 33500 lb, RW fuel, Rear c.g.

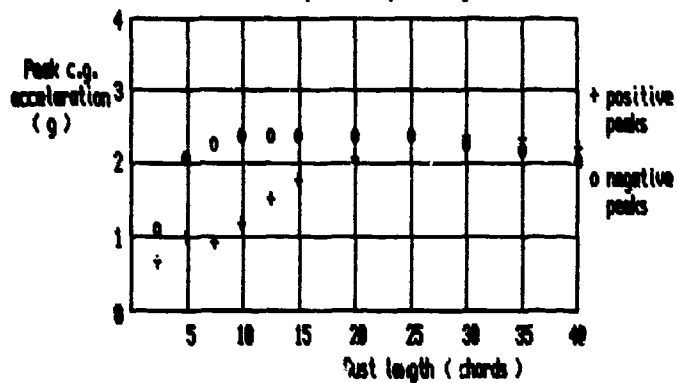


FIGURE 13

Aircraft Type U, 260 KTS (Uc), 20000 ft
RW = 53000 lb, RW fuel, Forward c.g.

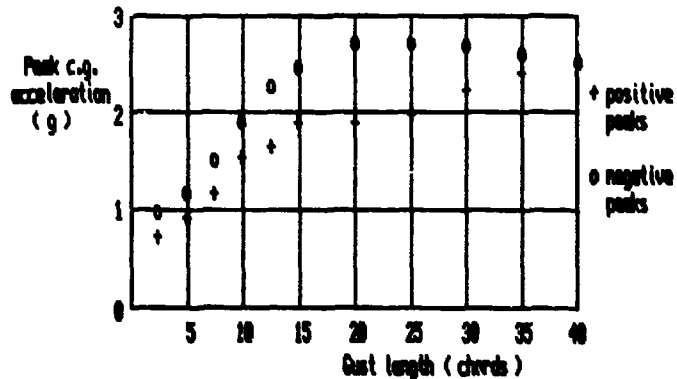
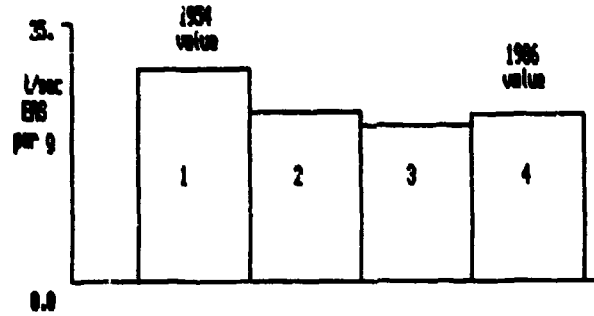


FIGURE 14

REVIEW OF GUST CONVERSION FACTORS

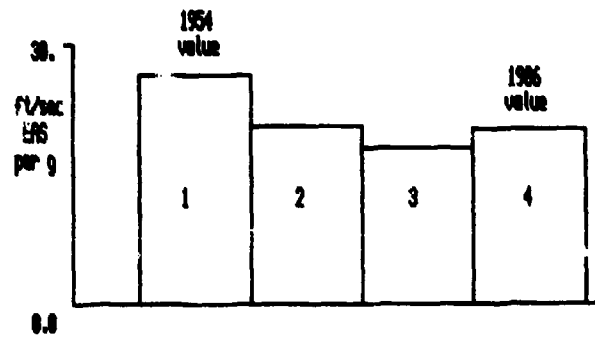
Aircraft Type E
Assuming mean cruise conditions

FIGURE 15



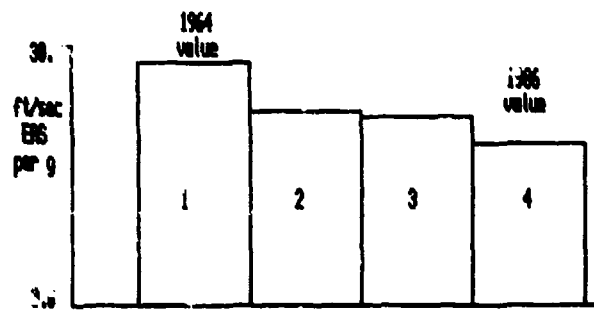
Aircraft Type J
Assuming mean cruise conditions

FIGURE 16



Aircraft Type V
Assuming mean cruise conditions

FIGURE 17



- 1: Pratt data solution for 12.5c gust (ref. NACA 1280).
- 2: Flexible aircraft solution for a 12.5c gust.
- 3: Flexible aircraft solution for a gust of equal amplitude to the 12.5c gust.
- 4: Flexible aircraft solution for a gust of equal probability to the 12.5c gust.

FIGURE 18

REVISION OF CURRENT GUST VELOCITIES

Gust probabilities believed valid for transport operations prior to 1958

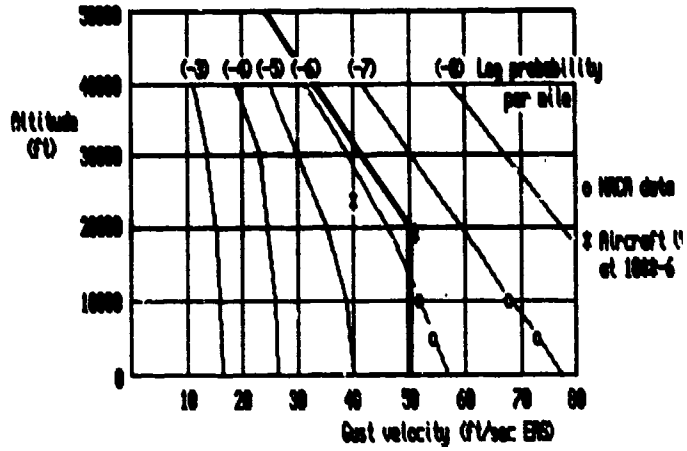


FIGURE 19

RE-ASSESSMENT OF DESIGN GUST VELOCITIES

Gust probabilities estimated as a result of the latest work

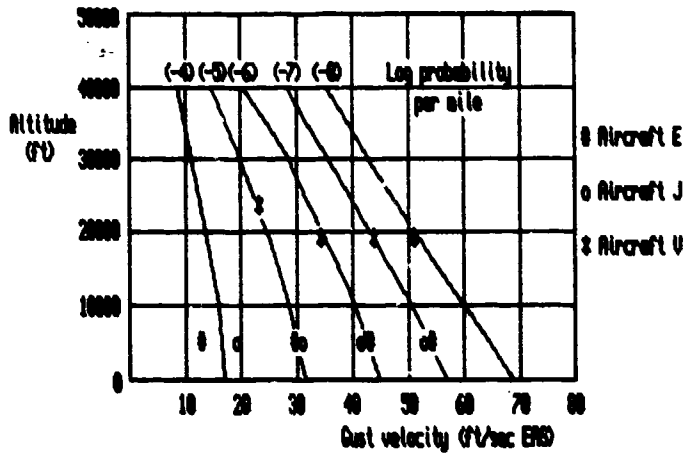
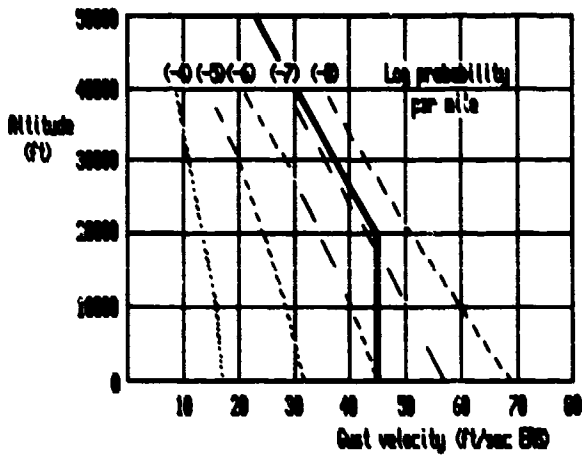


FIGURE 20

RE-ASSESSMENT OF DESIGN GUST VELOCITIES

Gust velocity expected to be met once in 50000 hours



REPORT DOCUMENTATION PAGE											
1. Recipient's Reference	2. Originator's Reference	3. Further Reference	4. Security Classification of Document								
	AGARD-R-734 Addendum	ISBN 92-835-0458-5	UNCLASSIFIED								
5. Originator	Advisory Group for Aerospace Research and Development North Atlantic Treaty Organization 7 rue Ancelle, 92200 Neuilly sur Seine, France										
6. Title	THE FLIGHT OF FLEXIBLE AIRCRAFT IN TURBULENCE — STATE-OF-THE-ART IN THE DESCRIPTION AND MODELLING OF ATMOSPHERIC TURBULENCE										
7. Presented at	the 65th Meeting of the Structures and Materials Panel in Cefme, Turkey on 4—9 October 1987.										
8. Author(s)/Editor(s)	Various		9. Date June 1988								
10. Author's/Editor's Address	Various		11. Pages 124								
12. Distribution Statement	This document is distributed in accordance with AGARD policies and regulations, which are outlined on the Outside Back Covers of all AGARD publications.										
13. Keywords/Descriptors	<table> <tbody> <tr> <td>Turbulence</td> <td>Data reduction</td> </tr> <tr> <td>Aircraft</td> <td>Accelerometers</td> </tr> <tr> <td>Flight characteristics</td> <td>Airborne equipment</td> </tr> <tr> <td>Surveys</td> <td></td> </tr> </tbody> </table>			Turbulence	Data reduction	Aircraft	Accelerometers	Flight characteristics	Airborne equipment	Surveys	
Turbulence	Data reduction										
Aircraft	Accelerometers										
Flight characteristics	Airborne equipment										
Surveys											
14. Abstract	<p>The large-scale use of flight recorders by commercial airlines, coupled with the enhanced quality of results offered by modern computer-based reduction processes makes it possible to broaden knowledge of the phenomenon of atmospheric turbulence. At the same time, new methods for predicting the response of flexible aircraft to turbulence are being proposed, and novel gust alleviation systems are being designed and tested. The Structures and Materials Panel held two Workshops on this topic, one in October 1986 and the other in October 1987.</p> <p>Presentations at the first Workshop, which concentrated on Measurements of Turbulence and Data Collection, are recorded in the main report — AGARD-R-734 — this volume records the presentations made at the second Workshop, which was held, under the chairmanship of Mr R.F.O'Connell, to discuss Methods of Analysis and Regulations. Papers include: (to DIV) ←</p>										

<p>AGARD Report No. 734 Addendum Advisory Group for Aerospace Research and Development, NATO</p> <p>THE FLIGHT OF FLEXIBLE AIRCRAFT IN THE TURBULENCE - STATE-OF-THE-ART IN THE DESCRIPTION AND MODELLING OF ATMOSPHERIC TURBULENCE</p> <p>Published June 1988 124 pages</p> <p>The large-scale use of flight recorders by commercial airlines, coupled with the enhanced quality of results offered by modern computer-based reduction processes makes it possible to broaden knowledge of the phenomenon of atmospheric turbulence. At the same time, new methods for predicting the response of flexible</p> <p>P.T.O</p>	<p>AGARD-R-734 (Addendum)</p> <p>Turbulence Aircraft Flight characteristics Surveys Data reduction Accelerometers Airborn equipment</p>	<p>AGARD Report No. 734 Addendum Advisory Group for Aerospace Research and Development, NATO</p> <p>THE FLIGHT OF FLEXIBLE AIRCRAFT IN THE TURBULENCE - STATE-OF-THE-ART IN THE DESCRIPTION AND MODELLING OF ATMOSPHERIC TURBULENCE</p> <p>Published June 1988 124 pages</p> <p>The large-scale use of flight recorders by commercial airlines, coupled with the enhanced quality of results offered by modern computer-based reduction processes makes it possible to broaden knowledge of the phenomenon of atmospheric turbulence. At the same time, new methods for predicting the response of flexible</p> <p>P.T.O</p>	<p>AGARD-R-734 (Addendum)</p> <p>Turbulence Aircraft Flight characteristics Surveys Data reduction Accelerometers Airborn equipment</p>
<p>AGARD Report No. 734 Addendum Advisory Group for Aerospace Research and Development, NATO</p> <p>THE FLIGHT OF FLEXIBLE AIRCRAFT IN THE TURBULENCE - STATE-OF-THE-ART IN THE DESCRIPTION AND MODELLING OF ATMOSPHERIC TURBULENCE</p> <p>Published June 1988 124 pages</p> <p>The large-scale use of flight recorders by commercial airlines, coupled with the enhanced quality of results offered by modern computer-based reduction processes makes it possible to broaden knowledge of the phenomenon of atmospheric turbulence. At the same time, new methods for predicting the response of flexible</p> <p>P.T.O</p>	<p>AGARD-R-734 (Addendum)</p> <p>Turbulence Aircraft Flight characteristics Surveys Data reduction Accelerometers Airborn equipment</p>	<p>AGARD Report No. 734 Addendum Advisory Group for Aerospace Research and Development, NATO</p> <p>THE FLIGHT OF FLEXIBLE AIRCRAFT IN THE TURBULENCE - STATE-OF-THE-ART IN THE DESCRIPTION AND MODELLING OF ATMOSPHERIC TURBULENCE</p> <p>Published June 1988 124 pages</p> <p>The large-scale use of flight recorders by commercial airlines, coupled with the enhanced quality of results offered by modern computer-based reduction processes makes it possible to broaden knowledge of the phenomenon of atmospheric turbulence. At the same time, new methods for predicting the response of flexible</p> <p>P.T.O</p>	<p>AGARD-R-734 (Addendum)</p> <p>Turbulence Aircraft Flight characteristics Surveys Data reduction Accelerometers Airborn equipment</p>

<p>aircraft to turbulence are being proposed, and novel gust alleviation systems are being designed and tested. The Structures and Materials Panel held two Workshops on this topic, one in October 1986 and the other in October 1987.</p> <p>Presentations at the first Workshop, which concentrated on Measurements of Turbulence and Data Collection, are recorded in the main report — AGARD-R-734; this volume records the presentations made at the second Workshop which was held, under the chairmanship of Mr. R.F.O'Connell, to discuss Methods of Analysis and Regulations.</p> <p>ISBN 92-835-0458-5</p>	<p>aircraft to turbulence are being proposed, and novel gust alleviation systems are being designed and tested. The Structures and Materials Panel held two Workshops on this topic, one in October 1986 and the other in October 1987.</p> <p>Presentations at the first Workshop, which concentrated on Measurements of Turbulence and Data Collection, are recorded in the main report — AGARD-R-734; this volume records the presentations made at the second Workshop which was held, under the chairmanship of Mr. R.F.O'Connell, to discuss Methods of Analysis and Regulations.</p> <p>ISBN 92-835-0458-5</p>
<p>aircraft to turbulence are being proposed, and novel gust alleviation systems are being designed and tested. The Structures and Materials Panel held two Workshops on this topic, one in October 1986 and the other in October 1987.</p> <p>Presentations at the first Workshop, which concentrated on Measurements of Turbulence and Data Collection, are recorded in the main report — AGARD-R-734; this volume records the presentations made at the second Workshop which was held, under the chairmanship of Mr. R.F.O'Connell, to discuss Methods of Analysis and Regulations.</p> <p>ISBN 92-835-0458-5</p>	<p>aircraft to turbulence are being proposed, and novel gust alleviation systems are being designed and tested. The Structures and Materials Panel held two Workshops on this topic, one in October 1986 and the other in October 1987.</p> <p>Presentations at the first Workshop, which concentrated on Measurements of Turbulence and Data Collection, are recorded in the main report — AGARD-R-734; this volume records the presentations made at the second Workshop which was held, under the chairmanship of Mr. R.F.O'Connell, to discuss Methods of Analysis and Regulations.</p> <p>ISBN 92-835-0458-5</p>

AGARD
NATO OTAN
7 rue Anacleto - 92100 AULNAY-SUR-SEINE
FRANCE
Telephone (1)47.36.57.00 - Telex 610 176

**DISTRIBUTION OF UNCLASSIFIED
AGARD PUBLICATIONS**

AGARD does NOT hold stocks of AGARD publications at the above address for general distribution. Initial distribution of AGARD publications is made to AGARD Member Nations through the following National Distribution Centres. Further copies are sometimes available from these Centres, but if not may be purchased in Microfiche or Photocopy form from the Purchase Agencies listed below.

NATIONAL DISTRIBUTION CENTRES

BELGIUM
Coordonnateur AGARD - VSL
Etat-Major de la Force Aérienne
Quartier Reims Elisabeth
Rue d'Evre, 1140 Brn

CANADA
Director Scientific Inf
Dept of National Def
Ottawa, Ontario K1/

DENMARK
Danish Defence Res
Ved Ldrætsparken
2100 Copenhagen

FRANCE
O.N.E.R.A. (Dire
29 Avenue de la
92320 Châtillon

GERMANY
Fachinformatio
Physik, Mathem
Karlsruhe
D-7514 Egger

GREECE
Hellenic Air Force General
Aircraft Support Equipment Directorate
Department of Research and Development
Hofagos, Athens. 15500

ICELAND
Director of Aviation
c/o Flugrad
Reykjavik

ITALY
Aeronautica Militare
Ufficio del Delegato Nazionale all'AGARD
3 Piazzale Adenauer
00144 Roma/EUR

LUXEMBOURG
Luxembourg

UNITED STATES
National Aeronautics and Space Administration (NASA)
Langley Research Center
M/S 180
Hampton, Virginia 23665

UNITED KINGDOM
Defence Research Information
Kentigern House
65 Brown Street
Glasgow G2 8EX

USA
National Aeronautics and Space Administration (NASA)
Langley Research Center
M/S 180
Hampton, Virginia 23665

NASA

National Aeronautics and
Space Administration
Washington, D.C.
20546

SPECIAL FOURTH CLASS MAIL
BOOK

Postage and Fees Paid
National Aeronautics and
Space Administration
NASA-451

Official Business
Penalty for Private Use \$300



THE UNITED STATES NATIONAL DISTRIBUTION CENTRE (NASA) DOES NOT HOLD STOCKS OF AGARD PUBLICATIONS, AND APPLICATIONS FOR COPIES SHOULD BE MADE DIRECT TO THE NATIONAL TECHNICAL INFORMATION SERVICE (NTIS) AT THE ADDRESS BELOW.

PURCHASE AGENCIES

National Technical Information Service (NTIS)
5285 Port Royal Road
Springfield
Virginia 22161, USA

ESA/Information Retrieval Service
European Space Agency
10, rue Mario Nikis
75015 Paris, France

The British Library
Document Supply Division
Boston Spa, Wetherby
West Yorkshire LS23 7BQ
England

Requests for microfiche or photocopies of AGARD documents should include the AGARD serial number, title, author or editor, and publication date. Requests to NTIS should include the NASA accession report number. Full bibliographical references and abstracts of AGARD publications are given in the following journals:

Scientific and Technical Aerospace Reports (STAR)
published by NASA Scientific and Technical
Information Branch
NASA Headquarters (NIT-40)
Washington D.C. 20546, USA

Government Reports Announcements (GRA)
published by the National Technical
Information Service, Springfield
Virginia 22161, USA

Printed by Specialised Printing Services Limited
40 Chigwell Lane, Loughton, Essex IG10 3TZ

ISBN 92-835-0458-5